University of Alberta
Department of Civil Engineering

Structural Engineering Report No. 102

Fatigue Strength of Trusses Made From Rectangular Hollow Sections

by
R. B. Ogle
and
G. L. Kulak

November, 1981

FATIGUE STRENGTH OF TRUSSES MADE FROM RECTANGULAR HOLLOW SECTIONS

by

R. B. OGLE

and

G. L. KULAK

DEPARTMENT OF CIVIL ENGINEERING

THE UNIVERSITY OF ALBERTA

EDMONTON, ALBERTA

NOVEMBER, 1981

ABSTRACT

This investigation was undertaken in order to examine the fatigue characteristics of full size HSS trusses made from rectangular sections. Present design standards including Canadian Standards Association CSA S16.1 do not make reference to fatigue requirements for joints made up of rectangular HSS sections. Recent research to establish guidelines for the fatigue behavior of HSS joints has been carried out almost exclusively on isolated joint specimens rather than full size trusses.

Two truss configurations, formed from overlap and gap K-type joints respectively, were investigated in this study. A static analysis was carried out to determine the stress distribution within each joint type and also to determine the load carrying characteristics of both truss configurations. This phase of the investigation was followed by cyclically fatigue loading the specimens to failure.

Results of the study show that both joint types fall below the most conservative fatigue category recommended by CSA S16.1. Therefore alternative methods of fatigue design are recommended for HSS joints. The study also indicated that the fatigue lives of full sized truss specimens may be less than the lives of isolated joint specimens. In addition, the tests confirmed that due to superior load transfer characteristics overlap K-type joints have significantly longer fatigue lives than gap K-type joints.

ACKNOWLEDGEMENTS

This study was carried out in the Department of Civil Engineering at the University of Alberta. It forms part of a continuing research investigation into the fatigue strength of structures made using hollow structural sections. Funds for the project have been provided by the Canadian Steel Construction Council and the National Sciences and Engineering Research Council of Canada.

This report is based on the thesis of Richard B. Ogle submitted to the Faculty of Graduate Studies and Research at the University of Alberta in partial fulfillment of the requirements for the degree of Master of Science in Civil Engineering.

Table of Contents

List of Tables

List of Figures

Figure Page

1. INTRODUCTION

1.1 General

Repeated or varying loads may cause failures at levels well below what is considered the static capacity of a member or structure. Such failures are characterized by the progressive growth of cracks initiating from micro-flaws, usually in areas of tensile stress. This crack growth may continue until the member cross section is so reduced in area that fracture occurs. Failure by such a process has been recognized as a design consideration for more than a century and is commonly known as fatigue.

Fatigue problems were first encountered in the design of machine components subject to cyclic or repeated stresses. Later, fatigue became a concern of the aircraft industry. Consequently, a large body of research concerned with fatigue has grown up in the areas of mechanical and aeronautical engineering.

It is only recently, however, that fatigue has become important in the context of civil engineering practices. Due to more sophisticated techniques of analysis and a better understanding of member behavior, modern steel structures tend to be more efficient than previous designs. When subjected to live loads, this results in increased stress ranges within the structure and, consequently, a greater susceptibility to fatigue. In addition, welding has

become the primary fastening method in many structures. This has led to a great variety of connection details, many of which do not have the relatively safe fatigue properties of older bolted and riveted connections (1). Finally, offshore exploration has introduced the drilling platform as a new type of engineering structure. Fatigue due to wave motion is an important design consideration in these platforms.

There are a number of variables that can influence the fatigue life of a structure. These include the yield point of the material, crystal structure, presence of flaws, inclusions, etc., residual stresses, detail type and load effects such as: stress range or stress ratio, random or constant load cycling and number of cycles of applied load. Researchers in the area of welded steel structures have shown that stress range, the number of load applications, and the detail type are usually sufficient to predict fatigue strength (2). This approach, commonly known as stress-life, relates the number of cycles to failure for a specific type of detail to the nominal applied stress range. Geometric properties and factors such as flaw size or weld profile are not considered explicitly since they are included in the type of detail being tested.

An alternative method of predicting fatigue strength is through the use of fracture mechanics. This type of analysis offers a more fundamental description of the physical process of fatigue. However, it also requires

knowledge of material fatigue properties, flaw sizes, and stress distribution. Fracture mechanics has often been used to verify experimental stress-life results. Such attempts have usually been successful in at least illustrating general trends.

1.2 Statement of the Problem

Due to their excellent structural properties, hollow structural sections (HSS) are finding increasing use in civil engineering structures. These sections can be classified as either circular (CHS) or rectangular, including square, (RHS). The joints formed by HSS members fall into three categories:

1. Circular web member to circular chord (C-C)
2. Rectangular web member to rectangular chord (R-R)
3. Circular web member to rectangular chord (C-R)

Present North American bridge design codes (3,4) and the Canadian design code for steel buildings (5) base their fatigue requirements primarily on tests on steel beams conducted under the National Cooperative Highway Research Program (6,7). These specifications group most common structural details into fatigue categories according to the fatigue strength of the detail. No information is given regarding the fatigue design of HSS connections, however.

Recently, researchers concerned with the fatigue behavior of HSS joints in offshore structures have produced

some design guides (8). This research deals almost exclusively with C-C joints and no specific suggestions have been made regarding C-R or R-R joints.

Some fatigue testing of C-R and R-R connections has been conducted in Europe (9,10,11). However, these tests involved isolated joints and therefore did not include the possible influence of secondary bending stresses on fatigue. In addition, the distribution of stresses in R-R joints and their effect on fatigue life is poorly documented.

1.3 Objectives

The objectives of this study are:

1. To investigate the fatigue behavior of trusses made from RHS members. The details of primary interest are overlap and gap R-R K-type joints.
2. To determine the nature and extent of secondary bending stresses in the trusses and their influence on fatigue strength.
3. To predict the stress distribution and stress concentration factors in the R-R K-type joint by use of the finite element method.
4. To predict the bending stresses by use of a simple direct stiffness program.
5. To compare test results with previous work done on isolated K-type joints.
6. To make recommendations for further work.

2. Literature Survey

2.1 General

Hollow structural section (HSS) joints were a development of improved fabrication and welding techniques of the 1960's. The first and most obvious concern was that of static strength, and it was found that the performance of most joint configurations was satisfactory. Usually, the only design guide necessary was a check of the punching shear of the web member with respect to the chord. This remains the most common static strength check used today.

The increasing use of HSS joints, especially in hostile offshore environments, led to a need for a more fundamental knowledge of how they behaved. This interest was focused on two areas, first on static or ultimate strength, and second on fatigue behavior. These areas of interest were not unrelated since it was recognized that a knowledge of the elastic stress distribution was required for an understanding of both. For this reason most investigators began with an elastic analysis of the HSS joint. The first such analyses usually attempted to predict the stresses theoretically by the solution of the governing differential equations. Later, during the 1970's, the more powerful finite element method was employed. In both cases, theoretical stresses were checked by stresses measured on laboratory specimens.

Once a knowledge of elastic stresses was obtained, investigators interested in ultimate strength moved on to solutions involving shell and plate buckling theory, yield line analysis, and sophisticated non-linear finite element programs. Those researchers concerned with fatigue strength used the elastic stress distribution for life predictions based on either a fracture mechanics or a stress versus life approach.

The distribution and relative magnitude of stresses within an HSS joint is primarily a function of geometry. In turn, the initiation and growth of fatigue cracks is dependent on the state of stress within the joint. For this reason, a variety of joint configurations have been tested and attempts have been made to correlate various geometric parameters with fatigue life. In addition to geometry, considerations such as flaws, residual stresses, nature of the loading function, etc., are important in determining fatigue strength. However, since these factors are common to the general body of literature regarding fatigue and fracture mechanics, fatigue studies of HSS joints have basically been directed toward the effect of joint geometry on fatigue life.

In context of civil engineering structures, secondary stresses are bending stresses which are induced in a connection as a result of the overall redundancy of the structure. Due largely to expense, virtually all fatigue testing has involved the axial loading of isolated joints.

This loading condition does not account for the presence of secondary stresses, which may be present in real structures. Therefore, in order to establish the influence of these stresses, it is necessary to conduct tests on entire structures.

2.2 Geometry and Joint Strength

2.2.1 Introduction

HSS joints can be classified by their overall shape and also by the nature of the members which frame into the joint. The most common joint types are T,Y,N and K joints,(Fig. 2.1), although more complex joints are possible. HSS joints also fall into three general categories:

1. Circular web member to circular chord (C-C)
2. Rectangular web member to rectangular chord (R-R)
3. Circular web member to rectangular chord (C-R)

Because of their extensive use in offshore structures, C-C joints have been the subject of most research.

In addition to overall shape and member type, there are a number of geometric parameters which influence joint behavior. Fig. 2.2 illustrates these parameters for a C-C joint. There is general agreement among researchers that the most important parameters are:

β - the ratio of the web member diameter to the chord

member diameter.

γ - the ratio of diameter to wall thickness for the chord member.

τ - the ratio of web member wall thickness to chord member wall thickness.

g/D - the ratio of gap length to chord diameter for K-type joints.

The parameters listed above are defined for C-C joints; analogous terms exist for R-R joints and are shown in Fig. 2.3.

Most theoretical and experimental measures of joint strength are expressed in terms of the geometric parameters noted above. This includes stress concentration factors used in fatigue analysis and also yield and ultimate loads for static strength considerations.

2.2.2 Theoretical Investigations (Elastic)

The earliest analytical attempts at determining elastic stress distributions in HSS joints involved the generation and solution of differential equations. This approach was used by Bijlaard (12), Dundrova (13), and Scordelis and Bouwkamp (14) to analyze joints idealized as laterally loaded cylinders. Although some reasonable results were obtained for C-C joints with T-type configurations, the solutions were cumbersome and limited to simple geometries. Thus, this approach soon gave way to the use of the finite element method. The first attempts to predict elastic

stresses using finite elements were made by Greste (15) and later by Kwan and Graff (16), Greimann, et al. (17) and Reber (18). In most cases, the primary element used was a shell element developed by Clough and Felippa (19). The important result of these analyses, from a fatigue standpoint, was the prediction of the magnitude and location of high or "hot spot" stresses. These early programs tended to be inefficient in terms of computational time and the preparation of input data. In the last five years similar but more sophisticated programs have been developed, culminating in such programs as PMBSHELL (20) and TKJOINT (21). These programs include features such as specialized elements, substructuring, and automatic mesh generation.

With the benefit of finite element programs, investigators have developed semi-empirical equations to estimate stress concentration factors for various C-C joint configurations. The most commonly used equations include those by Reber (18), Visser (22), and Potvin, et al. (21). The general form of the equations involves a number of dimensionless geometric parameters, including β, γ, τ, and g/D, which were defined in Fig. 2.2. In order to generate these formulae, many finite element solutions were obtained. The results were then used to develop correlation equations. Essentially, this method established the influence of one parameter on a hot spot stress while holding other parameters constant.

Dijkstra, et al. (23), have compared several stress concentration factor formulae to experimentally measured values. They found substantial differences between measured stresses and those predicted by the formulae. In addition, they also found substantial differences among the formulae themselves. It was concluded that the equations proposed by Reber (18) and Potvin, et al. (21), both of which were based on finite element parameter studies, most nearly approximated test results. However, it was also pointed out that even these formulae only gave a general indication of the real stress concentration factors. Nevertheless, fatigue design using stress concentration factors from such formulae is considered acceptable since the error introduced by their use does not appear to be greater than the total error introduced by other assumptions used during the fatigue design process, for example, the scatter inherent in any stress range versus cycle life plot due to initial flaw size or weld profile. If an extremely accurate prediction of the stress concentration factors for a particular joint is desired, then a separate finite element analysis of that joint should be conducted. Continued refinement of the element mesh would lead to an increasingly accurate estimate of the stress concentration factors.

While a great deal of work has been published regarding elastic stresses in C-C joints, there has been little work on C-R or R-R joints. This is not due to the complexity of the geometry, in fact C-R and R-R joints are simpler than

C-C joints, but because C-C joints are extensively used in offshore applications. Eastwood, et al. (24,25) have examined C-R and R-R joints using both the finite element and finite difference techniques. However, the results appear inconclusive and there is no evidence that any attempt was made to determine equations for stress concentration factors. Mang and Dutta (26) proposed a "spring model" which appears to have the capability of computing stress concentration factors for R-R joints. Unfortunately, documentation for this method is poor and no formulae or values for stress concentration factors have yet been published. Because C-R and R-R joints have relatively simple geometries, there is little doubt that programs such as PBMSHELL (20) or TKJOINT (21) could be adapted to generate stress concentration formulae for these type of joints.

2.2.3 Experimental Investigations of Static Strength

The first comprehensive experimental investigations into the static strength of HSS joints were conducted by Bouwkamp (27), and Beale and Toprac (28). Beale and Toprac tested isolated C-C joints with T,Y, and K configurations for both elastic stress distribution and ultimate strength. Stress patterns for circumferential, longitudinal, and normal stresses were determined by strain gauge measurements. It was found that circumferential stresses had the greatest magnitude and were therefore considered the

most important. The primary variable considered in the study was the web to chord diameter ratio, β. However, the influence of other joint parameters was also studied and empirical formulae for principal stresses were developed. These equations were based on relatively few data points and subsequent investigations have shown them to be of limited value (23). Nevertheless, the precision of the test measurements and the care taken in recording crack growth has caused the work of Beale and Toprac to be used as an experimental basis of comparison for many later analytical studies. Graff (29) summarized the experimental results of elastic and ultimate investigations to the year 1970.

Although interest has recently been focused on the study of the fatigue behavior of HSS joints, static tests have also been conducted. Static testing often takes place prior to fatigue loading in order to determine the magnitude and location of hot spot stresses. Examples of such work are Toprac and Louis (30), Bouwkamp and Stephen (31), and several Japanese investigators (32,33).

Most of the work concerning the static behavior of R-R and C-R joints has been carried out by British researchers at the University of Sheffield (24,25). Attempts were made to predict the stress distribution in the joints using the finite element and the finite difference method and also to verify these predictions experimentally. However, the analysis involved rather crude two-dimensional models and there were difficulties associated with the specification of

input loads and deflections. It is not clear whether the authors were successful in predicting elastic stresses or stress concentration factors as a function of joint geometry. The remainder of the research concerning the static strength of C-R and R-R joints deals with ultimate strength and its relationship to various geometric parameters. Davie and Giddings (10), Eastwood and Wood (34) tested K and N-type joints for ultimate strength as a function of gap ratio and parameters analogous to γ and β. These tests resulted in several empirically determined curves. More recently, Wardenier (35), Mouty (36), and Packer (37) have proposed formulae for ultimate strength of R-R joints. Wardenier's equations are based largely on experimental data, while both Mouty and Packer's work incorporate yield line theory.

2.2.4 Experimental Investigations of Fatigue Strength

Fatigue testing programs for C-C, C-R, and R-R joints were undertaken at roughly the same time, but, due to interest in offshore structures, C-C joints have been studied more intensively. The earliest tests on C-C joints were conducted by Bouwkamp and Stephen (31) and later by Toprac and Louis (30). Bouwkamp found that in N-type joints, the wall thickness of the chord member was important in determining fatigue performance. He also made the observation that overlapping web members are not as strong as gapped web members in fatigue loading. This conclusion

was not in agreement with the findings of other investigators. Toprac and Louis carefully measured the elastic stress distributions in T, Y, and K-type joints. They then made the important observation that, under fatigue loading, cracks initiated and grew from regions of high stress. As was expected, the joints with the highest stress concentration factors had the shortest fatigue lives. In this regard, T and Y-type joints were found to be weaker than K or N-type joints. For N-type joints it was found that the greater the amount of overlap, the lower the stress concentration factors, and, accordingly, the longer the fatigue life for a given stress range. In addition, Toprac and Louis observed the influence of other joint parameters such as γ and τ on fatigue strength. Finally, stress versus life plots for various joint configurations were presented.

Japanese investigators (38,39,40) have also carried out fatigue testing programs on K and N-type C-C connections. These studies include not only valuable data for the generation of stress versus life curves, but important observations on crack growth, stress distribution, and failure modes. Kurobane, et al. (39) confirmed that within regions of high stress, the distribution of strain range for strains that were known to be plastic was very similar to the strain range distribution for elastic strains. The explanation for this is that plastic material in hot spot locations was surrounded by elastic material and therefore was effectively being elastically strain-cycled.

A consequence of this behavior is that stress concentration factors computed by an elastic analysis can be used to predict strain ranges in hot spot locations even if their strains exceed the yield strain. Kurobane and Konomi (40) observed that fatigue strength was strongly related to the ultimate static strength of the joint. The ratio of load range to ultimate load was plotted against number of cycles to failure. (The ultimate load was estimated by the semi-empirical equation developed at Osaka University when actual static tests were not available (40).) The strong dependence of fatigue strength on ultimate strength that was revealed by this treatment confirmed an intuitive feeling of many researchers and also offered a method of predicting fatigue life on the basis of static strength.

Some of the most recent research on the fatigue of C-C joints attempts to predict fatigue life using the principles of fracture mechanics. Such an approach requires more information than a stress versus life approach and involves the precise measurement of crack growth rates, local stresses, and flaw sizes. More work must be done in this area before fracture mechanics can be used as a design guide for HSS joints. Details of the approach are given in Appendix A.

Examples of the fatigue testing of C-R or R-R joints are not numerous. Babiker (41) tested C-R N-type joints and produced several stress versus life curves, including a comparison of three gap spacings. It was found that joints

with overlap performed better than gap joints. Eastwood, et al. (34,42) tested both C-R and R-R N-type joints. For similar sized members, R-R joints showed slightly better fatigue characteristics than C-R joints. Once more it was found that overlap joints performed better than gap joints. It was also found that stiffening the chord face with a welded plate was not as effective in improving fatigue life as providing sufficient overlap. Further research on both C-R and R-R joints has been conducted by Mang and Dutta (26) and De Koning and Wardenier (9) under the sponsorship of CIDECT, a European organization concerned with research on hollow structural sections. These investigators have confirmed that gap joints are more susceptible to fatigue than overlap joints, that fatigue life tends to be independent of the applied stress ratio, and, finally, that the thickness of the chord wall becomes important as the diameter ratio, β, decreases. In addition, it was found that in regard to HSS joints, groove welds tended to perform better than fillet welds.

Because of the limited number of C-R and R-R joints tested, it is difficult to make specific statements regarding the influence of various joint parameters. However, it appears that CIDECT will continue to direct work in this area. A fracture mechanics approach has not yet been attempted for C-R or R-R joints.

2.2.5 Influence of Joint Parameters on Static and Fatigue Strength

Since it is not economical to examine the effect of all possible parameters on joint strength, researchers have been forced to test limited numbers of specimens and to study the influence of only a few variables, usually only within narrow limits. The result is that the comparison of different experimental programs is often very difficult. For this reason there is an increasing interest in more analytical methods such as fracture mechanics or the finite element method. It is also the reason that attempts have been made to relate fatigue strength to ultimate static strength.

It is obvious that the overall joint type, T,Y, or N has influence on both static and fatigue strength. An investigation of C-C joints by Beale and Toprac (28) revealed that Y-type joints had lower stress concentration factors than T-type joints, other geometric parameters being equal. The difference was found to be roughly 30% and thought to be reasonable, since forces perpendicular to the chord may cause significant bending stresses while stresses caused by forces parallel to the chord are not so severe. Similarly, it was found that the stress concentration factors in K-type joints were less than those in Y or T-type joints. The explanation for this is that in a K-type joint, forces perpendicular to the chord are transferred from branch to branch rather than carried entirely by the chord

wall, as is the case in a T or Y-type joint. As might be expected, the fatigue strength of T,Y, and K-type joints is a reflection of the static stress state. Toprac and Louis (30) found that, under the same nominal stress ranges, K-type C-C joints performed better than T or Y-type C-C joints. Similar behavior would be expected for C-R and R-R joints.

When K-type joints are tested, the geometric parameter most often studied is the gap ratio, g/D. Research on C-C joints has confirmed that overlap joints are stronger than gap joints in both static and fatigue loading (30). With regard to these tests and virtually all HSS joint testing, it should be noted that both static and fatigue loads are applied to isolated specimens in the axial direction. There is some evidence that the magnitudes of stress concentration factors are different for loads that result in bending. Toprac and Louis (30) found that overlap K-type joints were sensitive to in-plane moments. This suggests that if secondary moments in trusses are large, they may have a significant influence on the magnitude of hot spot stresses and, hence, fatigue life.

The influence of gap or gap ratio is similar for C-R and R-R N-type joints. Babiker (41) and Eastwood, et al. (42) found that C-R joints with 100% overlap were satisfactory in both static and fatigue loading. In the case of fatigue performance, the joints were compared to the stress-life curve assumed in British Standard Code of

Practice 153 (43) which refers to welded tubes in steel bridges. Joints with 47% overlap were found to perform well statically, but showed a reduced fatigue strength, falling below the BS 153 Class F curve. This was attributed to high local stresses introduced by intersecting weld beads required to form the joint. Gap joints were not satisfactory in fatigue loading and were often inadequate under static loads as well. Eastwood and Wood (34) reported similar findings for N-type R-R joints. However, De Koning and Wardenier (9) found that for N-type R-R joints, those joints wih 48% overlap actually showed slightly longer fatigue life than those with 100% overlap. Again, it was found that gap joints were very susceptible to fatigue.

Researchers are almost unanimous in the explanation given for the poor performance of gap joints. Load normal to the chord is transferred from one web member to the other through the top face of the chord, distorting the chord wall and inducing large bending stresses. This leads to a reduced fatigue life. On the other hand, an overlap joint permits load to be transferred more directly through the web members without involving the chord, thus, bending stresses are not as severe.

The web member width to chord width ratio, β, is also important in determining joint strength. Beale and Toprac (28) found that for C-C joints, elastic stresses in the chord became smaller and more uniform as β was increased. Several investigators (11,34) have reported greater ultimate

strength for larger β ratios in both C-R and R-R joints. Dijkstra, et al. (23) found that the degree of influence of β in various stress concentration factor formulae was different but that the general trend was for increasing stress concentration factors with decreasing β. In the case of C-R and R-R joints, Mang and Dutta (26) suggested that increasing β increased joint fatigue strength.

It is believed that as β increases, load is transferred more directly to the stiff sidewalls of the chord. This results in less distortion of the chord face, and hence, lower bending stresses. β also affects the influence of gap ratio on joint strength. For large β values virtually all the load is transferred through the sidewalls and the affect of gap is negligible. For smaller β values, however, the chord face becomes sensitive to gap. Thus, even small amounts of overlap can increase joint strength significantly.

The ratio of web member wall thickness to chord member wall thickness, τ, also affects joint strength. For C-C joints, Beale and Toprac (28) found that the stress concentration factor (measured in the chord) increased with increasing τ. This seems reasonable since increasing the web member wall thickness while holding the chord wall thickness constant (for the same nominal web stress) would require that the chord resist more load. Finite element analysis has confirmed this relationship (44). τ is also important identifying whether a fatigue crack will form in

the chord or in the web. τ is an indication of the relative bending stiffness of the web and chord which is in turn important in determining the maximum stress in the chord and web members. The critical value of τ for C-C joints has been reported as 0.56 (30). Below this value, fatigue cracks form in the web, while for τ ratios above 0.56, cracks form in the chord.

The chord diameter to thickness ratio, γ, is also an important parameter in both the static and fatigue strength of HSS joints. Several investigators (8,22) have found that the ultimate strength of C-C joints decreases with increasing γ. Dijkstra et al. (23) have confirmed that, for C-C joints, increasing γ results in larger stress concentration factors. The influence of γ on the strength of C-R and R-R joints has not been explicitly stated. γ is analogous to the span to depth ratio of a strip beam. γ is also important in ultimate strength design and is often reflected by punching shear efficiency.

2.3 Other Factors Influencing Fatigue Strength

The influence of connection geometry on the stress distribution and the fatigue life of HSS connections has been described in Section 2.2. There are several other important variables which may influence fatigue strength, these include:

1. The effect of local changes in geometry that are usually

not accounted for in a general stress analysis of the joint, for example: weld profile, notches or other abrupt changes in geometry.

2. The effect of flaws, inclusions, or gas porosities.
3. The nature of the applied load: constant amplitude, random, stress ratio, etc.
4. The material from which the connection and weldments are made.

There is general agreement that the last category, material parameters, is not likely to affect the fatigue strength of structural steels. Fisher et al. (6,7), in an extensive study of steel beams, found that yield strength was not significant in predicting fatigue life. The crack growth rate constants used in a fracture mechanics description of fatigue have been shown to be dependent on material type. However, for ferrite-pearlite steels, Rolfe and Barsom (45) report that the constants are relatively unchanged by the grade of steel tested. Pan and Plummer (46) successfully used crack growth constants derived from fatigue data published for several different tubular joints and steel grades to predict fatigue life. More recently, however, Bouwkamp (47) has suggested that the fatigue resistance of HSS joints is related to the yield point for steels with a yield strength of less than 50 ksi.

Local changes in geometry may increase the magnitude of stresses significantly. For example, the surface stresses at the toe of a non-load carrying fillet weld can be

magnified by a factor of roughly 2.0. Welds with poor profiles can increase stresses even more. To account for this weld variation in the stress-life approach, Marshall (8) has proposed a number of magnification factors according to weld profile.

Flaws and porosities located in regions of high tensile stress are the sites for crack initiation. In a stress-life approach the effect of flaw size is automatically included in the data generated by specimen tests. Much of the scatter found in stress-life curves is due to differences in flaw size, along with variations in weld profile. If fracture mechanics is to be used to predict fatigue life, then the initial crack size is required. When actual flaw measurements are not available, an average value must be estimated. Fisher and Hirt (48) have produced equivalent initial flaw sizes taken from measurements on steel beams. These flaw sizes, based on a penny-shaped crack model, were used successfully to predict the fatigue life of test specimens.

Laboratory fatigue tests on welded details usually involve constant amplitude, sinusoidal loading. However, real service loading is a random variable. The growth of fatigue cracks under random loads is complicated by such phenomenom as overstressing, in which a single large overload may retard crack growth for subsequent lower loads. This may be attributed to a zone of compressive residual stress induced at the crack tip by the overload. There has

been some success in formulating fatigue crack growth in terms of statistically averaged values such as the root mean square of the stress intensity factor range. The study of random loading is beyond the scope of this report and the reader is referred to References (45) and (49) for more details.

Constant amplitude sinusoidal loading can be described in terms of stress range, Sr, and stress ratio, R, where:

$$Sr = Smax - Smin$$

and

$$R = Smin / Smax$$

For most welded connections, fatigue life tends to be independent of stress ratio. This can be attributed to the presence of tensile residual stresses, in the order of yield stress, found adjacent to welded and heat affected metal. These stresses raise the mean stress level, that is, they tend to keep the crack open and in tension, making even compressive loads damaging. Once fatigue cracks leave a zone of residual tensile stress and are subjected to compressive stresses, crack growth stops. The stress ratio may become an important consideration for stress-relieved specimens or plain unwelded specimens. A detailed treatment of the fatigue of welded connections is given in References (50) and (51).

2.4 Effect of Secondary Stresses on HSS Joint Strength

There is little information regarding the testing of complete HSS trusses in either static or fatigue loading. Blockely (52) found that for purposes of static design, truss joints could be considered pinned. Secondary moments would be considered negligible in such an analysis. Dasgupta (53), however, reported that static failure loads in C-R trusses were up to 30% less than for comparable isolated joints. Mang and Dutta (26) suggest that fatigue tests on complete R-R trusses have been carried out and show good agreement with tests on isolated joints. They conclude that experimental results from isolated joints can be applied to joints in actual structures. Unfortunately, no details of the experimental program are given. Tajima et al. (54) tested full size trusses with RHS members for fatigue strength. The members were built-up sections and the connections involved gusset plates and, as such, the results of this study are not directly applicable to R-R HSS connections. However, it was found that the fatigue lives of joints in the full size truss specimens were approximately 30% less than the fatigue lives of small scale joints tested in the same manner. The investigators felt that the adverse effect of residual stresses on the trusses may have been responsible for their poorer performance.

Sharpe and Noordmark (55) tested full-size C-C aluminum trusses under fatigue loading. They found that a static truss analysis was most accurate when assuming the truss

chords were continuous and the web members were hinged at their ends. In addition it was found that secondary bending due to frame action was significant.

2.5 Present Code Requirements

CSA S16.1 - M78 (5) makes no specific reference to fatigue requirements for HSS connections. The Stelco Design Manual for Connections (56) contains a stress-life plot for C-R K-type joints based on the work of Eastwood et al. (34). Curves are plotted for 100% overlap joints, 47% overlap joints, and gap joints. It is noted that these curves are also applicable to R-R joints. Apart from overlap, no other variables are considered and a design procedure is not explicitly stated.

Most offshore structures are designed in accordance with either AWS D1.1 - 79 (57) or the British Code BS 153 (43). AWS D1.1 - 79 includes stress-life plots for several categories of weldments and connection details which are based on data published by WRC (51). Contained within this information are plots for T and K-type C-C joints, (Fig.2.4). These curves are based on "typical" connection geometries and it is recommended that they not be used if information regarding stress concentration factors can be obtained. The preferred design procedure for C-C joints, as outlined by Marshall (8), involves the use of AWS curve 'X', Fig. 2.4, and is as follows. The stress concentration

factor for the hot spot stress in a particular joint would be determined by either a finite element analysis or the use of an appropriate formula such as those presented by Reber(18) or Potvin et al. (21). The designer would also determine, usually from a statistical analysis the number of cycles of load applied at enough discrete stress ranges to adequately describe the random loading function. An estimate of fatigue life can then be made using a cumulative damage rule such as Miner's Law (45), which can be stated as:

$$D = \sum_i \frac{n_i}{N_i} \qquad (2.1)$$

where:

D = damage ratio.

n_i = number of cycles applied at 'i' stress range.

N_i = number of cycles to failure at 'i' stress range as determined by a constant amplitude stress-life curve.

In order to determine N_i, the designer would multiply the nominal stress range by a stress concentration factor and enter a stress-life plot such curve 'X' in AWS D1.1 - 79. Curve 'X' is based on stress transverse to full penetration groove welded plate specimens. If the weld profile in the HSS joint is more severe than a typical groove weld, then the nominal stress range could be further increased by a factor, as proposed by Marshall (8). A damage ratio, D, of

1.0 or greater indicates that the connection will not survive the particular loading condition. In such a case, the connection would have to be redesigned to reduce stress concentration factors. The procedure outlined above can be applied to C-R or R-R joints if the stress concentration factors for these geometries can be computed.

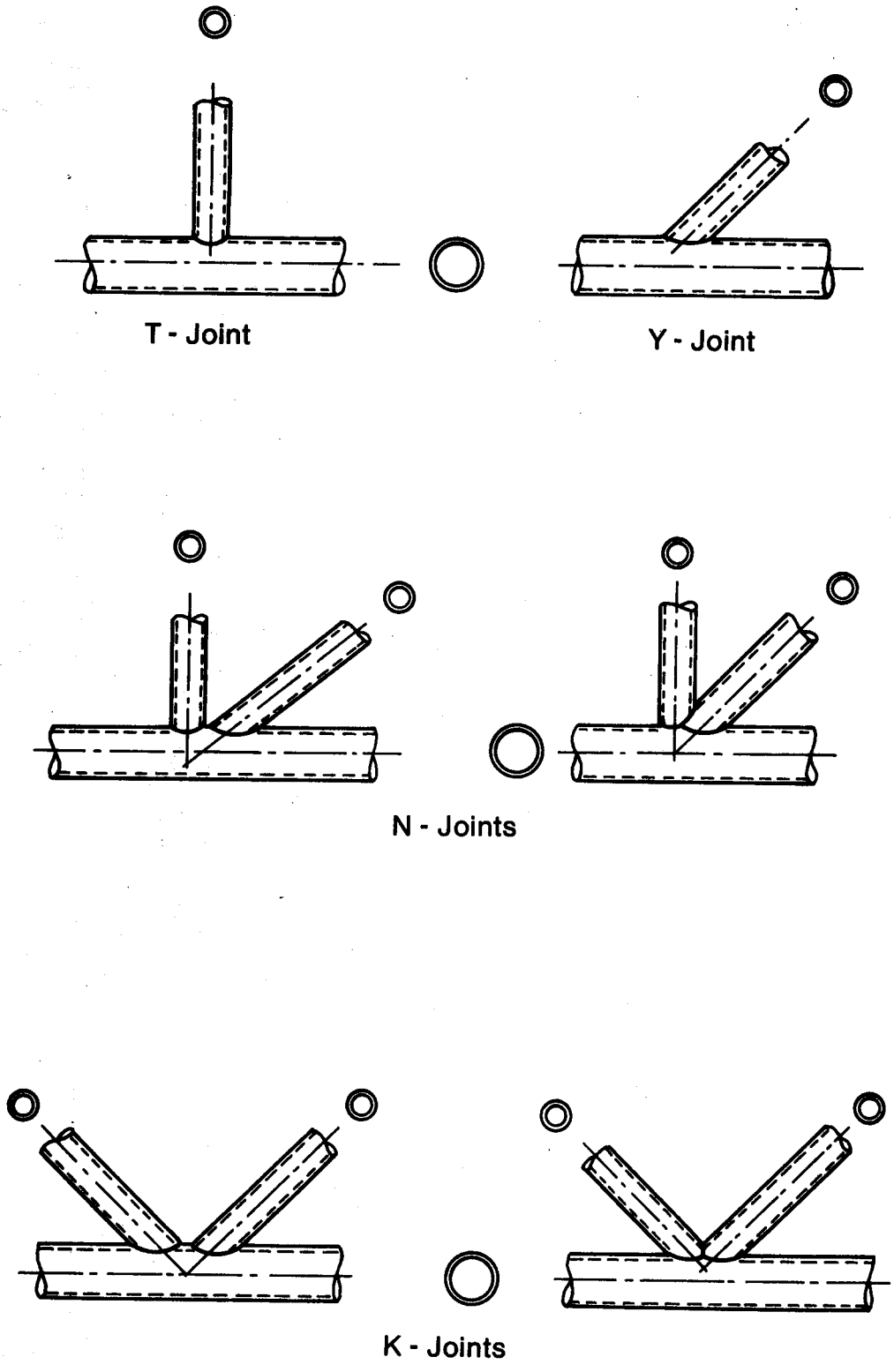

Figure 2.1 Typical Configurations for Tubular Joints

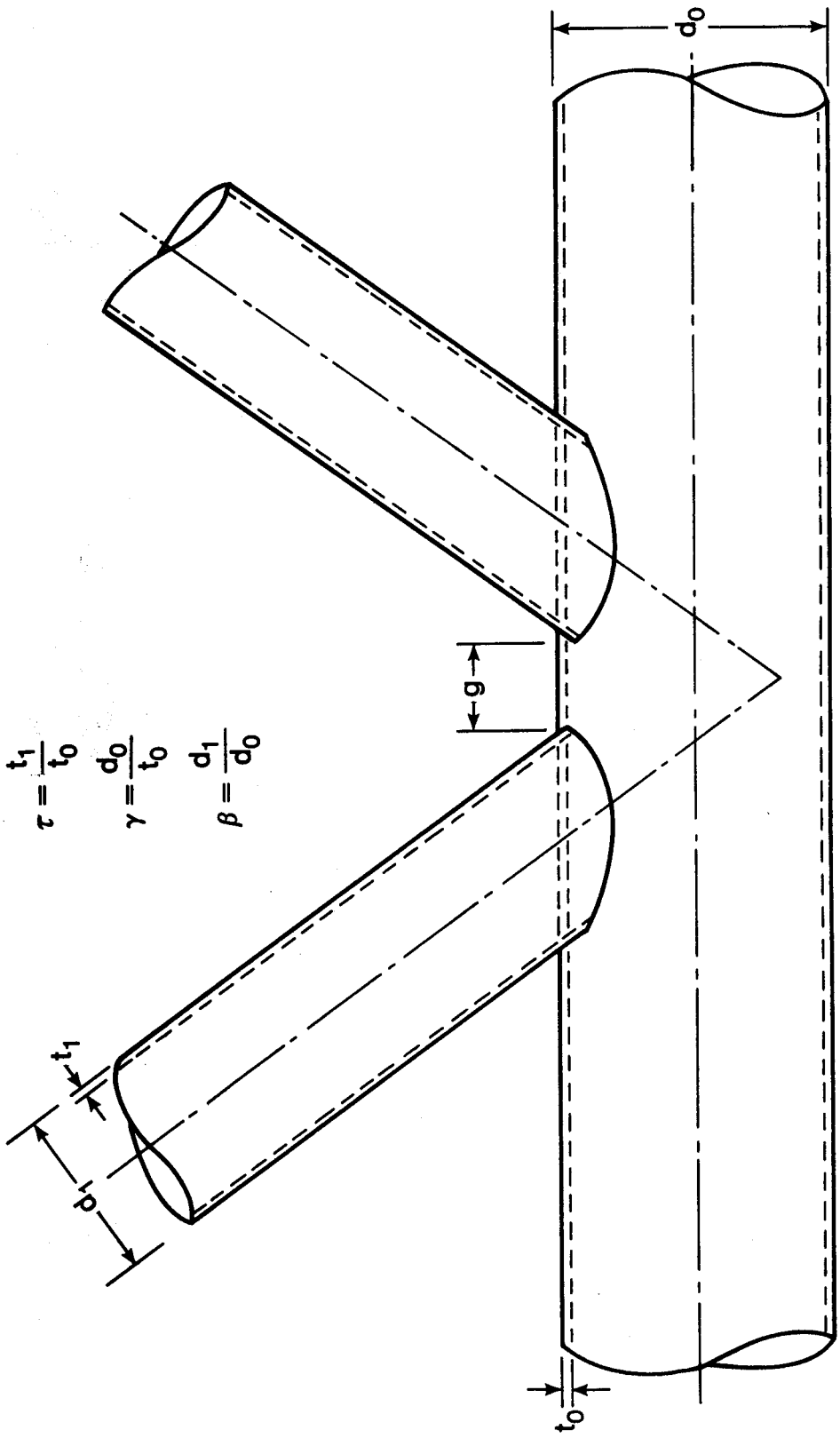

Figure 2.2 Joint Parameters for a C-C K-Type Joint

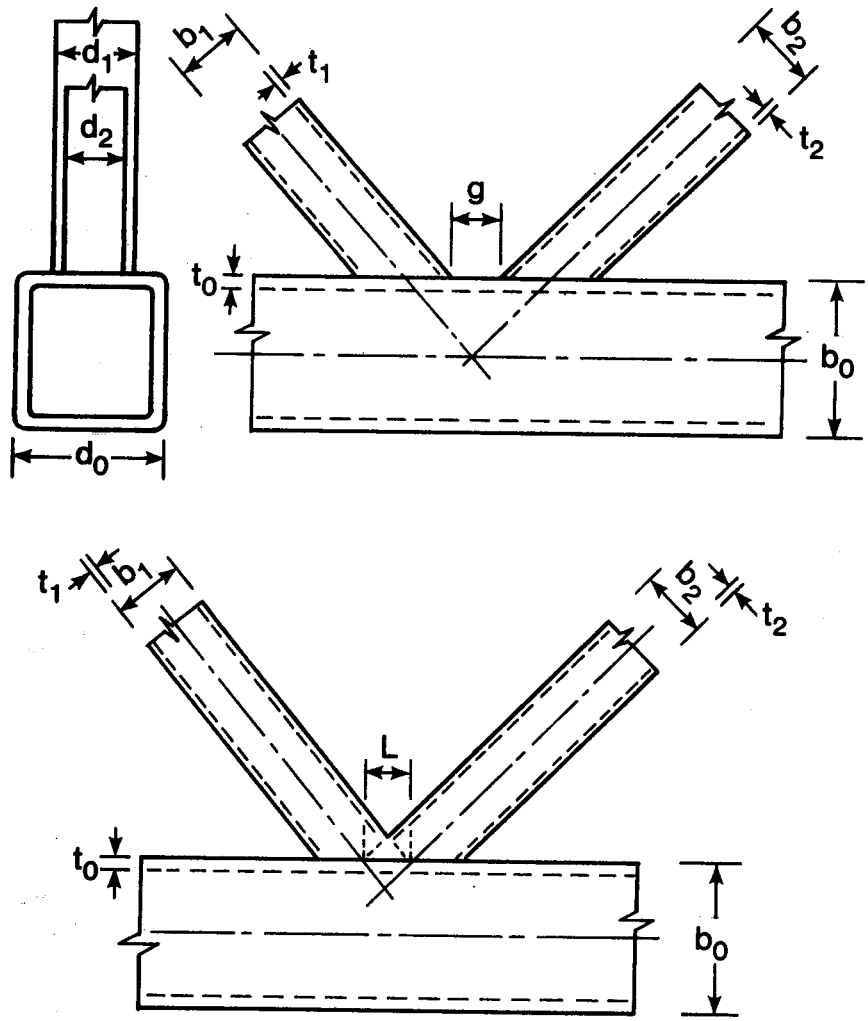

$$\text{Overlap} = \frac{L}{\left(\frac{b_1 + b_2}{2}\right)} \qquad \text{Gap Ratio} = \frac{g}{d_0}$$

$$\text{Thickness Ratio} = \frac{t_1 + t_2}{2t_0} \qquad \text{Diameter Ratio} = \frac{d_1 + d_2}{2d_0}$$

$$\text{Chord Thinness Ratio} = \frac{d_0}{t_0}$$

Figure 2.3 Joint Parameters for R-R K-Type Joints

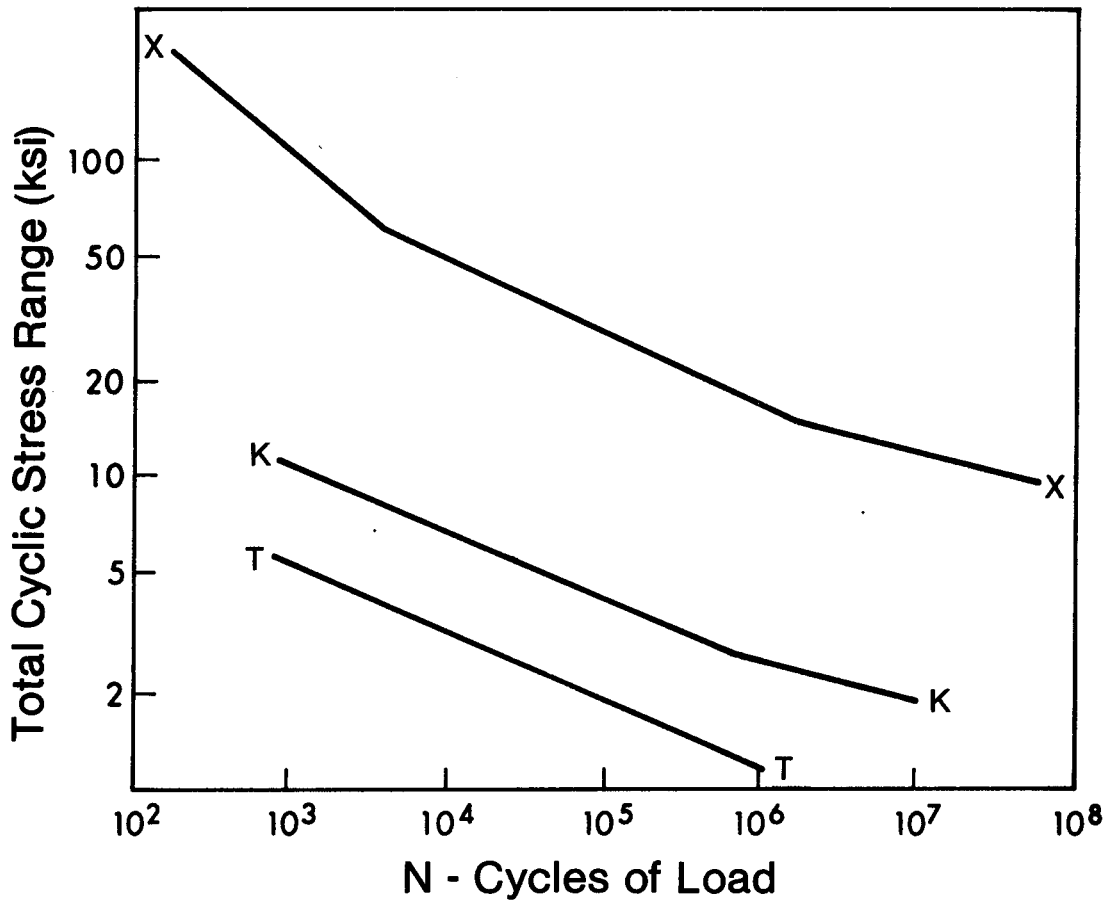

Figure 2.4 Allowable Fatigue Stress Ranges for Categories K, T, X

3. Experimental Program

3.1 Scope

The purpose of the experimental program was to determine the fatigue strength of full size HSS trusses with welded connections. This required two test procedures. First, specimens were loaded statically in order to find axial and bending stresses in individual members. In addition, stresses at various locations within what was considered the critical joint were measured during this stage. The second phase of testing involved the application of a fluctuating load to the truss specimens. Loading was continued until failure due to fatigue cracking occurred. The experimental results were then compared to studies conducted on isolated joints and to joint strength as predicted by current practices.

A testing program on the fatigue strength of HSS trusses was undertaken by Comeau and Kulak (58) in 1979. Three identical HSS trusses of CSA G40.21 50W Class H (hot-rolled) material were tested. The overall geometry of the trusses can be seen in Fig. 3.1. All joints were overlapped and had zero eccentricity, the overlapped joint L1 is illustrated in Fig. 3.2. This program will be referred to in this report as Test Series 1.

As a continuation of this project, the present study tested two series of three trusses each. The trusses in the

first series (Test Series 2) were geometrically identical to those tested by Comeau and Kulak, however the material used in this case was CSA G40.21 50W Class C (cold-rolled). The trusses in the second series (Test Series 3) were of Class H material but the K-type joints were gapped rather than overlapped. The truss layout for Series 3 is shown in Fig. 3.3 and the gap K-type joint L1, is illustrated in Fig. 3.4.

3.2 Specimen Description

In order to obtain realistic member proportions, the overlap joint trusses, Series 1 and 2, were designed to resist a factored static load of 315 kips. The design procedure followed the recommendations of CSA S16.1 - M78 (5) and the STELCO Design Manual for Connections (56). To ensure that static failure would be controlled by member strength rather than joint strength, the joints were designed with sufficient overlap. Three member sizes were used; the chords were HSS 6 X 4 X 0.250, the outer web members were HSS 6 X 6 X 0.375 and the inner web members were HSS 3.5 X 3.5 X 0.188.

The member cross section sizes were kept the same for Series 3. However, in order to accommodate the gap joint configuration it was necessary to slightly alter the overall dimensions of the truss. This small change in geometry did not appreciably affect member forces or behavior.

All truss specimens were constructed by a local steel fabricator using normal shop practices and tolerances. Welding was performed using the manual shielded arc process and AWS E70 electrodes. The location of tack welds used during fit-up was noted before final welding took place.

In all test series, the principal joint studied was the K-type joint located at midspan on the lower chord. However, all joints were monitored for fatigue cracking during testing. This revealed that in particular, cracking occurred within the upper joint, U2, in some tests. The joint U2 for the Series 2 and 3 trusses is illustrated in Figs. 3.5 and 3.6, respectively.

The overlap K-type joint, Fig. 3.2, was designed for zero eccentricity since the centrelines of the component members intersected at a single point. This resulted in an overlap of 40% ; overlap is defined in Fig. 2.3. The joint was formed using both groove and fillet welds. A full penetration groove weld using a back-up bar was applied to the intersection between the two 3.5 X 3.5 X 0.188 web members. The remainder of the joint was fillet welded.

The gap K-type joint shown in Fig. 3.4 was designed with a gap of 1.188 inch resulting in an eccentricity of 1.688 inch. The gap configuration permits easy fit up and welding procedures and requires only simple end profiling of the web members. The remainder of the joint was fillet welded.

Under preliminary testing for Series 1, it was found that excessive flexing of the vertical tube walls occurred at the loading point and at the reactions of the truss specimens. Therefore, to prevent premature fatigue failures in these areas, the chord members in all test specimens were stiffened by filling them with expanding grout for a distance of 18 inches in from the end of each member. It was considered that this modification would not effect the overall behavior of the truss.

3.3 Test Set-Up

The trusses were tested as shown in Figs. 3.1 or 3.3. Fig. 3.7 is a photograph of the loading arrangement and lateral bracing. A single compressive load was applied at the upper chord joint U1. The line of action of the load was directed through the intersection point of the centrelines of the web members. The support conditions were a roller at the reaction nearest the load point and a pin at the far reaction. In addition, lateral support was provided by bracing the upper joints in the out-of plane direction.

An Amsler dynamic testing machine was used in all tests. Compressive load was applied by a hydraulic jack (maximum capacity 110 kips) activated by a variable stroke hydraulic pump. Static load was measured by a pressure gauge in the testing machine and also by a flat compressive load cell placed directly underneath the jack. Dynamic load

levels were established by reading strain gauges placed on the tension web member at midspan; the resulting wave form was monitored on an oscilloscope. The dynamic loading rate was 500 cycles per minute for all specimens.

3.4 Test Procedure

Before testing was begun, the trusses were aligned in order to reduce out-of-plane bending. This was accomplished by adjusting the lateral bracing and placing shims under the reactions. A load of 30 kips was applied to the truss and strain readings, from gauges placed on the in-plane faces at the midpoints of members L0-U1 and L2-U2 were taken. The truss was considered aligned when the readings on opposite faces differed by less than 10%.

In order to determine the strain (stress) distribution within the K-type joints under static load, strain gauges were placed on specimens T5F and T8F of Series 2 and 3, respectively. The strain gauge pattern for Series 3 is shown in Fig. 3.8. Gauges, although fewer in number, were placed on all other specimens in probable hot spot locations. In addition, gauges were mounted on both out-of-plane faces of all members in specimens T9F and T10F of Series 3. These gauges allowed bending stresses throughout the truss to be computed. In other specimens, strain gauges were applied at mid-length in order to compute nominal axial forces. Static load was applied in 10 kip

increments up to maximum of 100 kips for Series 2 and 60 kips for Series 3. These load levels were well below that which would be expected to cause buckling or inelastic behavior in the joints. Strain readings were taken at each load level for all gauges. Dial gauges were used to measure the vertical deflection of the chord directly beneath the K-type joint in Series 3.

Stress range was considered to be the most important non-geometric variable in the study of joint fatigue life. Thus, each specimen was tested with a specified nominal stress range in the tension member L1-U2. In all tests, the minimum load level was adjusted to cause a minimum tension stress of 1.3 ksi in this member. The maximum load was set at a level which would produce the desired stress range. These limits were held constant for a given test. The loading waveform between these values was sinusoidal.

Before fatigue testing was begun, the joint areas were stripped of strain gauges and white-washed for easier detection of cracks. Because there was little prior knowledge as to when and where fatigue cracks would form, an observer was always present during testing. A crack growth history from first observation to final failure was recorded. Failure was assumed to have occurred when approximately one quarter of the cross section of member L1-U2 was cracked through.

3.5 Crack Initiation and Growth

In all three test series, fatigue cracking was observed in the lower K-type joint, L1, and in six of the nine specimens tested, final failure was a result of cracking in this joint. Failure in the other three specimens occurred in the upper K-type joint, U2. Table 3.1 summarizes the fatigue lives of all specimens, and a brief description of fatigue crack growth follows.

For specimens T2F, Series 1, cracking initiated in the vicinity of the groove weld in joint L1. On one side of the joint, a crack began in the vertical position of the groove weld and propagated both upwards and downwards. The lower end of the crack grew through the horizontal fillet weld, turned sharply, and propagated along the lower edge of the weld. The upper end of the crack propagated along the horizontal edge of groove weld. On the opposite side of the joint, a crack started at the toe of the horizontal groove weld and grew across the tension member L1-U2 in a direction roughly perpendicular to the longitudinal axis of the member, as can be seen in Fig. 3.9. In addition, cracks were also observed starting at the corners of the fillet weld on the underside (heel) of the tension member. This cracking, as shown in Fig. 3.10, did not occur until late in the fatigue life of the truss and was not responsible for failure.

Failure in trusses T3F and T4F was a result of crack growth in the upper joint, U2. In both cases, cracks

propagated along the weldment connecting the tension member L1-U2 to joint U2. These cracks were present on planes parallel to the plane of the truss. The cracks appeared to be stepped, suggesting several initiation sites. Cracks were also observed along the toe of the fillet weld where member L1-U2 entered joint L1. However, these cracks had not penetrated through the thickness of the member before failure occurred at joint U2.

The specimens in Series 2 all failed as a result of fatigue cracking in the overlapped K-type joint, L1. In all cases, cracks initiated in the groove weld near the horizontal to vertical weld transition. Although cracking was always observed on both sides of the joint, crack initiation was not simultaneous and one crack had usually grown 1 to 2 inches before crack growth was detected on the opposite side of the joint. In trusses T5F and T7F, these cracks propagated across the tension member L1-U2 in a direction approximately transverse to the member axis. This growth is illustrated in Figs. 3.11 and 3.12. Characteristically, the cracks cut through the horizontal fillet weld at 45 degrees and began growing along the bottom edge of this weld. In truss T6F, one crack behaved as described above while on the other face a crack initiated at the top of the groove weld and grew directly down the vertical face until it reached the horizontal fillet weld where it there sliced across the weld at 45 degrees and propagated along its bottom edge.

Both tests T5F and T6F were stopped before cracks penetrated the chord wall. Cracking in T7F was allowed to continue until the cracks grew through the top chord wall and into the sidewalls of the member. The crack pattern for T7F can be seen in Fig. 3.12. In additions to cracks initiating in the groove weld area, cracks were observed growing in the fillet weld at the back corners of the tension member L1-U2 for specimens T5F and T7F. These cracks were not observed until cracking in the groove region was well advanced. Specimen T7F also had a small crack in the upper end of member L1-U2, parallel to the member axis. This crack did not grow significantly after first observation.

The trusses T8F and T10F of Series 3 failed in an identical manner. A crack initiated at the toe of the tension member fillet weld in the K-type joint, L1, and spread rapidly across the width of the member. As the crack reached either end of the weld, the rate of growth slowed as it began to change direction and turn down into the vertical sidewalls of the chord. Because fatigue cycling was never stopped, it was not possible to determine at what point in its development the crack penetrated the thickness of the chord wall. At about the time the crack began growing into the vertical sidewalls, additional cracks were observed growing from the underside of the tension member near the corners of the fillet weld and propagating along the fillet weld back toward the toe of the tension member. The crack

growth pattern for T8F and T10F is shown in Figs. 3.13 and 3.14. Arrows indicate the direction of crack growth. A crack was also observed at the toe of the tension member L1-U2 in the upper joint U2 for specimen T10F. However, this crack did not initiate until cracking in the lower joint, L1, was far advanced.

In specimen T9F, initial cracking was first observed in the lower joint, L1. However, final failure actually occurred in the upper joint, U2. Cracks appeared at roughly the same time at the corners of the fillet weld, at the toe of tension member L1-U2 in joint L1. These cracks, one above the fillet weld, and one below, propagated toward the centre of the member. Eventually, the cracks overlapped and the upper crack crossed the fillet weld to joint the lower crack. At this time, initiation of a crack was observed at the toe of the tension member L1-U2 fillet weld in the upper joint, U2. This crack propagated rapidly across the width of the tension member and turned both corners of the weld simultaneously, continuing along the edge of the weld. Failure was eventually due to this crack. The gap K-type joint in truss T8F was sawn open after fatigue testing had been completed and a detailed inspection of the crack surface was made including examination with a scanning electron microscope. From this inspection it appeared likely that the crack had initiated on the top surface of the chord, directly at the toe of the fillet weld, perhaps where the weld to chord intersection created the most severe

angle. No large or obvious defects from which the crack may have originated were observed in this region. It was not possible to say whether the crack grew as a single eliptical surface crack until it had penetrated the chord wall or whether several surface cracks coalesced then propagated as a single edge crack. Fig. 3.15 shows the crack surface within the chord magnified 3000X. Distinct fatigue striations can be seen towards the centre of the photograph, each striation is the result of a single cycle of load.

A thin but distinct band of material with high manganese sulfide content was observed to run at mid depth of the chord wall. Large portions of this band were cracked, possibly opening during the fatigue process, Fig. 3.16. The formation of the region is probably associated with the rolling process. There was no evidence to suggest that it played an important role in the fatigue process, however.

Table 3.1 Fatigue Test Results

TRUSS	STRESS RANGE (ksi)	CYCLES TO FIRST CRACK	CYCLES TO FINAL FAILURE
T2F	7.3	69,000	423,000
T3F	4.7	----	1,911,000
T4F	5.5	----	924,000
T5F	6.0	804,000	1,200,000
T6F	8.0	129,000	255,000
T7F	4.0	6,670,000	7,510,000
T8F	6.0	144,000	174,000
T9F	4.0	1,600,000	2,180,000
T10F	5.0	327,000	366,000

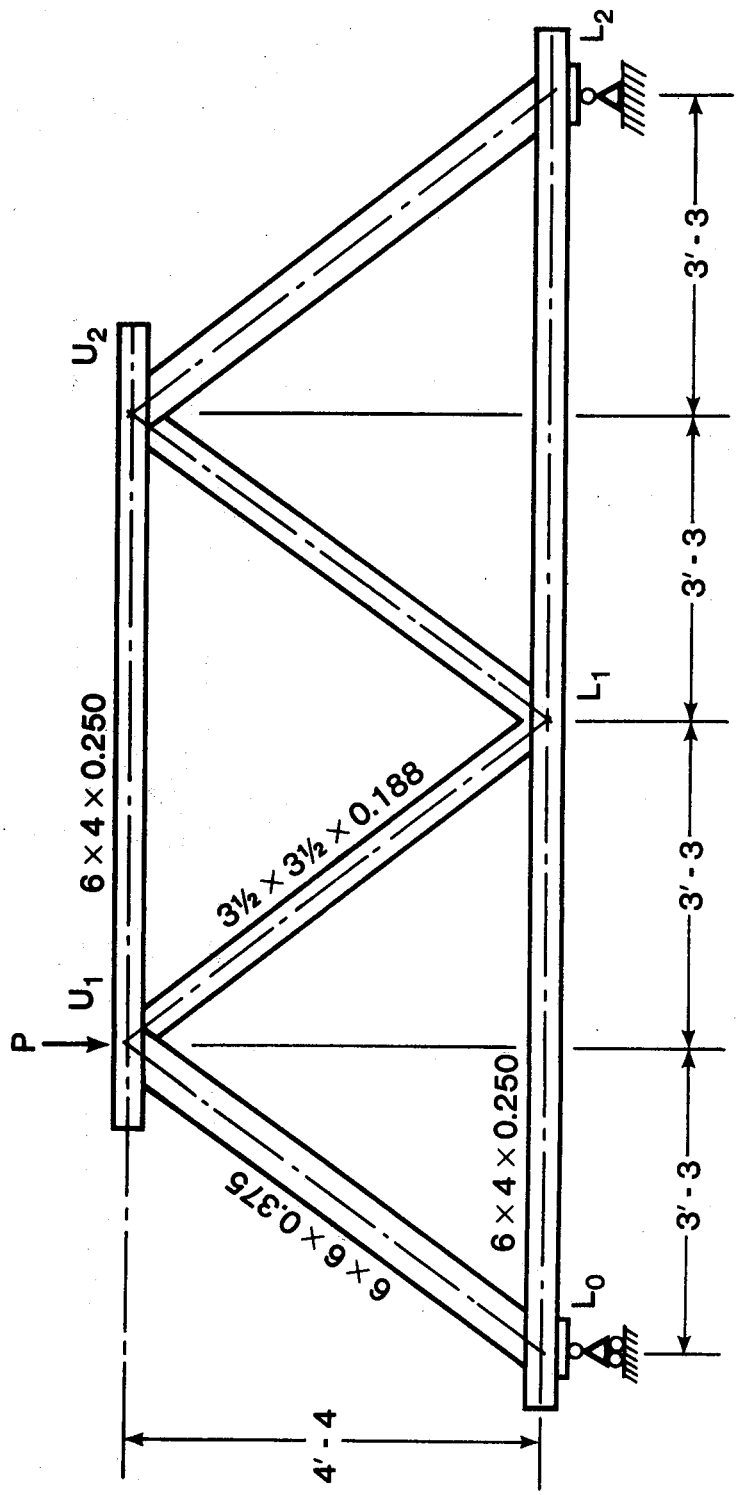

Figure 3.1 Overlap Joint Truss Specimen Layout
(Series 1 and 2)

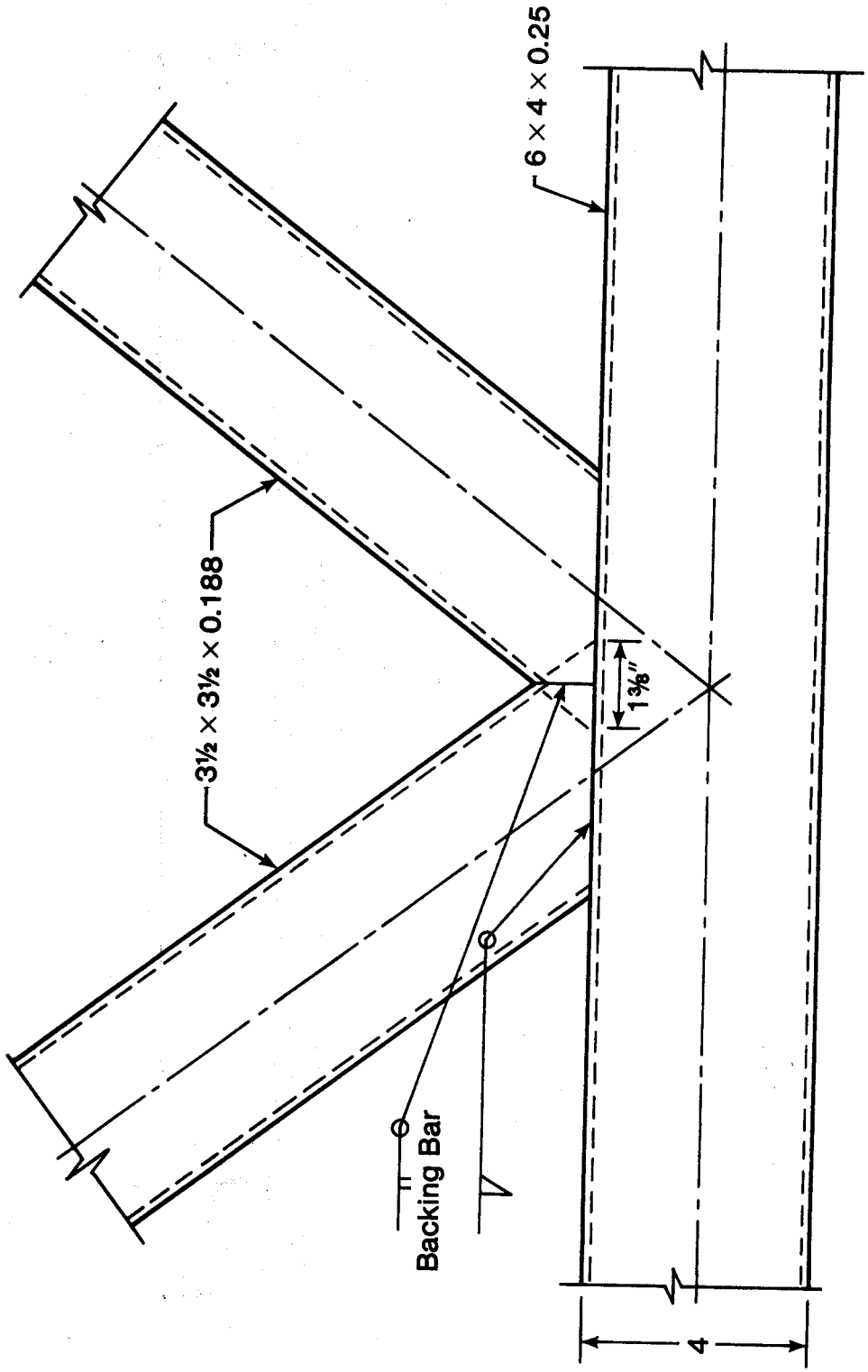

Figure 3.2 Detail of Overlap Joint L1 (Series 1 and 2)

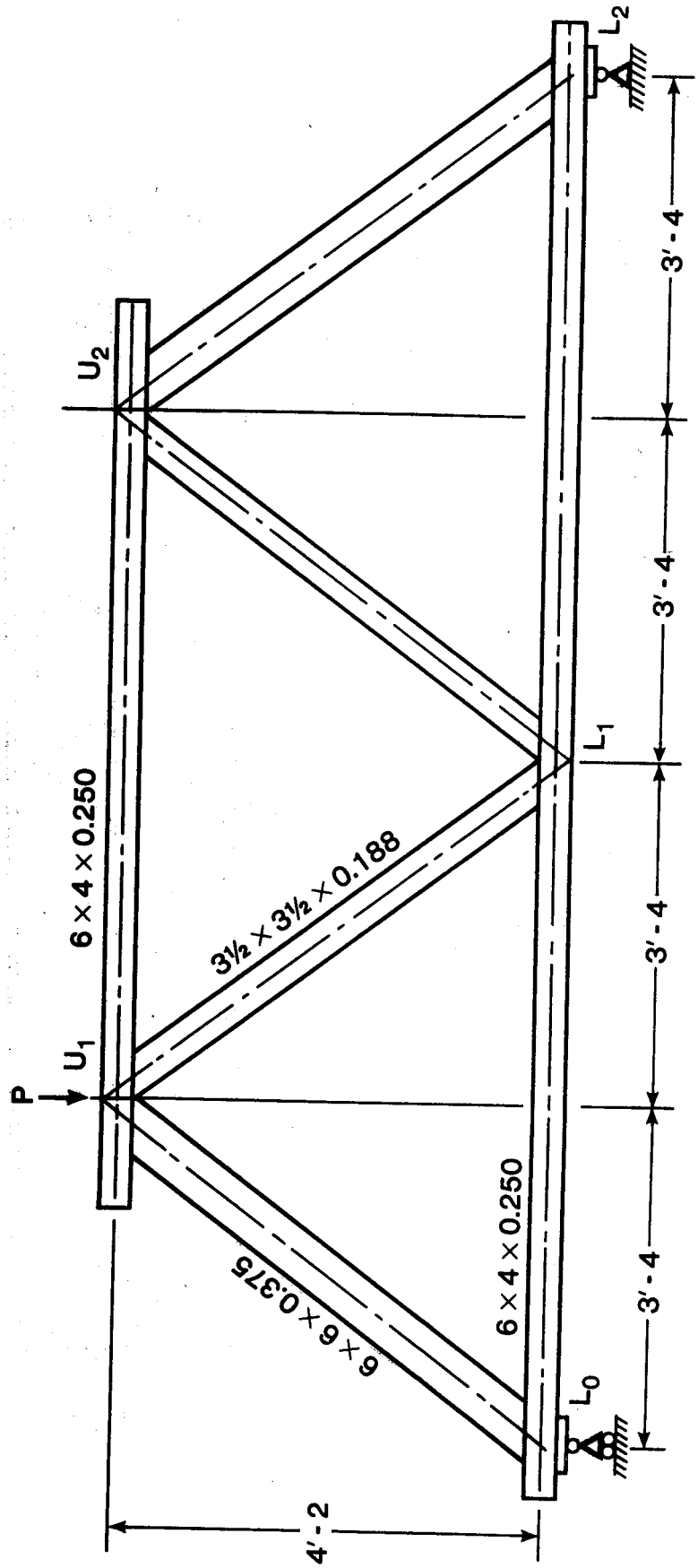

Figure 3.3 Gap Joint Truss Specimen Layout (Series 3)

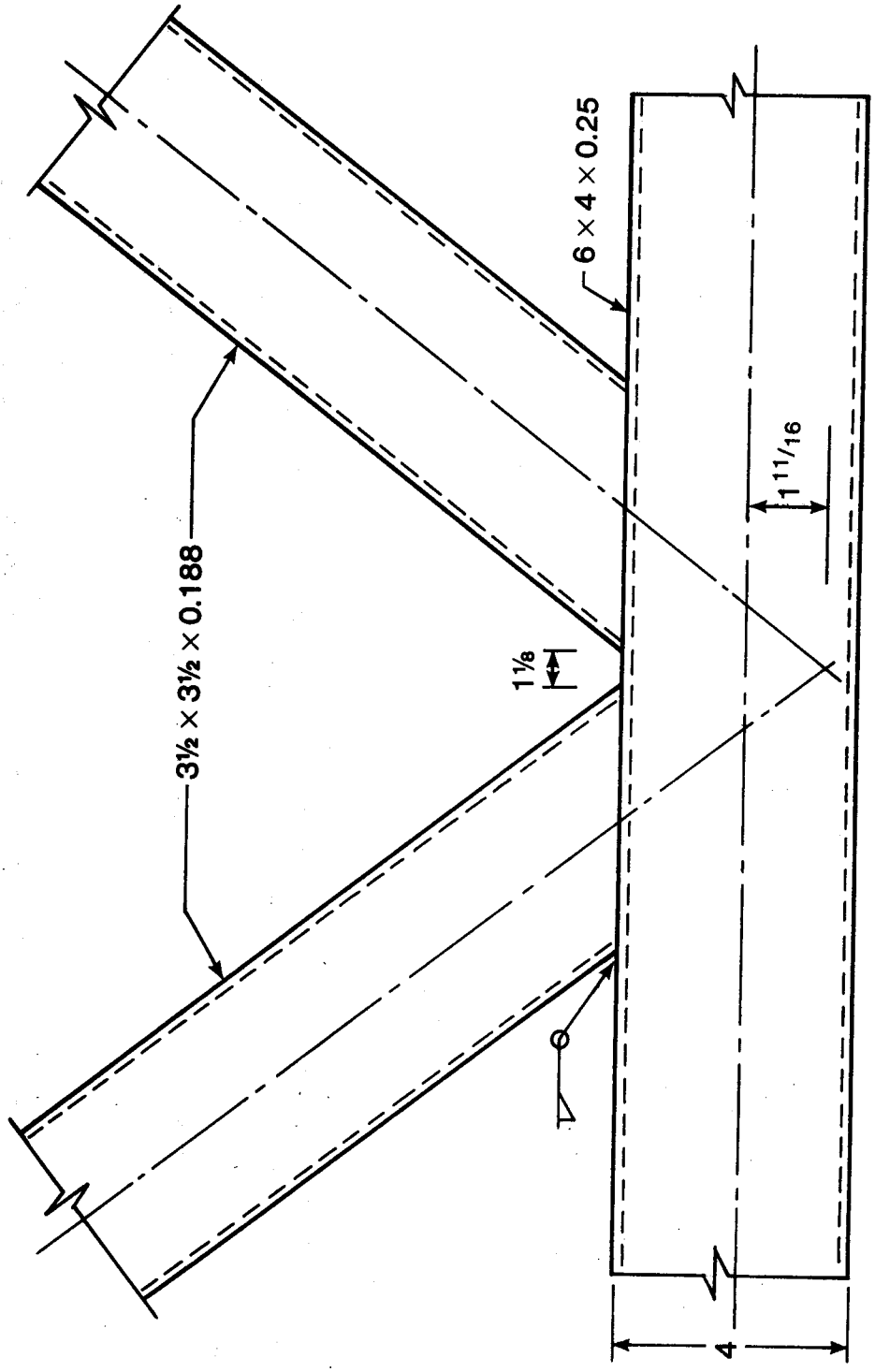

Figure 3.4 Detail of Gap Joint L1 (Series 3)

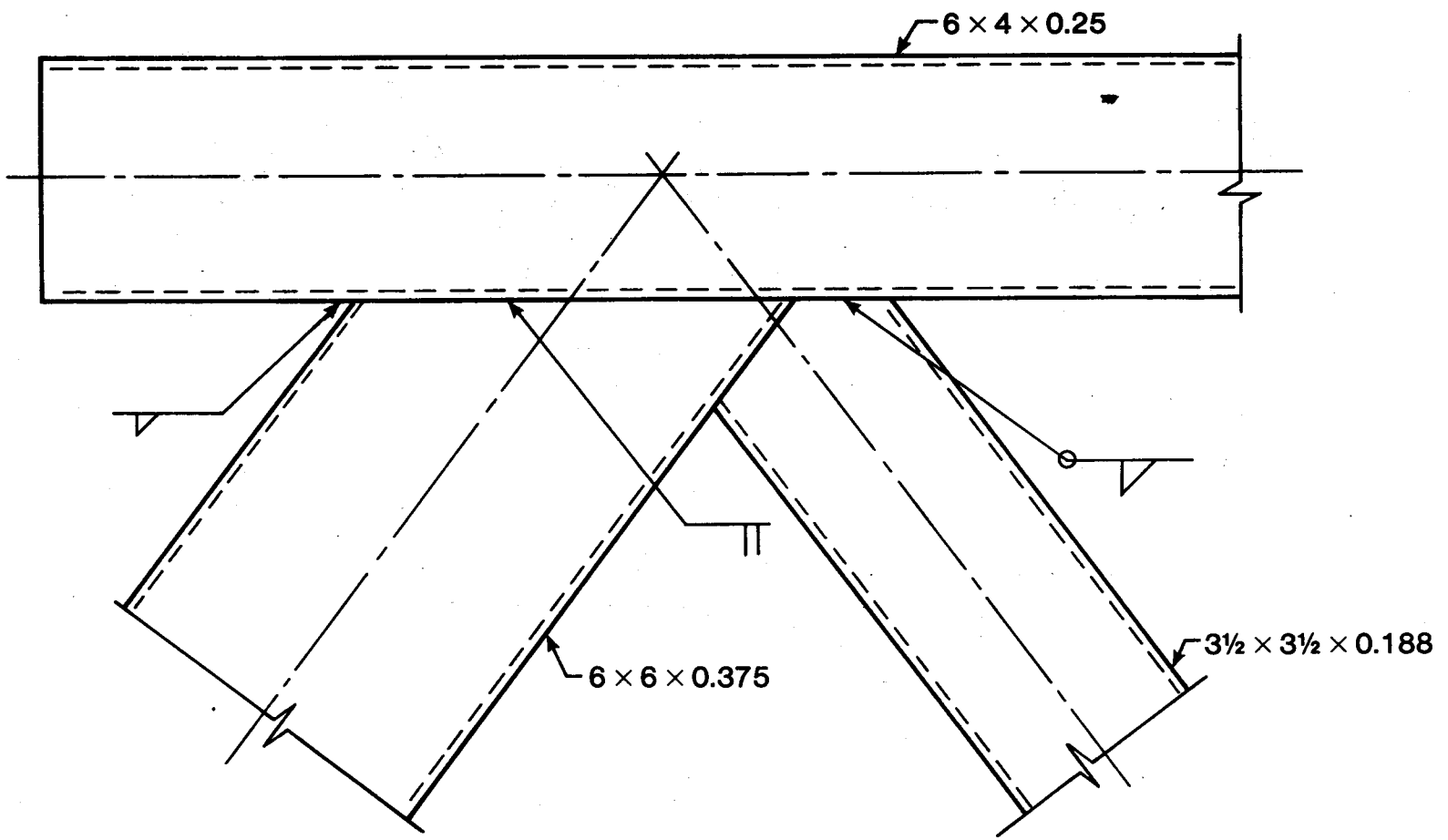

Figure 3.5 Detail of Overlap Joints U1 and U2
(Series 1 and 2)

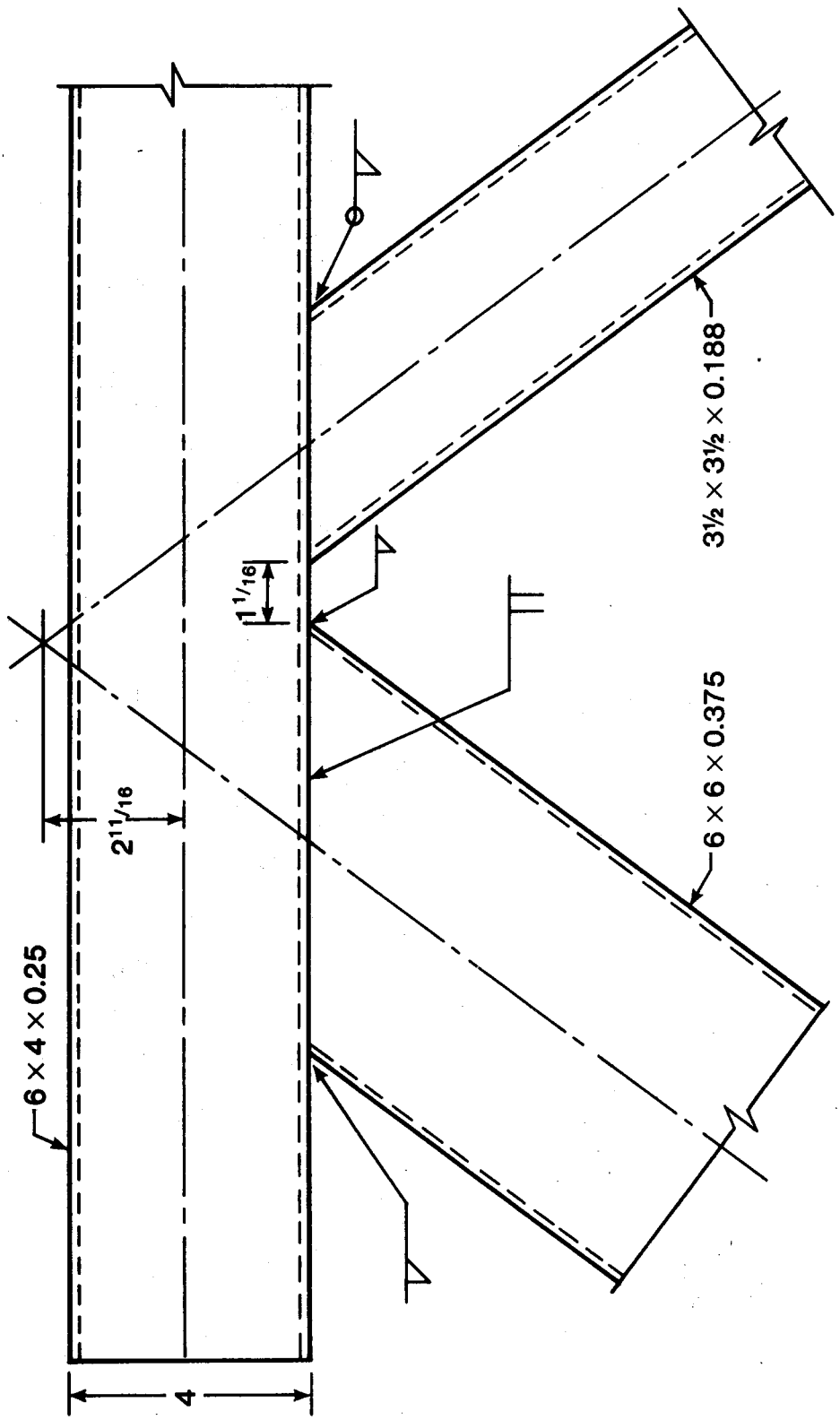

Figure 3.6 Detail of Gap Joints U1 and U2 (Series 3)

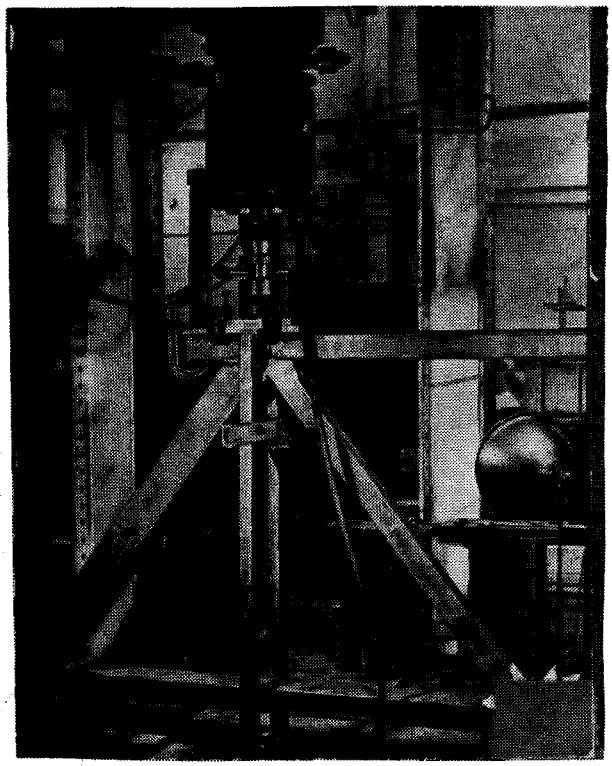

Figure 3.7 Test Set-up

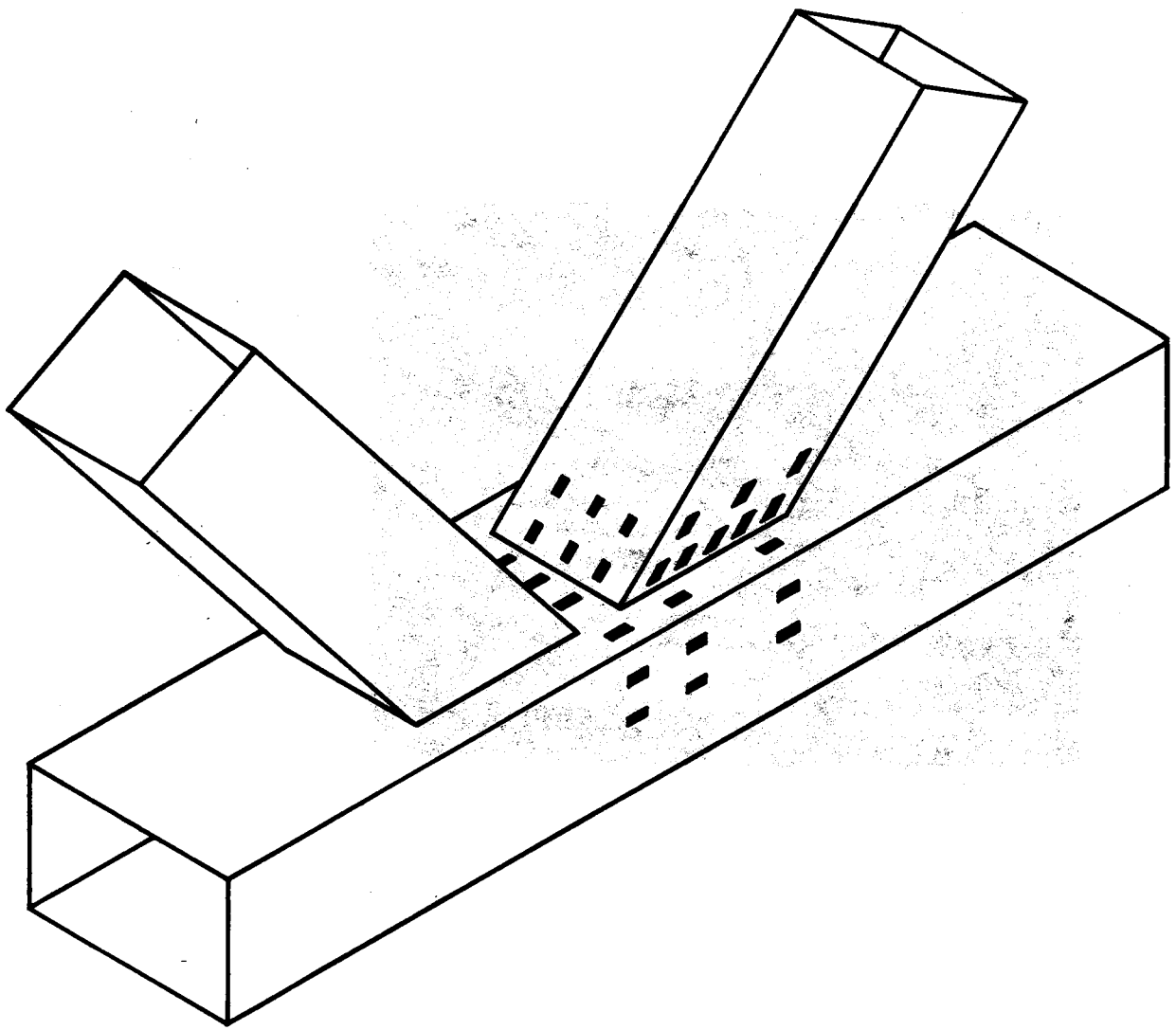

Figure 3.8 Strain Gauge Pattern for Gap Joint L1 (Series 3)

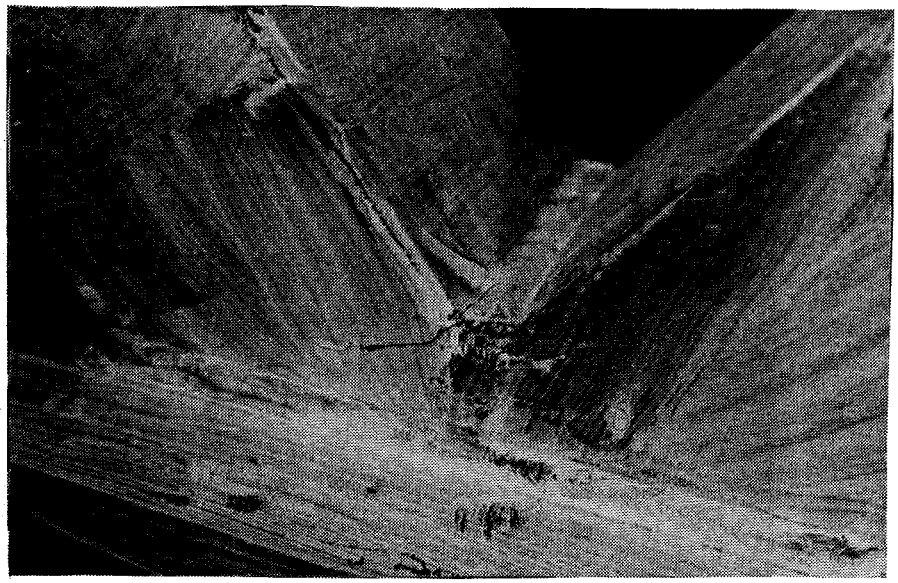

Figure 3.9 Fatigue Crack in Joint L1 (T2F)

Figure 3.10 Fatigue Crack in Joint L1 (T2F)

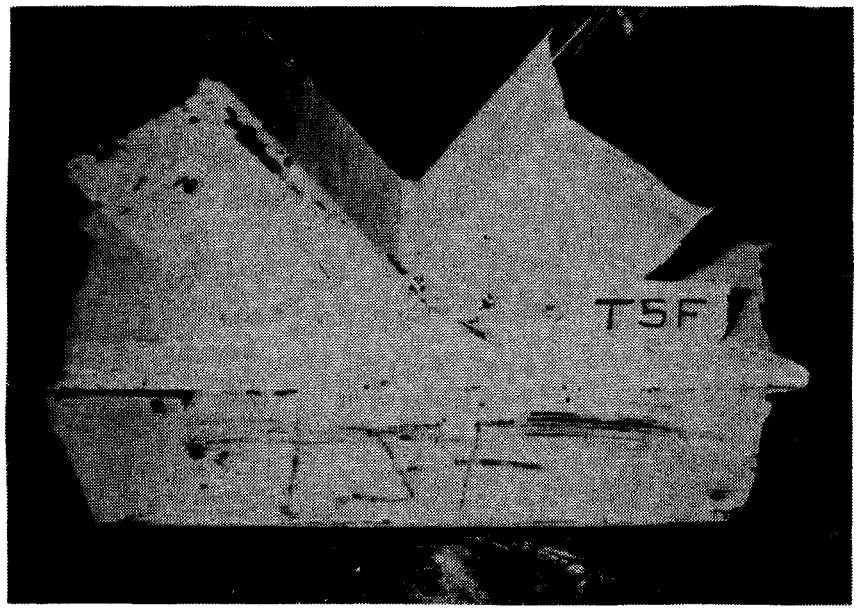

Figure 3.11 Fatigue Crack in Joint L1 (T5F)

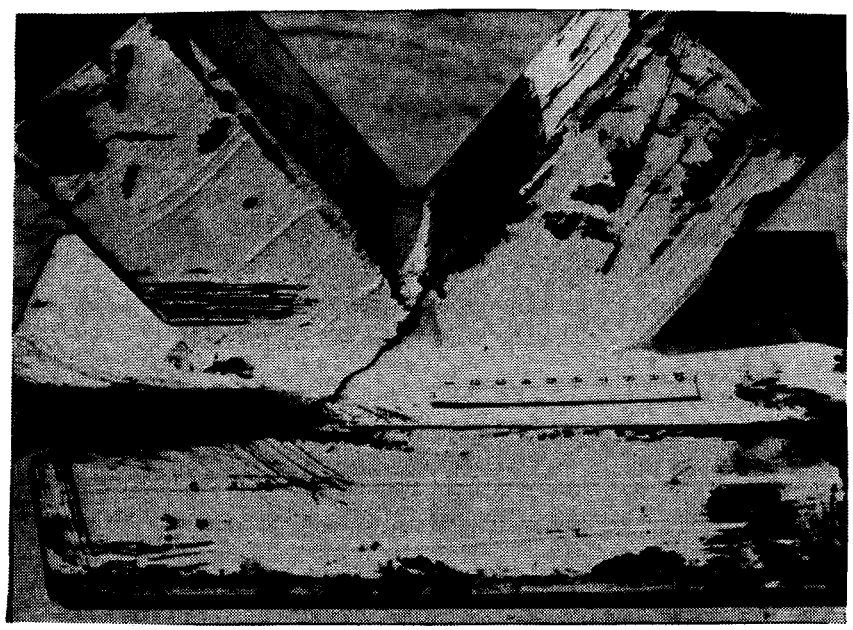

Figure 3.12 Fatigue Crack in Joint L1 (T7F)

Figure 3.13 Fatigue Crack in Joint L1 (T8F)

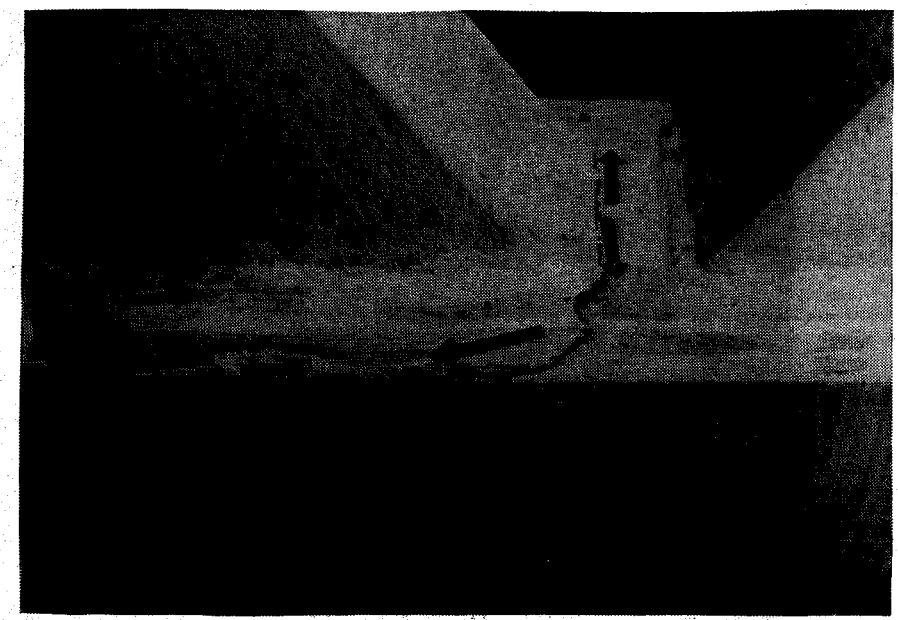

Figure 3.14 Fatigue Crack in Joint L1 (T10F)

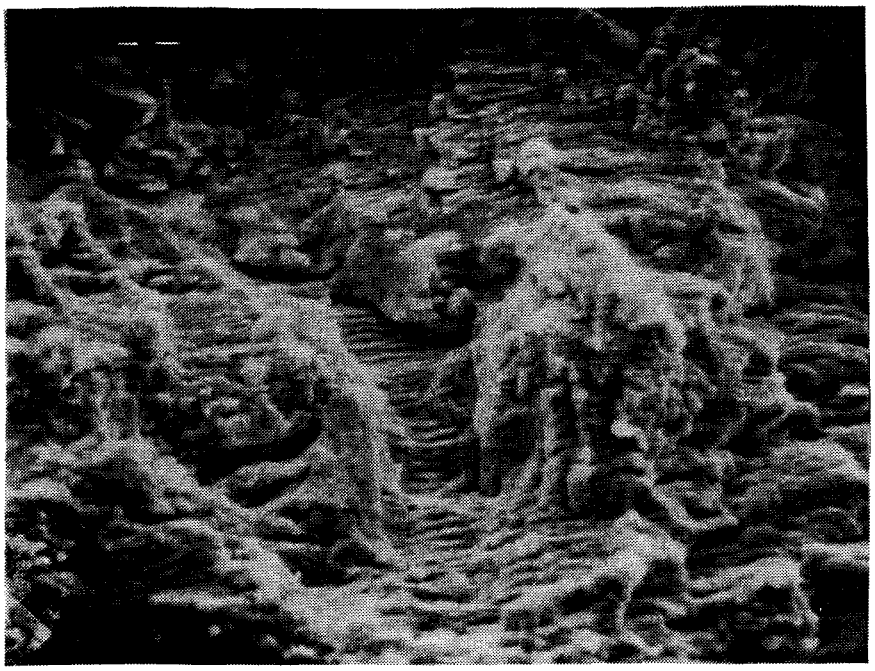

Figure 3.15 Fatigue Striations in Fatigue Crack found in Joint L1 (X3000)

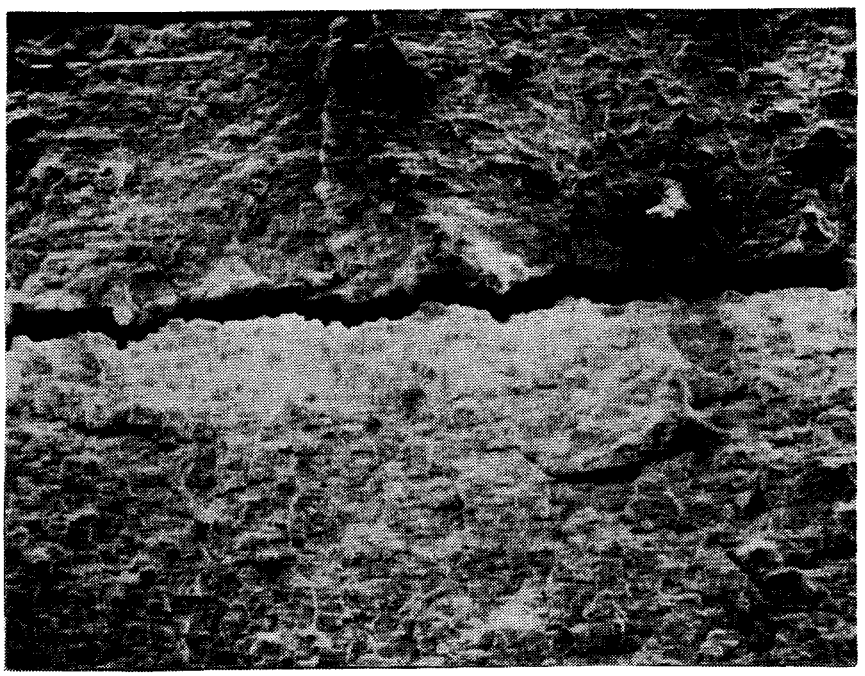

Figure 3.16 Crack in Chord Wall of Specimen T8F (X100)

4. Discussion of Test Results and Finite Element Analysis

4.1 Introduction

The growth of fatigue cracks within a structure has been shown to be strongly dependent upon the number of cycles of applied load, and upon the stress range created in various components of the structure by this load. The intensity and distribution of stresses within an HSS joint are a function of both the joint geometry and the forces and moments present in the members which frame into the joint. In order to compute these forces, a general analysis of the entire structure must be undertaken. Such an analysis will, in turn, depend on the geometric and stiffness properties assigned to individual joints.

Most of the fatigue testing of HSS joints has been conducted on isolated specimens under the influence of axial loads. This loading condition corresponds to the member forces that would be obtained from the analysis of a structure using the assumption of pinned connections. Obviously such an analysis disregards the presence of bending moments and shears which exist in real structures due to joint fixity. The effect of these "secondary" moments and shears on fatigue life may be an important consideration. Thus, in this study an attempt was made to theoretically predict secondary moments and shears in the truss specimens and to verify these predictions with

experimental measurements.

Given a set of forces and moments, the stresses within an HSS joint are dependent on a variety of geometric parameters, as discussed in the literature review. Because there has been little work published regarding the elastic stress distribution in RHS joints, it was decided to analyze both the overlap and gap K-type joints using a numerical technique, namely the finite element method. By control of the input model forces to the finite element model it was possible to observe the relative contributions of shear, moment, and axial force to the hot spot stresses. In addition, predicted stresses were compared to measured stresses at several locations in both joint configurations.

Finally, the fatigue life of the truss specimens was compared to published data for isolated joints, and fatigue life estimates based on stresses predicted by the finite element method were compared to experimental results.

4.2 Static Behavior of Truss Specimens

4.2.1 Member Behavior

In order to predict member forces and moments, the trusses were analyzed using PFT, a direct stiffness program developed by staff in the Department of Civil Engineering, University of Alberta. This program requires that the trusses be idealized as an assemblage of beam elements,

which are defined by the specification of 'i' and 'j' nodal points. These nodal points were considered to fall on the centrelines of the truss members. The geometry of all PFT models used can be seen in Figs. 4.1 and 4.2. Fig. 4.1 applies to the overlap joint truss specimens (Series 1 and 2). In Model 1 the joints are pinned while in Model 2 the joints are considered rigid. Models 3 and 4 are idealizations of the gap joint trusses, Fig. 4.2. Model 3 assumes that all joints are rigid while Model 4 has pinned interior web members with the remainder of the members continuous. Finally, Model 5 has continuous chords and pinned web members.

The loading condition in all PFT models was a single vertical load directed through the intersection point of the centrelines of web members L0-U1 and L1-U1. This corresponds to the actual static and dynamic loading point of the truss specimens. Output from the PFT program includes member shears, moments, and axial forces and these can, if desired, be converted to stresses. The results of the PFT analysis will be discussed later in this section.

Strain gauges were placed on several truss specimens in order to compare predicted axial forces and stresses with experimental values. Series 1 trusses had strain gauges applied at the mid-length of each member. The gauges were located at the centre of each of the four faces of the member. Strain readings were taken at several load levels up to a maximum of 100 kips. The readings were then used to

calculate nominal axial forces. To determine bending stresses (in addition to axial stresses) for Series 3, the gap joint specimens T9F and T10F had complementary strain gauges placed on the out-of-plane faces of each member at approximately the quarter points. Gauges were also placed at positions corresponding to the boundary sections of the finite element model of the gap K-type joint. This enabled model loads computed from actual strain readings to be used as input for the finite element analysis. In this test series, load was applied in increments of 10 kips up to a maximum of only 60 kips in order to avoid any inelastic behavior. The strain reading at the quarter points were converted to stresses and these were, in turn, converted to shears, moments, and axial forces.

The nominal axial forces as computed by the PFT stiffness program and as measured in the tests are presented for both overlap and gap joint truss types in Tables 4.1 and 4.2. The results show that all PFT models give similar results for axial forces. In addition, these forces are in reasonable agreement with those obtained from strain measurements. It can be seen that, in most cases, experimental and predicted forces differ by less than 10%. It may also be noted that experimental values are consistently lower than the pedicted values. The explanation for this is not readily apparent but may be linked to calibration of the test equipment. Axial forces in the interior web member L1-U1 and L1-U2 of Series 3

specimens appear to be proportionally lower than other member forces. This may be attributed to the fact that the ends of the interior web member are connected to the relatively flexible chord wall faces. This flexibility would tend to reduce the amount of load carried by the inside diagonals and increase the forces and moments carried by the outside members since these are more rigidly connected by their stiff sidewalls.

The experimental bending moments, which were measured only for Series 3, are compared to those predicted by PFT Model 3 in Figs. 4.3 through 4.9. It is evident from an examination of these figures that although bending moments are predicted accurately for some members, large differences are apparent for others. In general, it may be concluded that while the direction and relative distribution of bending moments and shears in the truss structure may be obtained from an analysis using PFT or a similar simple stiffness program, significant error in the magnitude of these moments can occur. A major source of error may be traced to assumptions which oversimplify the structural behavior of the truss joints. In the PFT analysis, joints are idealized as either pinned or fully rigid and are assumed to be located at the intersection of member centrelines. In fact, the stiffness properties of a real joint are complex and certain amounts of relative rotation and axial displacement may occur between the members forming the joint. The properties associated with each joint will,

of course, influence the overall behavior of the truss. For example, as was mentioned earlier, the relatively flexible nature of the chord face may have reduced the axial loads in the interior web members.

It is not likely that a simple stiffness program such as PFT could be easily adapted to predict, with high accuracy, the shears and moments in a general RHS structure. Such an analysis could best be accomplished by a finite element analysis of the entire structure or, alternately, by the derivation of stiffness properties for typical joints, also by applying the finite element method, and the use of these substructures in a stiffness program such as PFT. Such an approach was considered beyond the scope of this study.

The need for determining secondary moments and shears in the design RHS structures depends, of course, on their influence on ultimate or fatigue strength. If the structure can be designed on the basis of axial forces alone, then, as is evident from Tables 4.1 and 4.2, an analysis based on PFT or a similar program is adequate. However, if secondary moments are significant, as is likely the case with gap joint trusses (53), then some estimate of their magnitude must be attempted. This could be accomplished by the finite element method, as discussed earlier, or, for the purpose of ultimate design, it has been suggested that moments can be computed and proportioned to RHS truss members according to axial forces and joint eccentricities (34).

The magnitude of the stresses created by the secondary moments measured in the Series 3 truss specimens appeared to be significant. Table 4.3 gives the maximum measured bending stress for a given member as a percentage of nominal axial stress. If the experimental moments shown in Figs. 4.3 through 4.9 are extrapolated to the member ends, then even larger stresses could be expected. Thus, for the Series 3 trusses, stresses due to secondary moments were possibly an important factor in fatigue life. Bending stresses for Series 1 and 2 were not measured. However, these stresses were probably small compared to those developed in Series 3 because of the overlap condition and zero joint eccentricity. Because a testing program on isolated joints was not undertaken, it was not possible to experimentally separate the effect of axial forces and bending moments on hot spot stresses. However, a finite element model was used to examine the effect of various member moments, shears, and axial forces on the stress intensity and distribution within both the overlap and gap K-type joint.

4.2.2 Stress Within the K-Type Joints

Before testing was begun it was anticipated that the K-type joint, L1, would be the critical joint with respect to fatigue for all three test series. This was confirmed by experiment, since six of nine specimens failed at this location. An attempt was made to determine the stress

distribution in the K-type joints both experimentally and by use of the finite element method. The crack growth process was studied to see if cracks initiated and grew in areas where high stresses were predicted.

The finite element analysis was undertaken using the SAPIV program (59). The element selected from the program library for this analysis was the "type 6" thin shell and plate element developed by Clough and Felippa (19). The type 6 element is a quadrilateral of variable geometry having five local degrees of freedom associated with each of its four nodes. A sixth degree of freedom, rotation about a normal to the element's surface, does not have an associated stiffness term. Therefore, for flat plate structures, it is necessary to suppress this rotation or add a type 7 spring element to avoid numerical difficulties. Type 7 elements were also used to provide support conditions for both isolated joints.

The finite element idealization included three mesh sizes for the gap joint and two mesh sizes for the overlap joint. The medium sized mesh for the gap joint is illustrated in Fig. 4.10. This figure shows that because of symmetry considerations it was only necessary to model one-half the joint. The assumption used here was that no torsional or out-of-plane loading occurred, an assumption consistent with the symmetrical nature of the truss and the applied loads. In order to enforce the symmetry condition, one translational and one rotational degree of freedom were

suppressed along the plane of symmetry.

The output from the SAPIV program was in the form of nodal displacements, element membrane stresses, and element bending and twisting moments. To aid in assessing the stress distribution throughout the joint, a program was written to convert this output into principal stresses and directions. Another program was written to convert the SAPIV output into strains in any specified direction. This enabled theoretical strains to be compared to experimentally measured strains.

4.2.2.1 Results of the Finite Element Model Study

Loading of the finite element model could be achieved by specifying either nodal displacements or nodal forces. It was found that force loading was the most convenient method for this study. Fig 4.11 shows the various load cases considered for all models. A brief description of the significance of each load case follows.

Load case 1 represents nominal axial loading for the lower joint, L1, as might be expected from a pinned joint analysis of the truss. If a similar joint occurred in the upper chord of a truss, then the web forces would be identical but the chord would be in compression rather than tension. This is modelled in load case 2 and it corresponds to past testing of virtually all isolated joints, which have precompressed chords. While precompression of chords may be a conservative condition in ultimate static tests where

buckling is likely, it is not so in fatigue tests, where tensile stresses are important. Thus, a comparison of the hot spot stresses for load cases 1 and 2 would indicate whether the practice of chord precompression, which has been the experimental procedure in a large number of tests (9,26), may be unconservative in the prediction of fatigue life. Load cases 3 and 4 isolate the effect of bending in the joint produced by shears or secondary moments in the truss members. The fifth load case uses shear, moment, and axial forces obtained from a PFT analysis for input at the boundary sections of the finite element model. Finally, load case 6 uses experimentally measured shears, moments, and axial forces as input for the gap joint model, rather than the theoretical values predicted from PFT analysis.

Comparison of the output from load cases 1 and 2 shows that chord precompression has a significant effect on the stresses in the gap region of the gap joint. When the chord forces were changed from compression to tension, maximum principal tension stresses in the most highly stressed elements of the gap were increased by a factor of approximately 1.4 . This suggests that if the stresses in this region are critical in the growth of cracks, fatigue life may be overestimated when testing isolated joints with precompressed chords. Tests on complete C-C trusses by Maeda, et al. (32) appear to support this conclusion. In ten of fifteen truss specimens tested by Maeda, failure occurred in a joint on a lower tension chord. The remaining

five specimens failed at a joint on the upper compression chord. Except for the sign of the chord forces, these joints were identical. A comparison of load cases 1 and 2 for the overlap joint model did not show any appreciable difference in the intensity of stresses in hot spot locations. This is probably because the regions of high stress in the overlap configuration are not associated with membrane stresses in the chord face.

The state of stress in the gap joint, as indicated by principal stresses on an element, was very similar for load cases 5 and 6 (load case 5 was obtained from a PFT analysis, while load case 6 used experimentally measured input stresses). The similarity of results is surprising since the input forces and moments for the two load cases were somewhat different. It is probable that the smaller axial loads of load case 6 were compensated for by larger input moments. Thus, while in this particular case a PFT analysis led to stresses similar to those obtained using experimentally measured forces and moments, such a result should not be expected in general.

Load case 6 was felt to be a realistic representation of the actual gap joint loading. When this case was duplicated by superimposing shear, moment and axial force load cases, it was found that shear and moment, that is, load cases 3 and 4, contributed up to 37% of the bending stress in hot spot locations. Since bending was the largest contributor to stress within elements in these regions, this

means that secondary shears and moments are significant sources of hot spot stress. A comparison of principal stresses in the gap region for load cases 2 and 6 shows that bending moments and shear increased the principal tension stress by a factor of approximately 1.45. This increase is important in view of the strong dependence of fatigue life on stress range. Stresses in other hot spot regions were not significantly increased by the moment or shear loads of cases 3 and 4. For example, stresses at the heel of the tension member were actually reduced; however, an increase would be expected if the direction of these loads was reversed.

Because bending strains were not measured in the overlap gap truss specimens, it was not possible to determine the contribution of secondary moments and shears to hot spot stresses. However, due to the load transfer mechanism of the overlap joint (to be discussed later) and the zero eccentricity condition, it is unlikely that the magnitude of secondary shears and moments would be sufficient to cause significant stresses. A preliminary analysis with PFT also suggests that secondary moments would be very small. In addition, a study of the finite element model suggests that in the crotch of the joint, where fatigue cracks were known to initiate, stresses were not increased appreciably by bending moments in the web members if these moments are in the same direction. A PFT analysis indicates that the moments would be in the same direction.

4.2.2.2 Comparison of the Theoretical and Measured Strains

Strains within both the gap and overlap joints were determined experimentally by placing strain gauges on several test specimens. The strain gauge pattern for the gap joint is illustrated in Fig. 3.8. In two of the gap joint specimens, gauges were placed only where large stresses were expected, that is, at the toe of the tension member in the gap region of the chord. Strain readings for specimens T5F (overlap) and T8F (gap) are compared to strains predicted by the finite element model in Tables 4.5 and 4.6. It can be seen that agreement between predicted and measured strains is not particularly good, especially in regions of high strain, where predicted strains are much larger than those measured experimentally.

The differences between theoretical and experimental strains may be traced to two sources, difficulties associated with the measurement of real strains, and the use of a numerical model, ie. the finite element method, which does not exactly reproduce the behavior of the real joint. With regard to experimental measurement, the relatively large strain gauges used on the overlap joints and the gap joint, T8F, could not be placed any closer than approximately 3/8 inch away from the toe of a weldment. This prevented the measurement of high stresses which could be expected close to the weld (60). However, when small gauges, which could be placed closer to the weld toes, were used at the toe of the tension member in specimens T9F and

T10F, strains up to 1.3 times greater than those measured with large gauges were recorded. The difficulties associated with strain gauge size are also well illustrated by measurements taken in the gap region of the gap joint. The strains in the chord face change very rapidly across the gap and an inflection point is present at the centre of the gap. When large gauges, which spanned this point, were placed in the gap, low and erratic strains were recorded. However, when smaller gauges were used on subsequent specimens, large strains were measured, likely due to the fact that they did not cross the inflection point. In general then, it may be concluded that strain gauge readings tend to under-estimate the strains that occur in the region of weldments. Some investigators (8) have estimated strains by extrapolating a curve based on the readings of several in-line gauges. Such a technique was not considered in this study.

The description of joint behavior using the finite element model may depart from reality for several reasons. A possible source of error is one common to many finite element analyses; an assemblage of discrete elements is used to describe the behavior of a complex state of stress and strain. The error associated with this approximation depends on the ability of the element to represent the true displacement field and actual loading conditions. The 'type 6 ' element in the SAPIV library is considered reliable and has been shown to yield acceptable results in the past for

this type of problem. A more likely source of error is the mesh size of the joint models. Figs. 4.12 and 4.13 are plots of displacement versus number of equations used in the finite element analysis of the gap joint. The displacements were chosen at a boundary node on the compression web member and also at a boundary node on the chord. The plots indicate that, for overall behavior, the model appears to be rapidly converging, behavior that is consistent with a valid finite element analysis. However, this trend does not necessarily apply to local regions such as wall intersections, especially where stresses are concerned. In these regions a further refinement of mesh size would be required to account for local geometry.

It is not clear whether refinement of the finite element mesh would result in higher or lower stresses in the region of hot spots. As a wall intersection is approached the intensity of stresses tends to increase rapidly and since the finite element stress output is an average value for an entire element, smaller elements close to the wall would tend to record larger stresses. However, in this particular model it is also possible that increasing the number of elements might alter the load carrying characteristics of the joint, possibly reducing stresses.

Another source of error in the finite element analysis may be associated with its failure to model weldments. Fig. 4.14 illustrates the intersection of the toe of the tension web member and the chord for the gap joint, as

actually fabricated and as is idealized by the finite element model. In this example the additional material furnished by the weld provides a more gradual transition from the chord to the web, tending to reduce stresses in the vicinity of the chord wall to web wall intersection. In addition, the presence of fillet welds on either side of the gap segment in the gap joint would increase the stiffness of this region, likely leading to a reduction of stresses. In a similar way, the finite element model does not account for the stiffening effect of the fillet welds when considering transverse effects. For example the fillet weld reduces the span between the sidewall of the chord and the sidewall of the diagonal member. Thus load would tend to be carried more directly into the stiff sidewalls of the chord member, thereby reducing bending stresses in the chord face.

Large stresses can be expected at the tips of weldments. These stresses are confined to very small regions and are usually neglected in a general finite element analysis used to compute stress concentration factors. Such stresses can not be measured by conventional strain gauges and thus would not affect the comparison of measured strains to predicted strains in this study. Nevertheless, these very localized stress concentrations are usually the origin of fatigue cracks. Marshall (8) accounts for the local state of stress by assigning one stress concentration factor to the weld tip and another to the general region close to the weld toe. The latter is called

a "structural stress concentration" and can be obtained from a finite element analysis, strain gauge measurements, etc. The stress concentration factor at the weld tip , K_t , depends on weld profile and, based largely on experience, Marshall has proposed values ranging from 1.0 to 3.0 (Fig. 4.15). Analytical solutions for fillet welds which do not carry load are available and a typical value for a 45 degree weld is 2.0 (6).

4.3 Load Transfer Characteristics of K-Type Joints

4.3.1 General

Both the finite element model and actual strain readings are useful in describing the general behavior of the gap and overlap K-type joints. Observations of the initiation and growth were also valuable in identifying regions of high stress; naturally the load transfer mechanisms changed as cracks propagated.

4.3.2 Overlap Joint

Two regions of high tensile stress can be identified in the overlap joint, one located in the sidewalls of the web members near the crotch of the joint, the other at the heel of the tension member and extending into both the chord face and the web member sidewalls (Fig. 4.16). The primary source of stress is different in both regions. At the

crotch, the web members tend to be much stiffer in their axial directions than in directions normal to their sidewalls and they are also stiffer than the top face of the chord. Thus, most of the axial force is transferred through the stiff vertical sidewalls, in the vicinity of the vertical groove weld. This region is one of high membrane stresses as illustrated in Fig. 4.17. On the other hand, high tensile stresses encountered at the heel of the web tension diagonal-to-chord intersection are primarily due to bending. The bending appears to be caused by the rotation of the stiff sidewalls with respect to the flexible upper face of the chord. This rotation, shown in Fig. 4.18, occurs despite the fact that the centrelines of all members intersect at a single point. The severe distortion of the chord face results in large curvatures and, hence, high bending stresses which tend to increase toward the heels of the joint. Curvatures are most pronounced at the corners of the heel where the chord face is flattened out in two directions. High bending stresses are also induced in the sidewalls of the web members near the heel of the joint since these elements were relatively stiff and compatibility of rotation with the chord face is maintained (Fig. 4.19). It was also observed that the membrane stresses in the out-of-plane faces at the joint heels were considerably reduced. This was probably caused by the axially stiff web member forcing the chord face to flatten out rather than curve or 'hump' directly beneath the web wall.

The behavior hypothesized above is based largely on the results of the finite element model of the joint. Experimental verification of the model was reasonably good in the crotch area of the overlap joint where membrane stresses predominated. For example, the maximum measured and predicted stress concentrations in this region were 2.17 and 2.70, respectively. However, in areas where high bending stresses were predicted by the finite element model, for example in the sidewall of the tension web member near the heel of the joint, measured stresses were not found to be large. As discussed in Section 4.2.2.2, this may be attributed to problems associated with experimental strain measurements, the presence of welds, or difficulties inherent in the finite element model.

During fatigue cycling, cracks initiated and grew in the groove weld region, as described in Section 3.5. Crack initiation and growth was also observed at the web tension diagonal-to-chord intersection at the heel of the joint. However, this occurred only after cracks in the groove weld region were well advanced. Thus, based on these observations, as well as strain gauge measurements, it appears that the finite element model significantly overestimates the stresses occurring in the heel region of the joint. Nevertheless, the model is useful in describing the load transfer mechanisms of the joint.

4.3.3 Gap Joint

The most obvious difference between overlap and gap joint configurations is that in the gap joint the stiff sidewalls of the diagonal web members are not connected. Thus, axial load from the web members is not transferred directly from one diagonal to the other; rather, the compression web diagonal pushes down into the flexible chord face while the tension web diagonal pulls the chord face upwards. This results in a severe distortion of the chord face, especially in the gap region (Fig. 4.20). The gap segment has an inflection point at the centre and large curvatures towards the toes of the web members, resulting in high bending stresses. From a fatigue standpoint the most serious of these bending stresses are tensile surface stresses which occur at the tip of the tension web member fillet weld. In addition to the gap region, bending stresses are found in the chord face along the web diagonal to chord intersection. As in the overlap joint, these stresses appear to be a result of curvatures caused by the displacement of the chord face by the axially stiff web members. Stresses are high at the corners of the joint where the chord is being flattened out in two directions. Bending stresses are also found in the sidewalls of the web members and are probably caused by the rotation of the chord face.

Bending moments in the diagonal web members are also important sources of stress within the gap joint. The

directions of experimentally measured moments cause the chord face to deflect in the manner shown in Fig. 4.21. When this load case is superimposed on the axial force case, (Fig. 4.20), it can be seen that deflections in the gap region will tend to increase while deflections at the heels of the tension and compression web member will decrease. This results in larger stresses in the gap region and smaller stresses in the chord and web walls towards the heels of the joint. Such behavior indicates that the state of stress in the joint depends on both the magnitude and direction of member moments.

In order to confirm that hot spot stresses in the gap joint were primarily a function of bending, the medium mesh model for the gap joint was rerun with the chord wall thickness reduced by one half. If the maximum stresses in the joint were directly related to bending then it was expected that reducing the wall thickness by one half would result in stresses roughly four times as great. Principal stresses in several highly stressed elements were computed and found to be 3.7 to 4.0 times greater than those in the original model, thus confirming the importance of bending.

Fatigue cracks in the gap joint specimens initiated and grew in the gap region, directly at the tip of the fillet weld connecting the tension web member to the chord. This corresponds to the region of highest tensile stress, as predicted by the finite element model and also as measured by strain gauges. Late in fatigue life cracks also grew

where the back corners of the tension web diagonal met the chord. The finite element analysis predicted that this would be a region of high tensile stress. However, it must be remembered that considerable cracking had occurred elsewhere in the joint by this time and therefore the load transfer mechanism of the joint had been altered.

4.4 Fatigue Strength Results

The initiation and growth of cracks in individual specimens was described in Chapter 3; Table 3.1 summarizes the stress range versus cycle life data for all three test series. The number of cycles at the time of both the first observable crack and final 'failure' are recorded in this table. The first observed crack, usually 1/4 to 3/8 inch long when discovered, would roughly correspond to a through crack in a simple welded plate test. Testing was not interrupted to determine when, in fact, the crack had penetrated the member wall. A through thickness crack is often used as a failure criteria in fatigue design; however, in this study final failure was assumed to have occurred when roughly 25% of the tension web member cross sectional area had been destroyed by cracking. The difference between these two criteria is small since the fatigue crack would be propagating extremely rapidly by the time it became a through crack.

Fig. 4.22 is a plot of nominal stress range in the tension member versus the number of load cycles to failure. All three test series are shown and data from isolated K-type joints tested by Mang and Striebel (61) also appear on the plot. Although the latter joints did not have the same dimensions as the specimens in this study, the important non-dimensional parameters were very similar, and a comparison was considered valuable. It can be seen that the isolated joint data generally plots above the data obtained from complete trusses, indicating that isolated joints may have a higher apparent fatigue resistance. This can be attributed to stresses caused by secondary bending in the truss specimens or perhaps to the fact that the isolated joints had precompressed chords. Although Mang does not state whether his specimens were precompressed, this has been the usual practice in most fatigue tests of HSS joints. The results of the finite element analysis of the gap joint in Section 4.2.2.1 revealed that measured bending moments could be expected to increase the principal tension stresses in the gap region by as much as a factor of 1.45. In addition, reversing the chord force from compression to tension increased tension stresses in the gap by a factor of 1.4. Since the slope of the Log Sr. v.s. Log N curve is approximately -4, the fatigue life is inversely proportional to the stress range raised to the fourth power, ie. $N = CSr^{-4}$. Hence, an increase of 1.45 could for example, result in a reduction of fatigue life of as much as $(1/1.45)^4 = 0.23$.

It should also be noted that Mang's tests were conducted under fully reversed load cycling, that is R=-1, while in this study the stress ratio in the tension web diagonal was always greater than zero. Thus, depending on the magnitude and distribution of residual stresses, it is possible that some portion of the reversed load may not have been damaging. This would, of course, lead to longer fatigue lives for Mang's specimens.

Fig. 4.23 presents the results of a linear regression analysis of Series 1,2, and 3. Because only a few data points were available for the analysis, the statistical significance of the lines is questionable. However, the analysis is useful for purposes of comparison. The Series 3 line (gap joints) and the lines for Series 1 and 2 (overlap joints) are separated by a distinct vertical distance, which represents a difference in stress range. This suggests that the hot spot stresses in the gap joints trusses were larger than those in the overlap trusses, a condition which was discussed in detail in Section 4.3. The slopes of the regression lines for the overlap truss specimens are -4.86 and -3.35 respectively, while for the gap trusses the slope is -6.30, indicating that the gap joint configuration may be more sensitive to stress range. The reason for this possible increased sensitivity is not clear. However, it is likely that the difference can be attributed to statistical scatter, since any significant change in slopes would reflect a change in fracture mechanism and material

properties, an unlikely occurence in this study. In any case an investigation as to the probable cause will have to await more data so that statistically valid regression lines can be established.

Inspection of Fig. 4.23 indicates that there is no significant difference in fatigue performance between hot rolled specimens (Series 1) and cold rolled specimens (Series 2). Any difference which does appear probably falls within the normal statistical scatter found in tests of this type. It is likely then, that the process of hot or cold rolling which affects the primary residual stress pattern is not an important factor when obtaining the fatigue strength of HSS joints.

The regression lines for both the overlap and gap joint trusses in Fig. 4.23 fall below the category F line, which was taken from the fatigue design recommendations of CSA S16.1 - M78 (5). Thus, if similar joints were to be designed strictly on the basis of nominal axial stress range, the results of this study suggest that two new fatigue categories would have to be considered. However, since every tubular joint offers a stress distribution peculiar to its own geometry, a nominal stress range versus life approach is not practical. Instead, the procedure most frequently followed is to use structural stress concentration factors in conjunction with fatigue curves that are based on simple test specimens. For example, the AWS curve 'X' (57), which was derived from tests on butt

welded plates, automatically takes into account extremely localized stress concentrations at the weld tip not considered in a finite element analysis. Increasing the stress range applied to these specimen types by stress concentration factors derived from a finite element analysis or another source simulates the stress condition in an HSS joint. It is also necessary to modify the method to include the effect of weld profile (8). This may be accomplished by further increasing the hot spot stress range by a factor, K_t . Values of K_t for several weld profiles are shown in Fig. 4.15. In this figure K_t values are relative to plain plate specimens rather than butt welded specimens.

Fig. 4.24 is a plot of modified stress range versus member of cycles to failure for all three test series. The modified stress range is the nominal stress range multiplied by a structural stress concentration factor. In this case, the stress concentration factors were taken from the finite element analysis for regions where cracking was observed to have started. No modification for weld profile was made since the welds appeared compatible with the AWS curve 'X' data (60). The data from Series 3 falls above curve 'X' in Fig. 4.24, indicating that the predicted stress range may be too large, that is, it would result in a conservative design. The data for Series 1 and 2 fall slightly below curve 'X', which suggests that for this joint configuration and weld profile the prediction is reasonably good but on the unconservative side.

There are several possible sources of error in the procedure outlined above. The structural stress concentration factors may not be accurate, as was discussed in Section 4.3. This is likely the case for the gap joint specimens where strains predicted in the gap region by the finite element method were much larger than measured strains. Much better values were obtained for the crotch region of the overlap joint. This is reflected by Fig. 4.24, where modified overlap joint data falls much closer to curve 'X' than modified gap joint data.

Another source of error may be the influence of weld profile; the fillet weld in the test specimens may have represented either a more or less severe condition than the butt weld used in the AWS curve 'X' specimens. Furthermore, for both the overlap and gap type joints, a significant portion of the fatigue life involved crack growth within weld metal or material otherwise affected by the welding process. The metallurgical properties of this material would not be exactly reproduced in the specimens used to generate the AWS curve 'X'. In regard to differences in weldments, Rodabaugh (60) did not attempt to modify data from C-C joints when using curve 'X'.

Finally, although the magnitude of the hot spot stress range can be approximated using stress concentration factors and applied to data from simple specimens, this is not an accurate description of the state of stress which occurs in the joint, since as the crack propagates, it will move into

regions where the stress and stress gradient is different from that of a simple specimen. In addition, changes in load transfer due to crack growth will not be the same in an HSS joint as in a simple plate specimen.

Rodabaugh (60) plotted fatigue data for C-C gap K-joints from several sources in a manner similar to Fig. 4.24. Stress concentration factors developed by Potvin et al. (21) were used to estimate hot spot stresses. It was found that the data fell above the AWS curve 'X' for all but low cycle fatigue, suggesting that the method is conservative.

Table 4.1 Axial Forces for Series 1 and 2, Load = 56 kip

MEMBER	PFT-1 (kip)	PFT-2 (kip)	MEASURED (average) (kip)
U1-U2	-21.0	-20.8	-18.5
L0-U1	-52.5	-52.2	-47.3
L1-U1	-17.5	-17.1	-14.7
L1-U2	17.5	16.8	15.2
L2-U2	-17.5	-17.5	-15.0
L0-L1	31.5	31.1	26.3
L1-L2	10.5	10.7	7.5

Table 4.2 Axial Forces for Series 3, Load = 56 kip

MEMBER	PFT-3 (kip)	PFT-4 (kip)	PFT-5 (kip)	MEASURED (average) (kip)
U1-U2	-22.1	-22.0	-21.1	-20.4
L0-U1	-52.8	-52.7	-52.8	-50.3
L1-U1	-17.5	-17.7	-17.8	-15.2
L1-U2	17.2	17.2	17.5	15.2
L2-U2	-18.1	-18.3	-17.7	-17.0
L0-L1	32.4	32.5	31.7	29.0
L1-L2	11.6	11.8	10.7	10.3

Table 4.3 Maximum Measured Bending Stress as a Percentage of Nominal Axial Stress

MEMBER	STRESS (% of axial)
U1-U2	85
L0-U1	17
L1-U1	33
L1-U2	21
L2-U2	110
L0-L1	19
L1-L2	48

Table 4.4 Location of Strain Gauges for Tables 4.5 through 4.8

LOCATION	DESCRIPTION
1	sidewall of tension web near crotch of joint
2	sidewall of tension web near centreline of member
3	sidewall of tension web near heel of member
4	out-of-plane face of tension web near crotch of joint
5	out-of-plane face of tension web near heel of joint
6	sidewall of tension web, 6" from crotch of joint
7	out-of-plane face of tension web, 6" from crotch
8	sidewall of chord member near centreline
9	chord face near heel of tension web member
10	web member corresponding to boundary of F.E. model
11	top face of chord close to gap region
12	directly at toe of tension web member
13	within gap region of chord face

Table 4.5 Measured and Predicted Strains for Overlap Joint T5F, Load = 63.8 kip

GAUGE	ELEMENT	MEASURED ($\times 10^{-3}$)	PREDICTED ($\times 10^{-3}$)	$\frac{\text{PREDICTED}}{\text{MEASURED}}$	LOCATION
23	510	0.6800	0.7390	1.09	1
24	518	0.3970	0.4981	1.25	1
25	520	0.3764	0.3689	0.98	1
26	523	0.2870	0.4369	1.52	2
27	526	0.2752	0.5858	2.12	3
45	482	0.5036	0.2011	0.40	4
36	543	0.1637	0.0852	0.52	5
37	543	0.1830	0.0852	0.47	5
28	567	0.3295	0.2506	0.76	6
29	566	0.2537	0.2568	1.01	6
30	564	0.1779	0.2622	1.47	6
43	563	0.3586	0.2477	0.69	7
44	563	0.3524	0.2477	0.70	7
16	110	0.0947	0.1370	1.45	8
17	106	0.1301	0.1702	1.31	8
20	250	0.1520	0.1124	0.74	8

Table 4.6 Measured and Predicted Strains for Gap Joint T8F, Load = 53.3 kip

GAUGE	ELEMENT	MEASURED ($\times 10^{-3}$)	PREDICTED ($\times 10^{-3}$)	PREDICTED / MEASURED	LOCATION
51	256	0.1381	0.3021	2.19	9
44	262	0.1699	0.3311	1.95	9
43	264	0.1687	0.1288	0.76	9
17	344	-0.1366	-0.1737	1.27	10
16	347	-0.2880	-0.3088	1.07	10
40	439	-0.9119	-0.0360	0.04	5
25	475	0.3283	0.4384	1.34	4
27	477	0.2179	0.2698	1.24	4
37	513	0.2983	0.4771	1.60	1
31	515	0.2925	0.2647	0.91	1
34	517	0.4621	0.5025	1.09	1
33	523	0.2227	0.2528	1.14	1
38	525	0.4659	0.5687	1.22	3
36	533	0.3842	-0.0427	----	3
35	535	0.1484	0.1759	1.19	3
39	541	-0.0455	0.4690	----	5
7	602	0.1444	0.1877	1.30	10
9	605	0.2707	0.2966	1.10	10
57	608	0.1229	0.1424	1.16	8
55	609	-0.0716	0.2616	----	8

Table 4.6 continued

48	630	0.0790	0.1137	1.44	11
54	631	-0.0186	0.1012	----	11
53	648	-0.0589	0.3222	----	8
49	650	0.3719	0.5973	1.61	11
28	663	0.8473	1.1180	1.32	12
30	664	0.7458	1.4780	1.98	12
32	665	0.3917	1.2200	3.11	12
29	475	0.3116	0.4384	1.41	7
44	262	0.1737	0.3311	1.91	9
41	541	-0.0148	0.4690	----	9
26	664	0.7748	1.4780	1.91	12

Table 4.7 Measured and Predicted Strains in Gap Region for Gap Joint T9F, Load = 53.3 kip

GAUGE	ELEMENT	MEASURED ($\times 10^{-3}$)	PREDICTED ($\times 10^{-3}$)	$\frac{\text{PREDICTED}}{\text{MEASURED}}$	LOCATION
49	635	0.8920	1.4530	1.63	13
50	633	1.1940	1.1900	1.00	13
51	635	0.8574	1.4530	1.69	13
53	662	1.0600	1.0870	1.03	12
54	663	1.0000	1.1180	1.12	12

Table 4.8 Measured and Predicted Strains in Gap Region for Gap Joint T10F, Load = 53.3 kip

GAUGE	ELEMENT	MEASURED ($\times 10^{-3}$)	PREDICTED ($\times 10^{-3}$)	$\frac{\text{PREDICTED}}{\text{MEASURED}}$	LOCATION
55	635	0.5070	1.4530	2.87	13
56	633	0.4980	1.1190	2.39	13
57	635	0.6112	1.4530	2.38	13
58	663	0.8260	1.1180	1.35	12
59	662	0.9335	1.0870	1.16	12
60	663	0.8767	1.1180	1.28	12

Table 4.9 Linear Regression Analysis for Test Series 1, 2 and 3

SERIES 1	Log N = 8.50 - 3.35 Log Sr
SERIES 2	Log N = 9.81 - 4.86 Log Sr
SERIES 1 & 2	Log N = 9.39 - 4.41 Log Sr
SERIES 3	Log N = 10.08 - 6.30 Log Sr

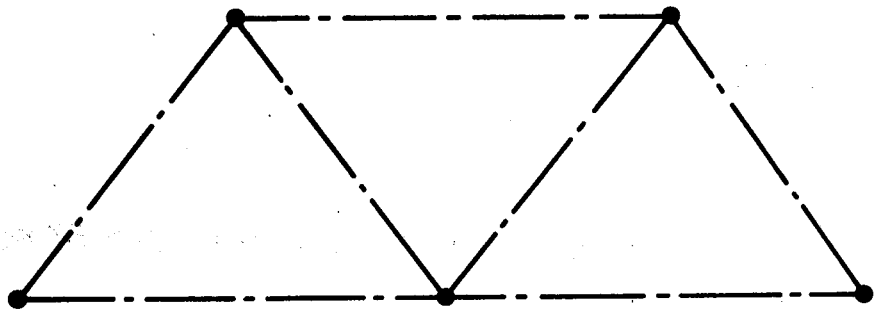

Figure 4.1 Geometry for PFT Models 1 and 2

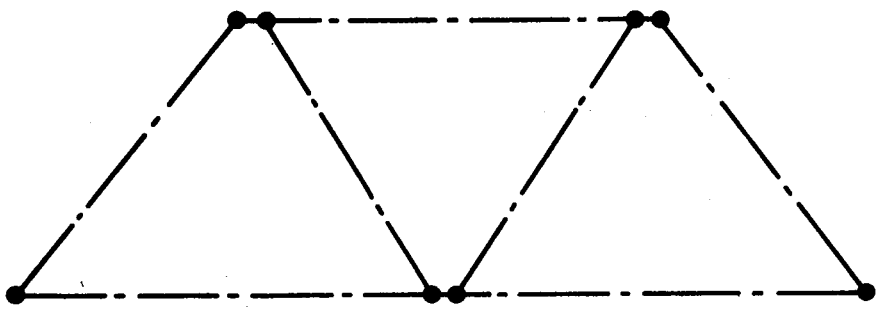

Figure 4.2 Geometry for PFT Models 3, 4 and 5

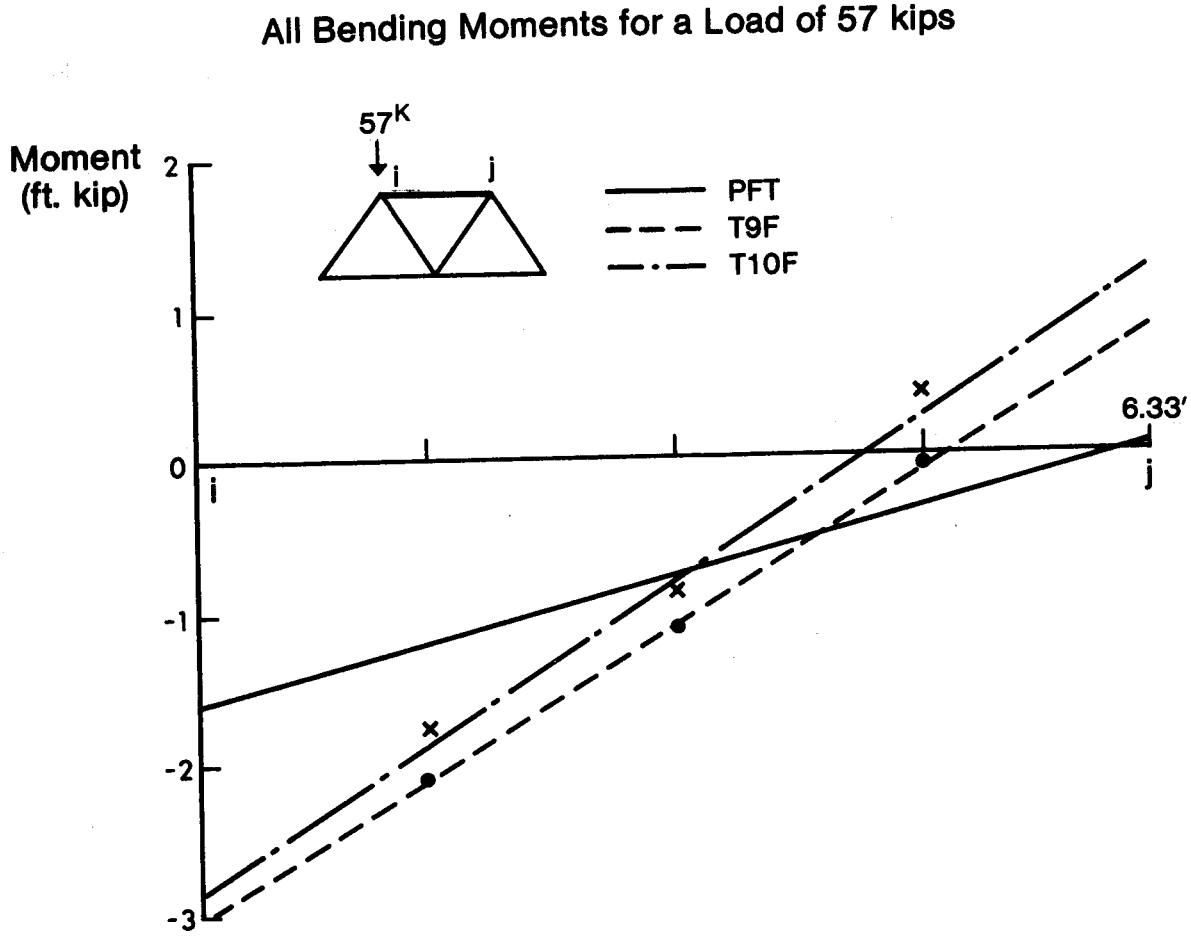

Figure 4.3 Bending Moments for Member U1-U2

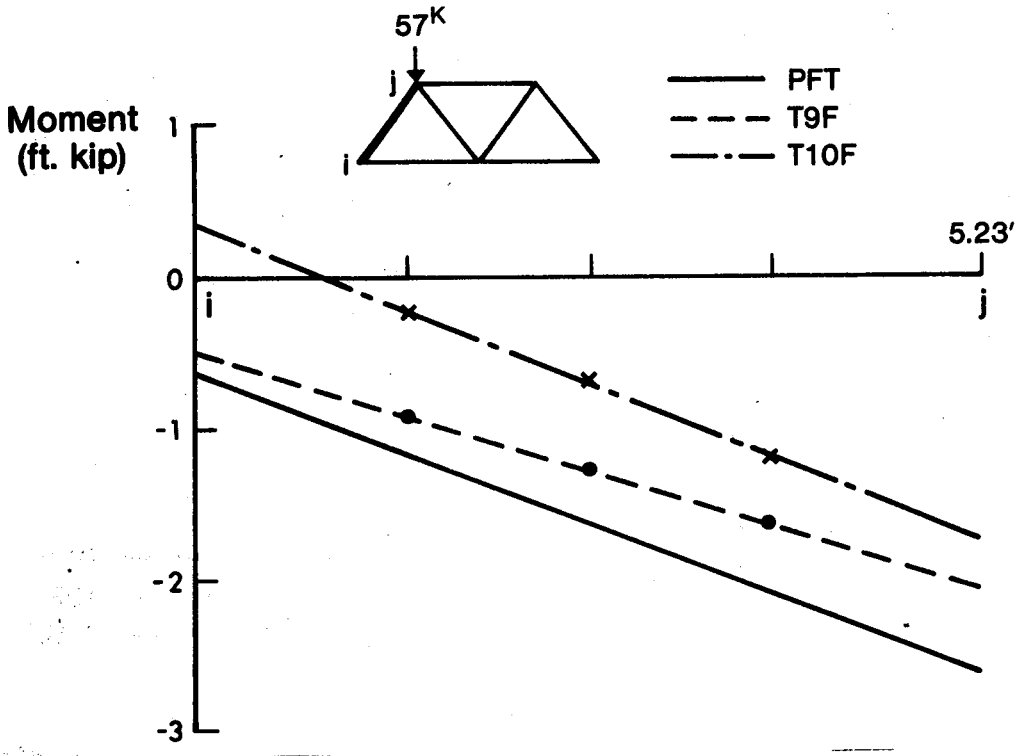

Figure 4.4 Bending Moments for Member L0-U1

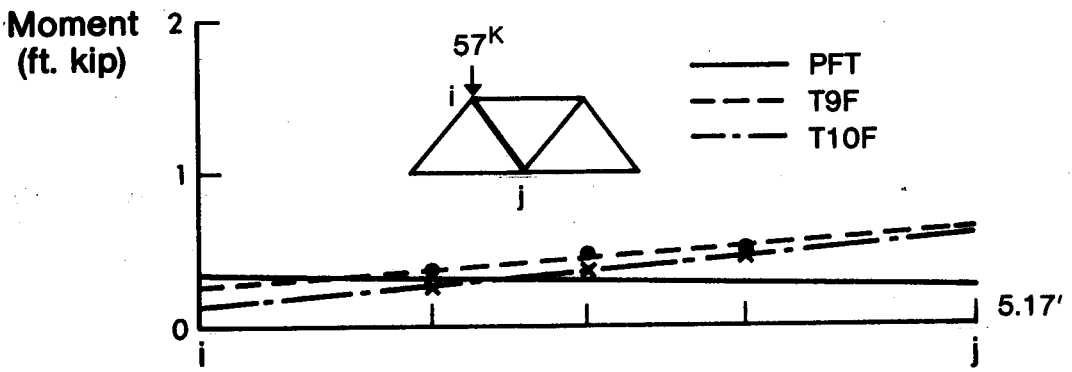

Figure 4.5 Bending Moments for Member L1-U1

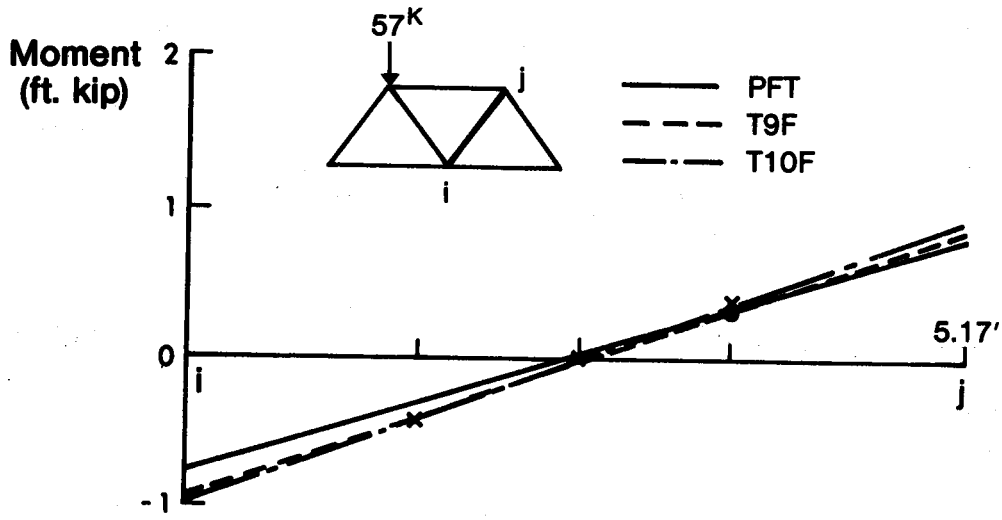

Figure 4.6 Bending Moments for Member L1-U2

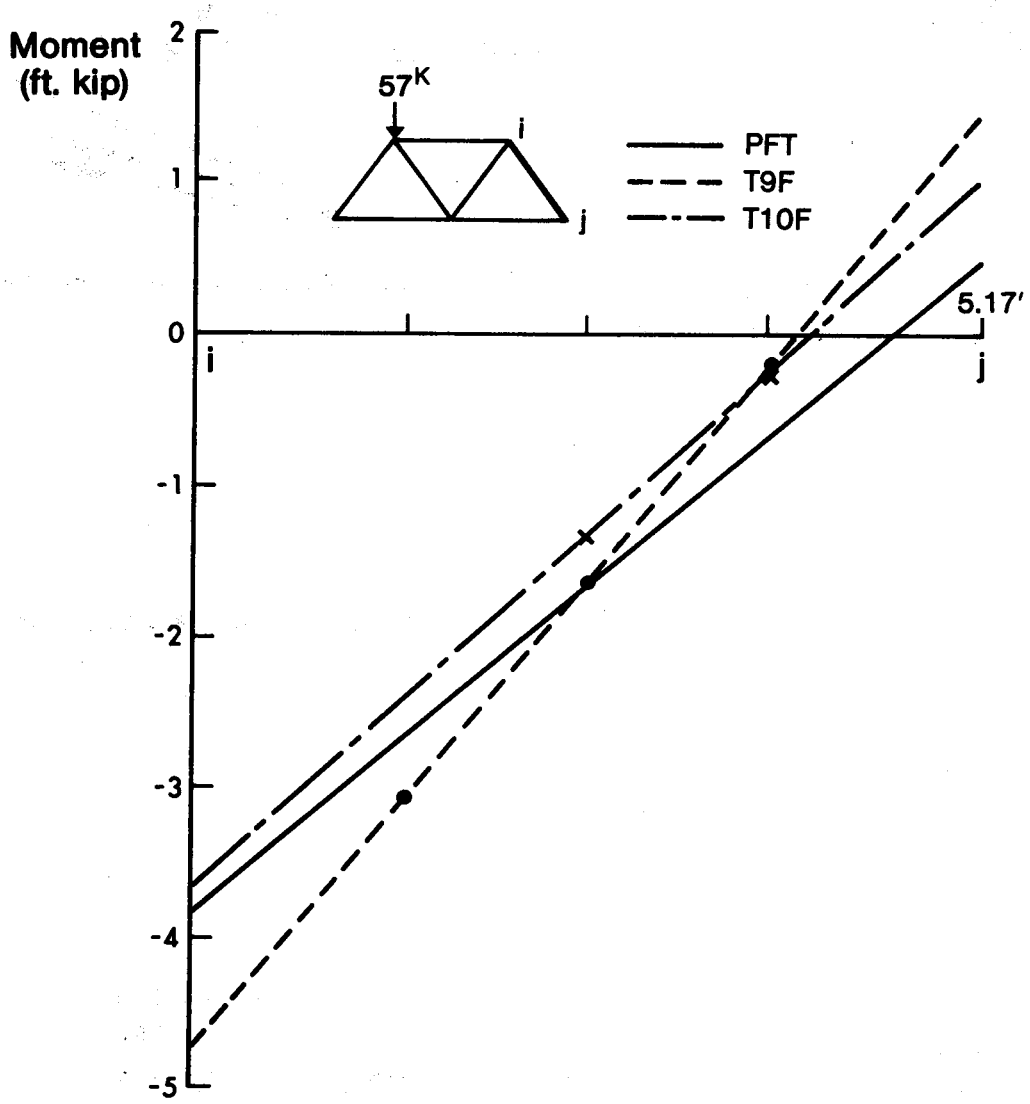

Figure 4.7 Bending Moments for Member L2-U2

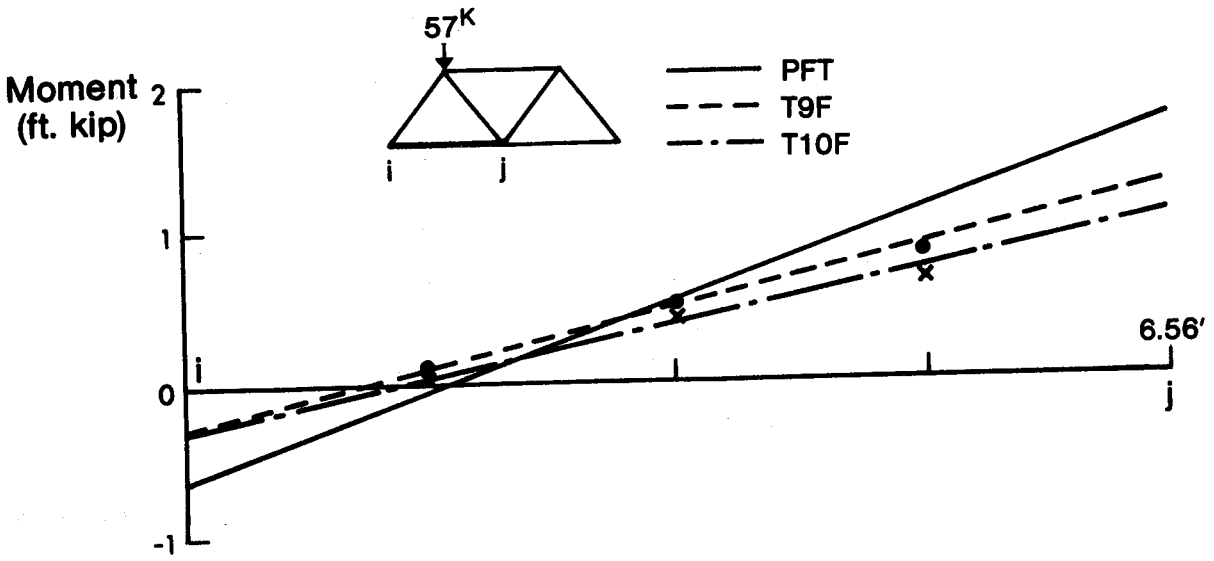

Figure 4.8 Bending Moments for Member L0-L1

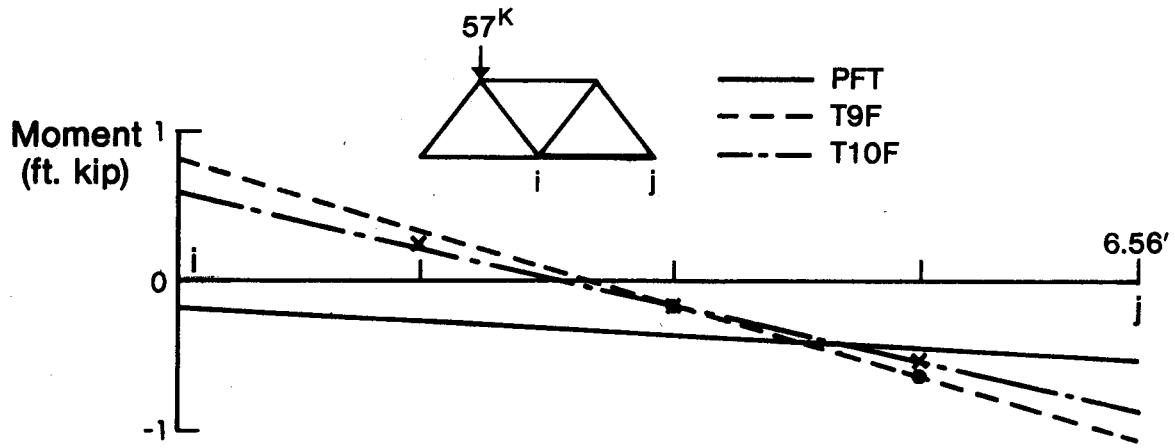

Figure 4.9 Bending Moments for Member L1-L2

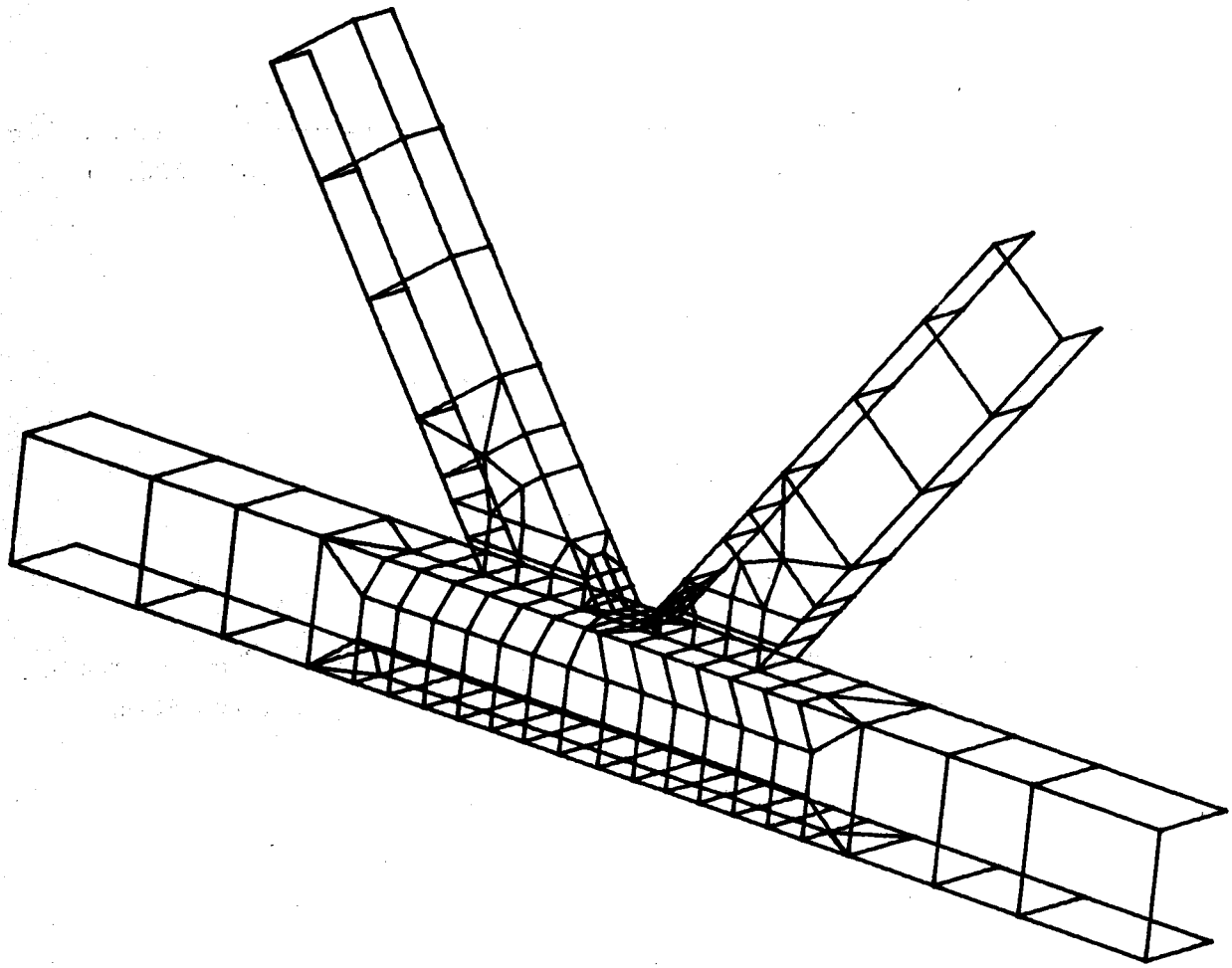

Figure 4.10 Finite Element Mesh for Gap Joint L1,
(Mesh Coarseness = Medium)

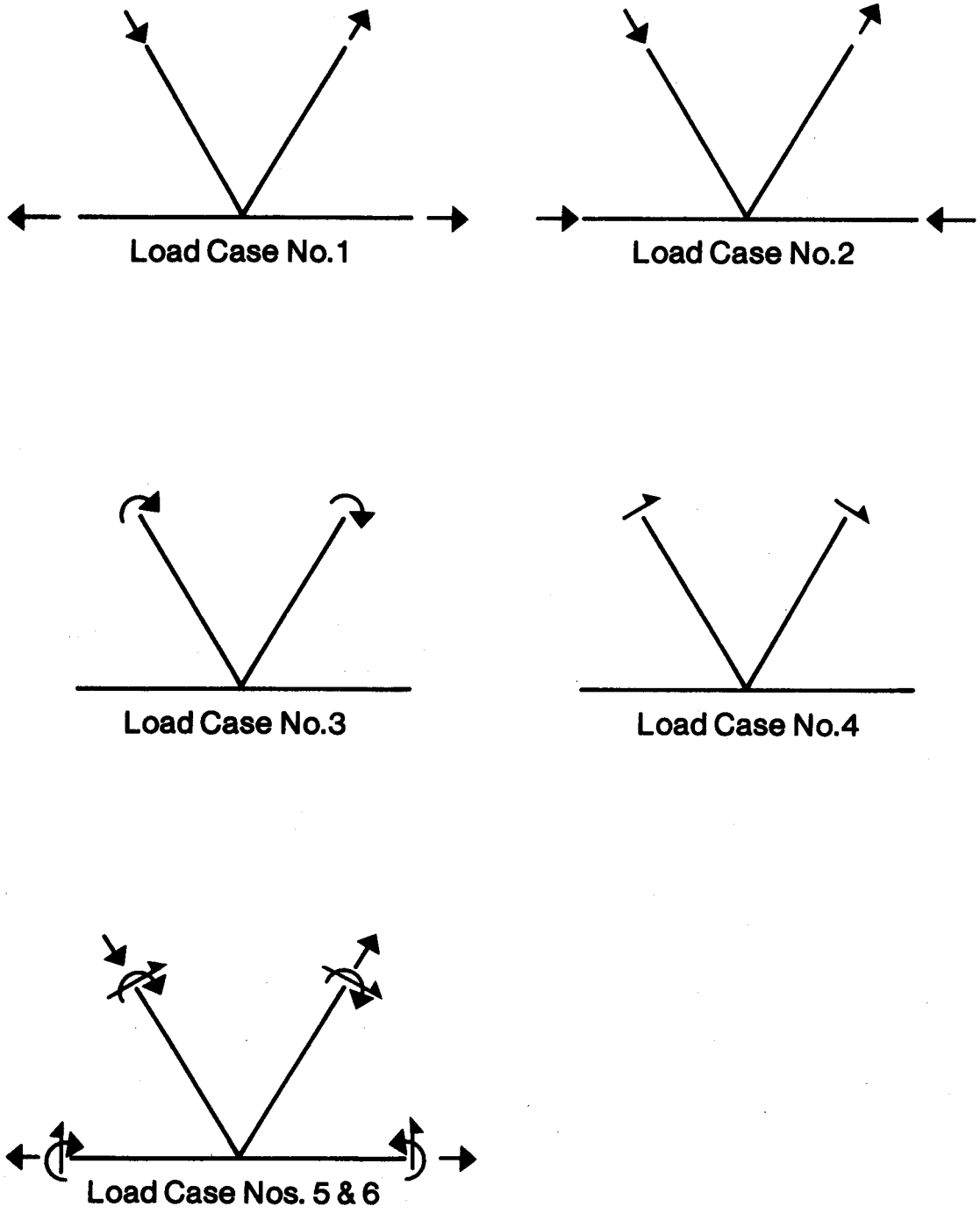

Figure 4.11 Load Cases for the Finite Element Analysis

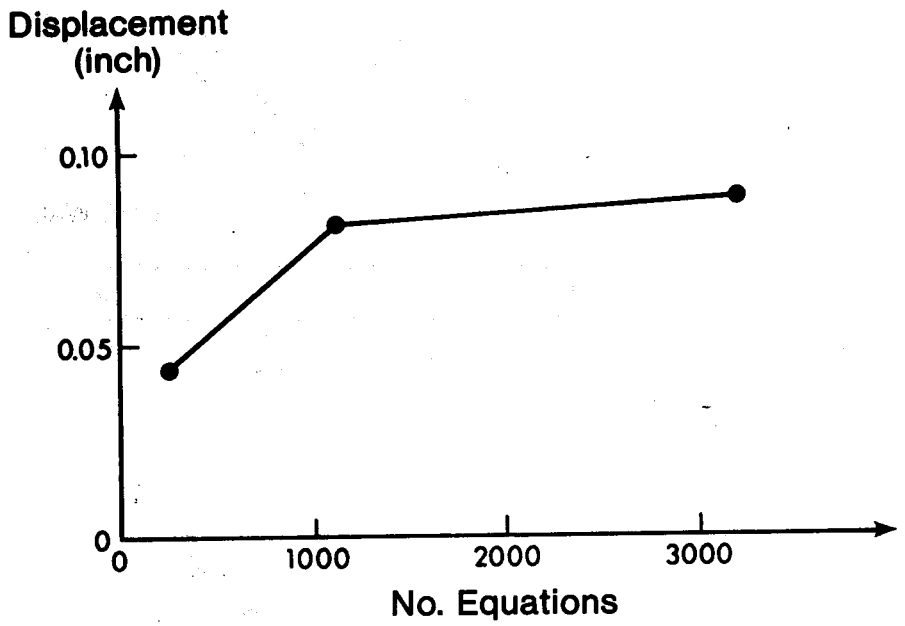

Figure 4.12 Displacement versus No. of Equations, for a Boundary Node on the Chord

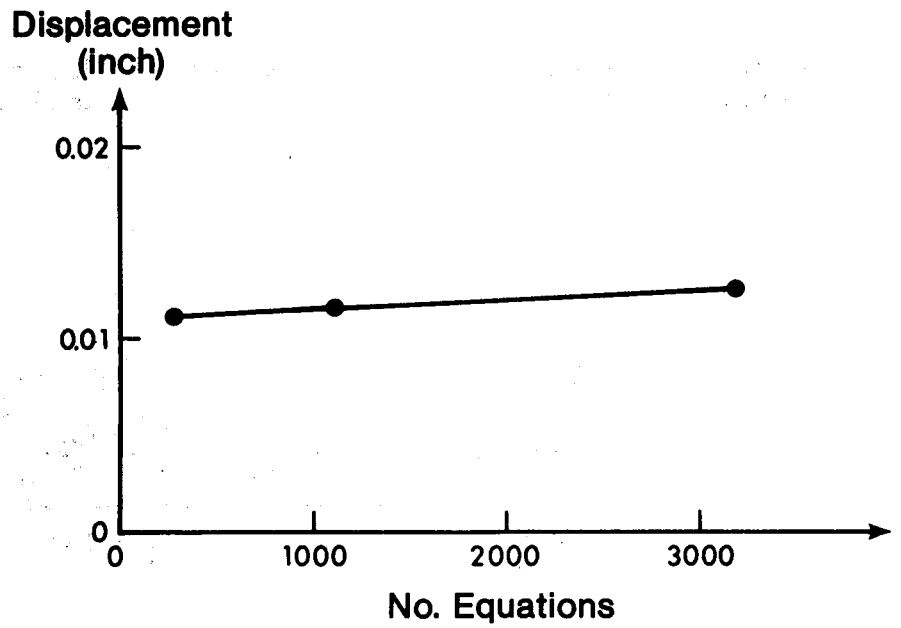

Figure 4.13 Displacement versus No. of Equations, for a Boundary Node on the Web

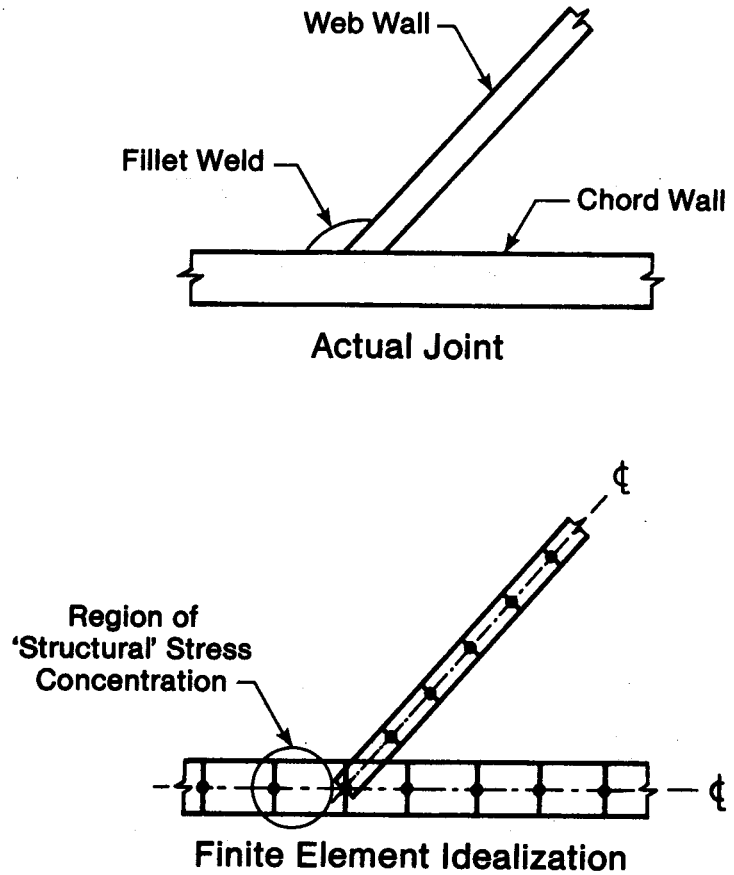

Figure 4.14 Comparison of the Actual Web - Chord Intersection and the Finite Element Idealization

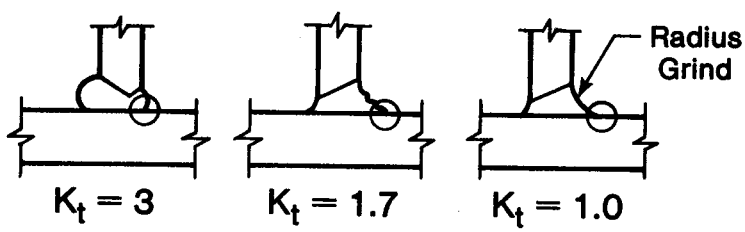

Figure 4.15 Stress Concentrations to Account for Weld Profile

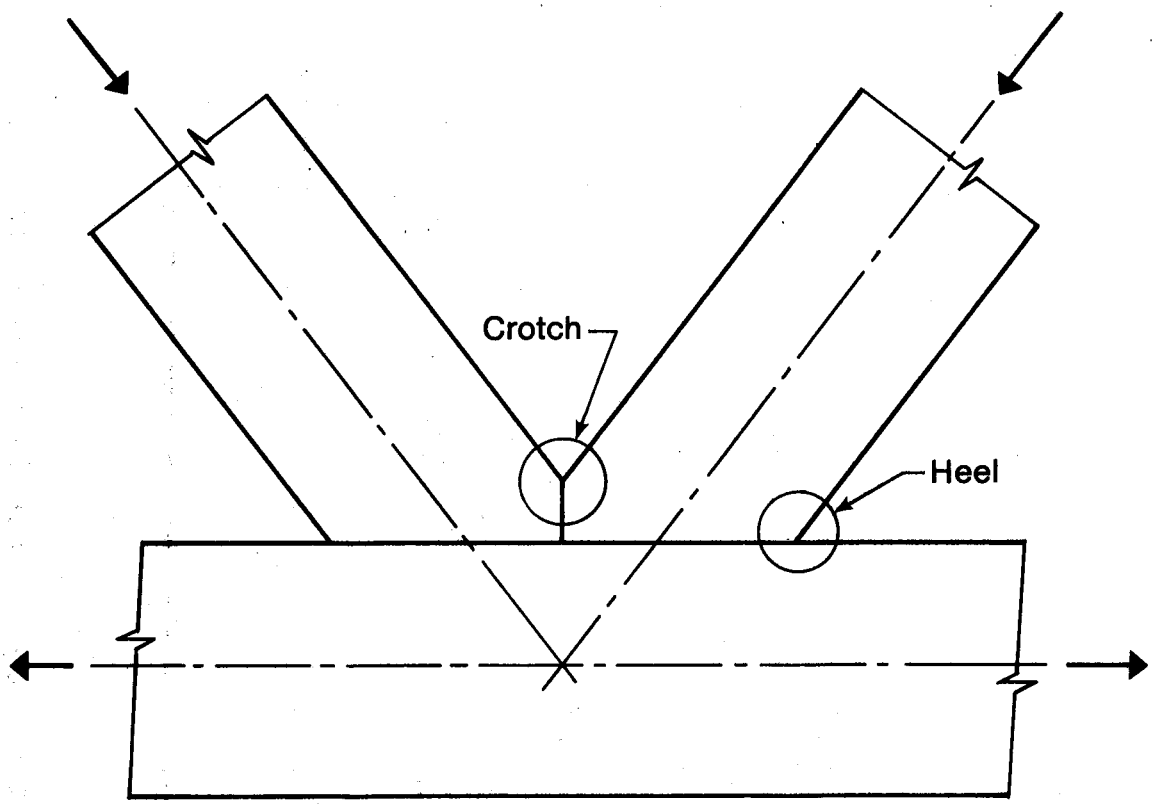

Figure 4.16 Regions of High Stress in the Overlap Joint

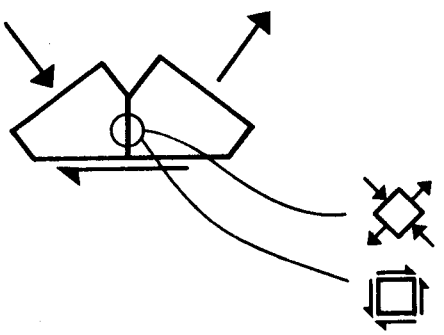

Figure 4.17 Membrane Stresses in the Stiff Sidewalls of the Crotch Region

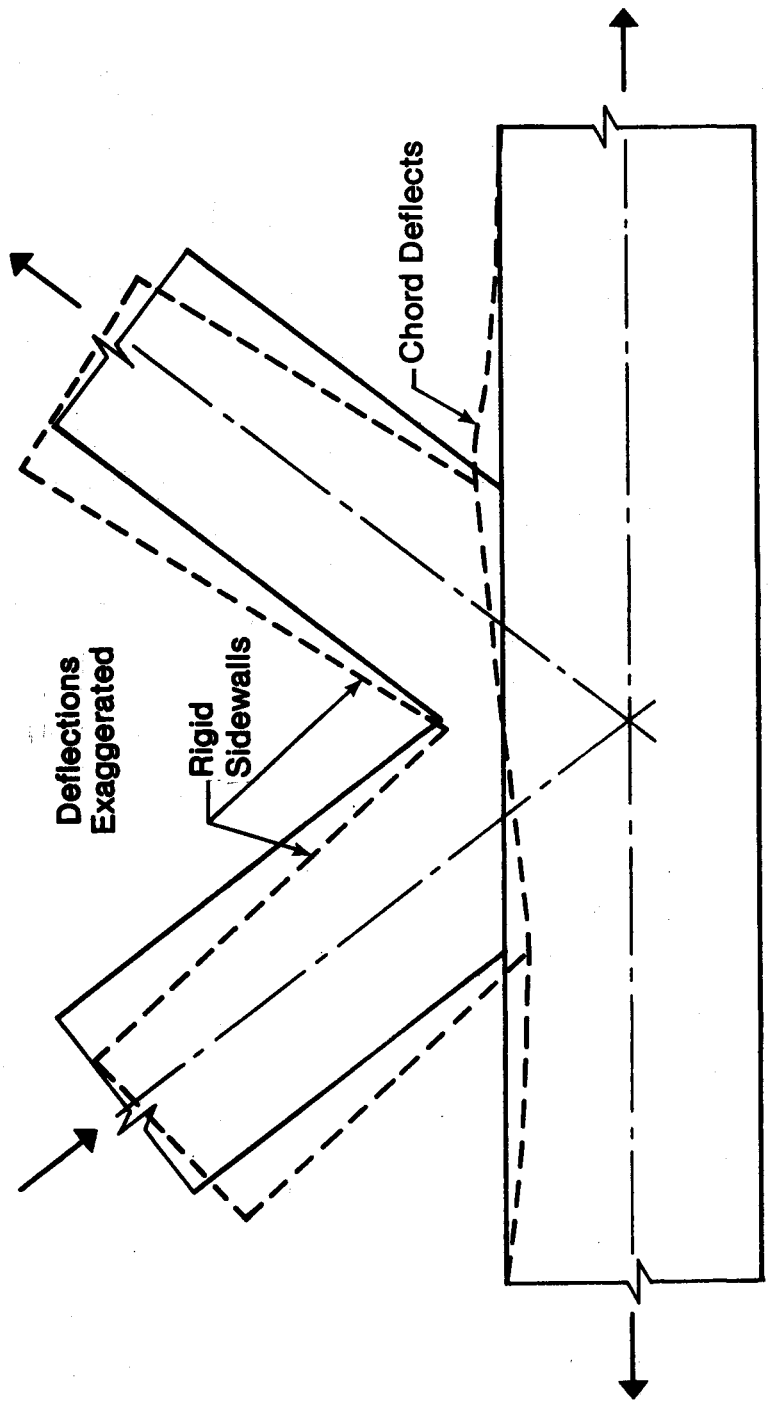

Figure 4.18 Deflection of the Chord Face in the Overlap Joint due to Axial Loads

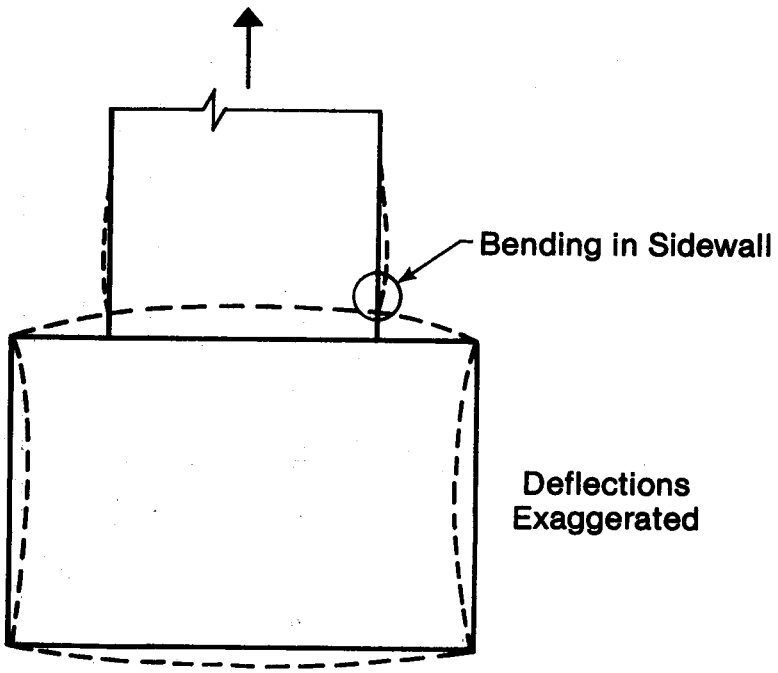

Figure 4.19 Section through the Overlap Joint Near the Heel of the Tension Member

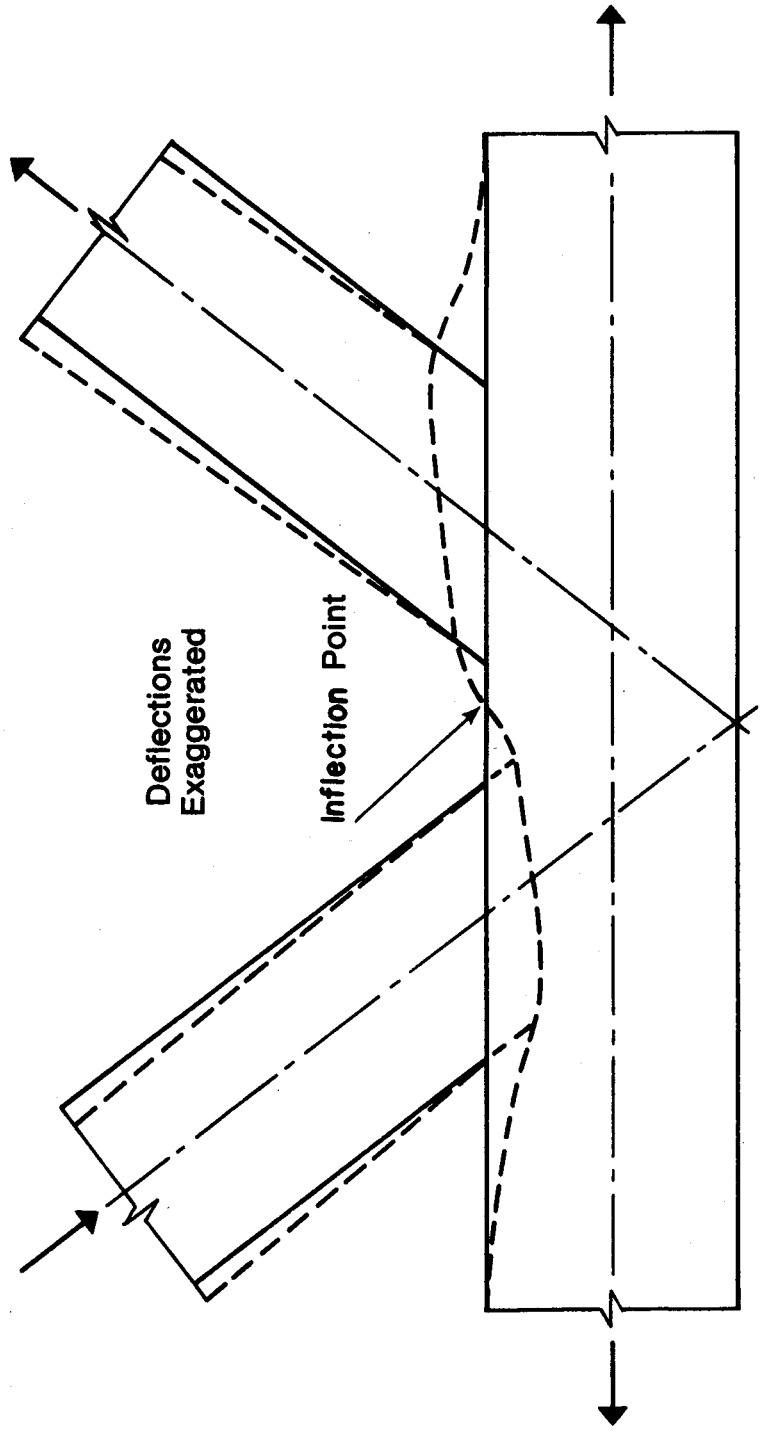

Figure 4.20 Deflection of the Chord Face in the Gap Joint due to Axial Loads

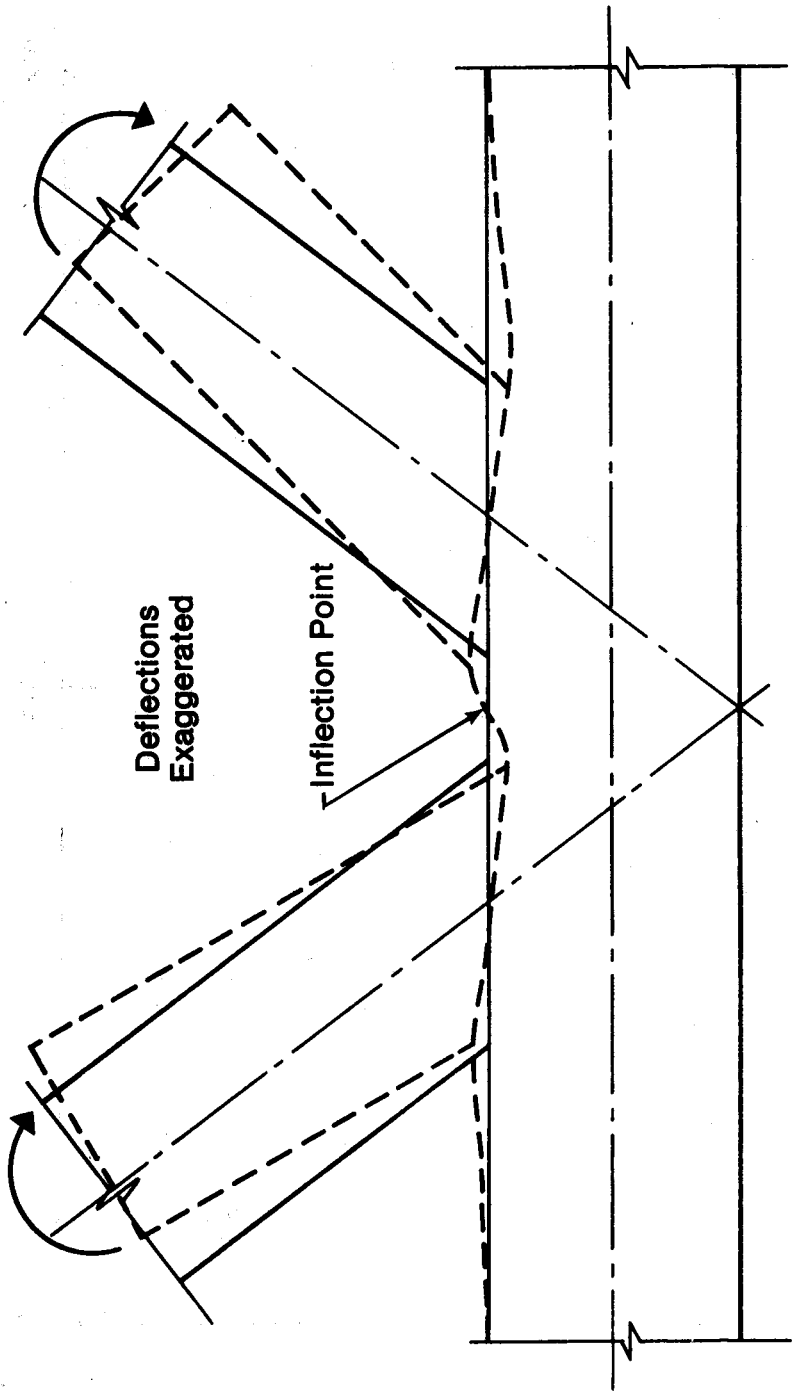

Figure 4.21 Deflection of the Chord Face in the Gap Joint due to Moment Loading

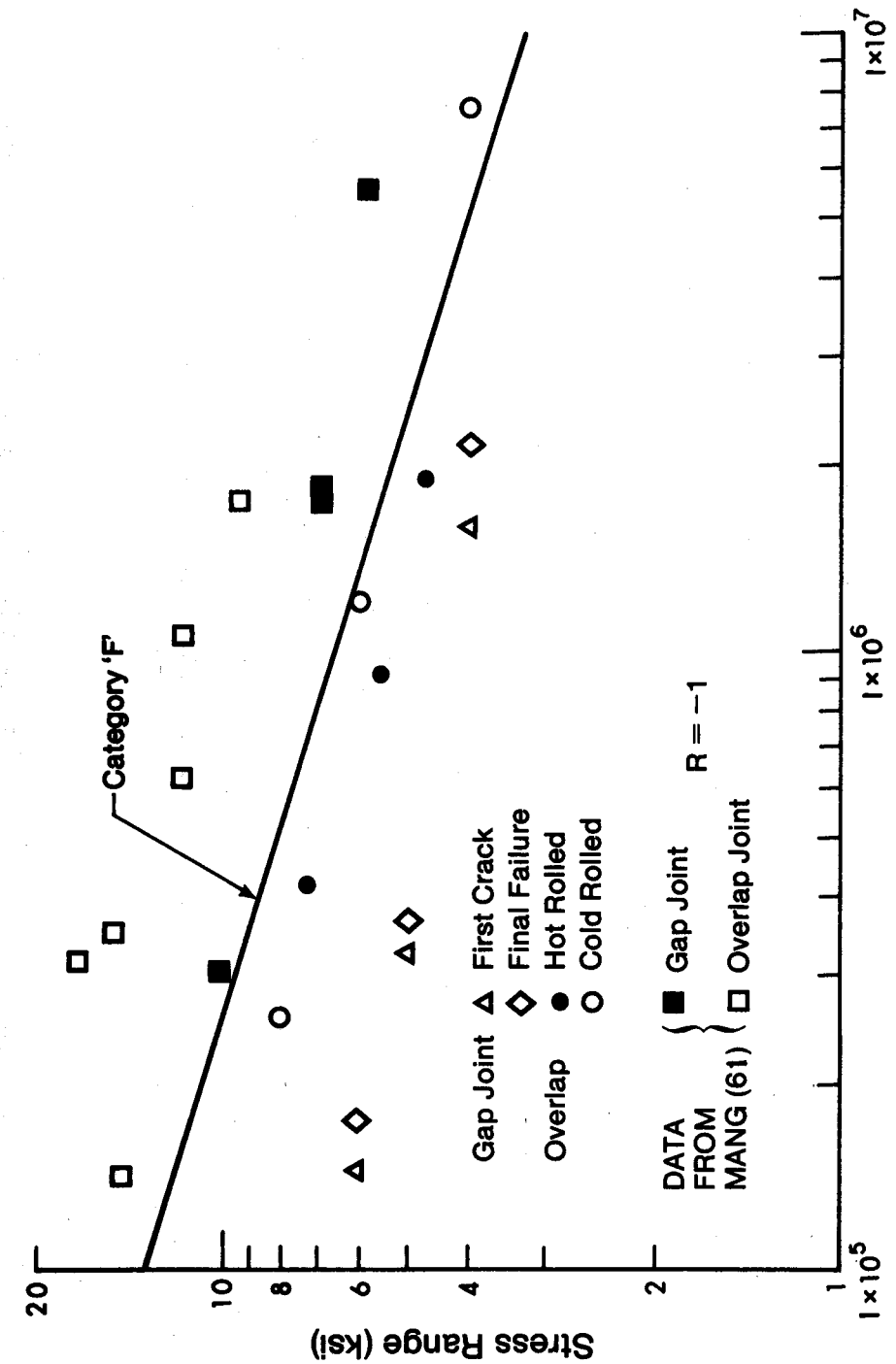

Figure 4.22 Nominal Stress Range versus Life for R-R K-type Joints

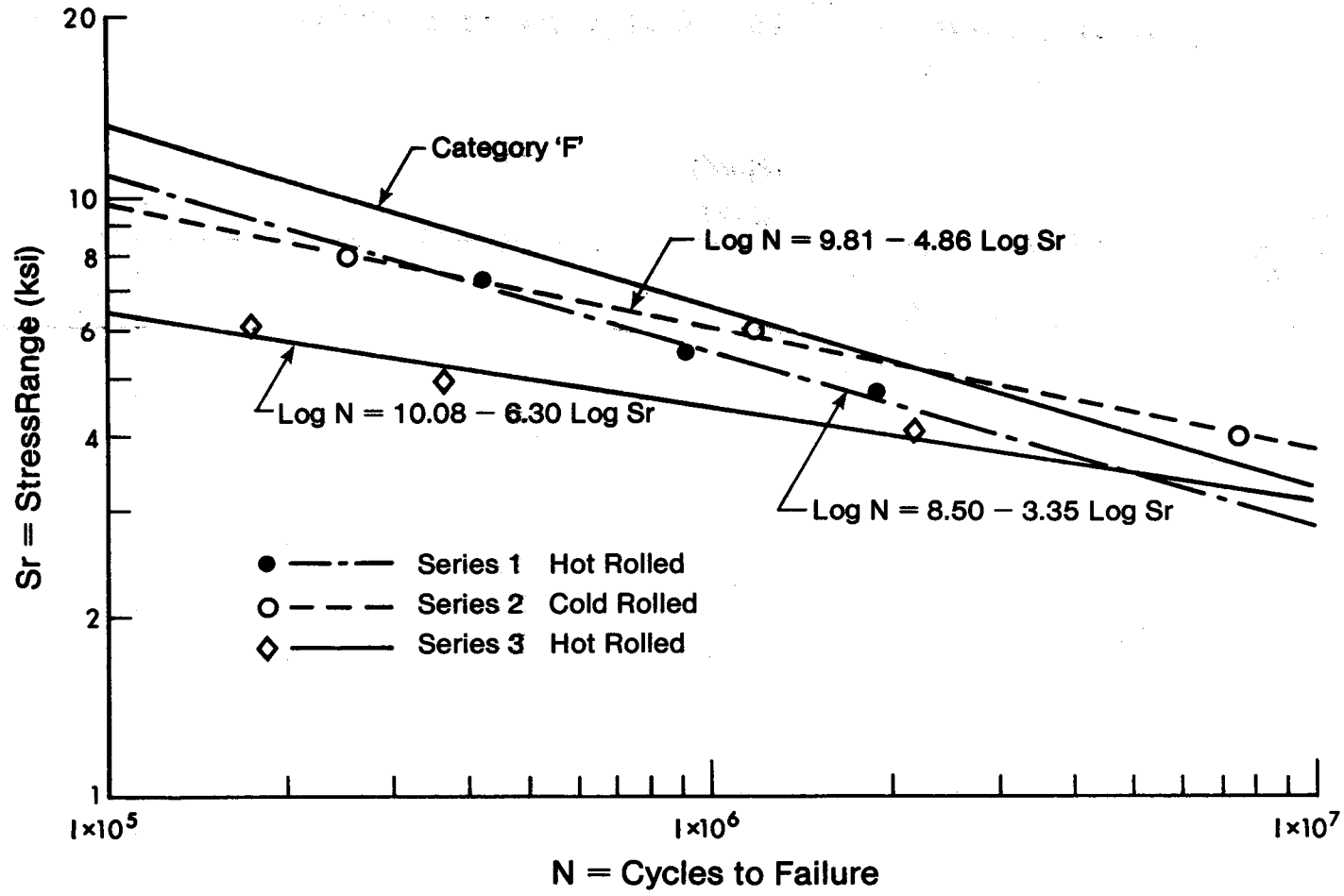

Figure 4.23 Nominal Stress Range versus Life for Series 1, 2 and 3

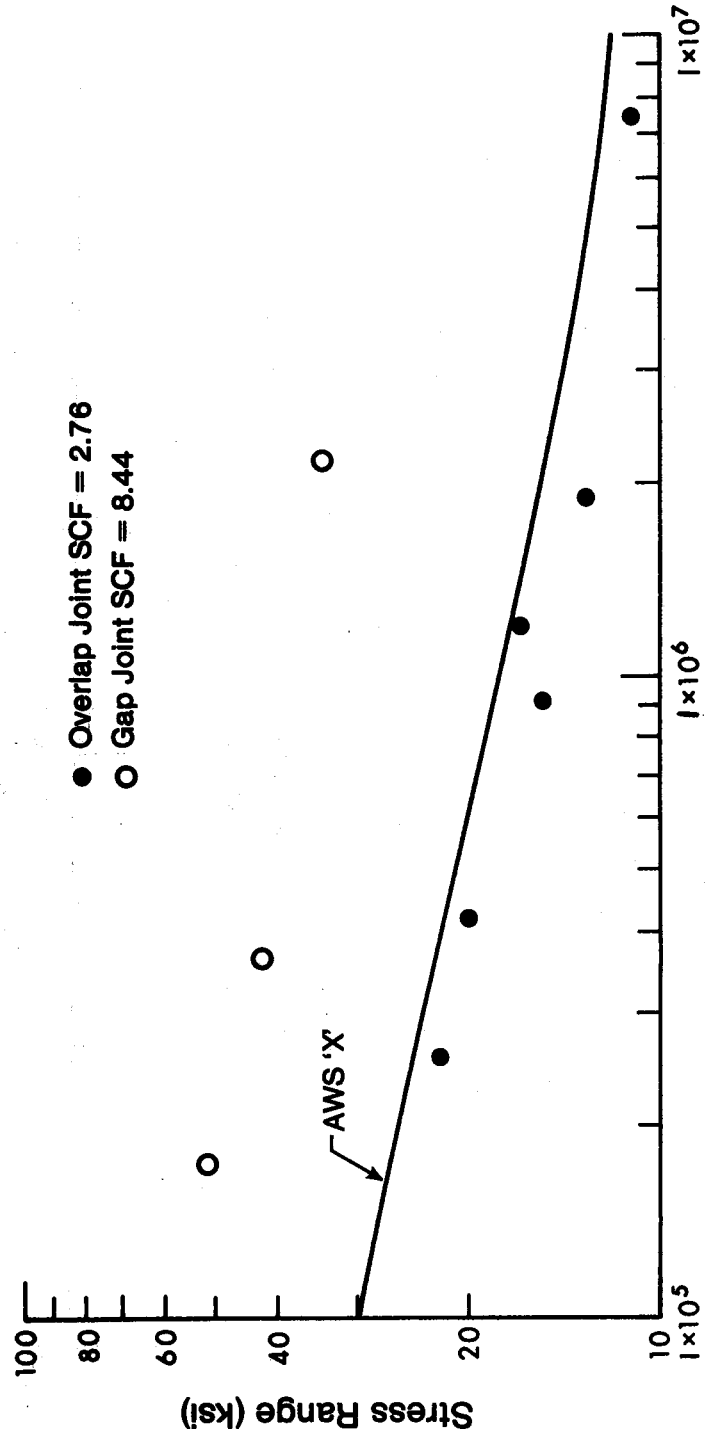

Figure 4.24 Modified Stress Range versus Life for Series 1, 2 and 3

5. Summary and Conclusions

5.1 Summary

This study deals with fatigue behavior of nine full size trusses made up of RHS members. In particular, two truss configurations were examined; six trusses had overlapped K-type joints while three trusses had gap K-type joints. The overlap specimens included three trusses of cold rolled steel and three trusses of hot rolled steel. The gap joint trusses were all hot rolled.

Since fatigue life has been shown to be dependent on the magnitude of hot spot stresses within a joint, static tests were conducted to determine elastic stresses before fatigue testing was carried out. This included the measurement of secondary bending moments and shears within the truss members, and the comparison of these measured values with those predicted by a simple stiffness program. In addition, both the overlap and gap joints were analyzed using the finite element method. The strains from the finite element analysis were compared to actual strain gauge measurements. The finite element method was also used to describe the load transfer mechanisms in both joints.

After static testing was completed the truss specimens were fatigue tested at various stress ranges by the application of a single fluctuating load. The stress range versus cycle life data for all specimens was analyzed and

comparisons were made between the overlap and gap joint configurations. In addition the effect of hot rolled versus cold rolled steel was examined. Truss data was also compared to the results of tests on isolated joints by other investigators.

5.2 Conclusions

5.2.1 Overall Static Truss Behavior

1. Significant bending moments were measured in members of the gap truss specimens. In some members, these moments caused bending stresses of the same magnitude as the nominal axial stresses. The moments appear to arise from both the eccentricity of the joints and from the relative rotations and displacements which occur between members framing into a joint.
2. An analysis of the gap truss based on a simple stiffness program was successful in predicting measured axial forces. However, such an approach did not show good agreement for bending moments.

5.2.2 Stress Distribution within K-type Joints

1. For equal axial forces, hot spot stresses within the gap joint were larger than those in the overlap joint. This observation is based both on experimental evidence and the finite element analysis.

2. For the gap joint, the largest stresses occurred in the chord face directly at the toe of the tension web member and within the gap region. These stresses appear to be primarily due to bending.
3. For the overlap joint, regions of high stress were predicted in the chord face at the heel of the tension web members and in the sidewalls of the tension web member in the region of the vertical groove weld. The importance of the latter region was supported by experimental evidence and appeared to be due primarily to membrane stresses.
4. Secondary moments have an important influence on the fatigue strength of trusses with gap K-type joints. Based on the finite element model it appears that bending moments of the order measured in the gap joint truss specimens can cause significant hot spot stresses.
5. Based again on the finite element model, compression of the chord of the gap joint was found to reduce hot spot stresses when compared to placing the chord in tension. It would appear that the practice of chord precompression in the fatigue testing of isolated joints may be unconservative.
6. In general, in regions of high local bending stress, the finite element model tended to overestimate experimentally measured strains.

5.2.3 Fatigue Strength

1. For K-type joints, overlap joints perform better than gap joints with respect to fatigue strength.
2. There was no significant difference in fatigue performance between hot rolled and cold rolled specimens.
3. Both gap and overlap K-type joints fell below category 'F' in the stress versus cycle life plot given by CSA S16.1 - M78.
4. Fatigue life predictions based on stress concentration factors derived from the finite element analysis and the use of AWS Curve 'X' were conservative for gap joints and slightly unconservative for overlap joints.
5. Fatigue cracks initiated in the crotch region of the overlap joint specimens and grew in the sidewall of the tension web member in a direction roughly transverse to the member axis.
6. In the gap joints, cracks initiated at the toe of the tension member fillet weld and propagated along the toe of the weld, penetrating the entire thickness of the chord face.

5.3 Recommendations for Design

1. K-type joints should be overlapped if possible. This will improve the load transfer characteristics of the joint, reducing hot spot stresses and also tend to

reduce secondary moments within the truss frame.

2. Since RHS trusses may fall below present fatigue categories in CSA S16.1 - M78, caution is advised in fatigue applications. If an accurate estimate of stress concentration factors can be made, the use of AWS curve 'X' to determine fatigue life is recommended.

5.4 Recommendations for Further Research

A literature review revealed that little work has been carried out on the fatigue behavior of joints made up of RHS members. Although tests on isolated joints have been conducted, work is lacking in several areas: the elastic stress distribution within RHS joints, the behavior of entire trusses, and, finally, a fracture mechanics approach to joint fatigue strength. Based on these observations and the present study, the following recommendations are made:

1. Further studies should be made to determine the effect of nondimensional geometric joint parameters on hot spot stresses within RHS joints. Such a study would use the finite element method followed by a parameter study. The result of this investigation would be stress concentration factors as a function of the joint parameters for several types of joints and loading conditions. A computer program which includes features such as mesh generation and substructuring would facilitate the study.

2. The nature of secondary bending within trusses made of RHS members should be examined. This study might include both an analytical approach using the finite element technique and experimental investigations including static and fatigue tests on both isolated joints and complete trusses.
3. A fracture mechanics approach to both overlap and gap RHS joints should be undertaken. This would require the careful measurement of crack growth rates and the computation of compliance factors to be used in the fracture mechanics crack growth equations.

References

1. Munse,W.H., *The Changing American Fatigue Design Specifications*, Proceedings of the Conference on Fatigue of Welded Structures, 6-9 July 1970, Vol. 1, Session 1, The Welding Institute, Abington, U.K.

2. Fisher,J.W., *Fatigue Strength of Welded Steel Details and Design Considerations*, Proceedings of the Canadian Structural Engineering Conference, Montreal, 1972.

3. CSA Standard S6-1974, *Design of Highway Bridges*, Canadian Standards Association, Rexdale, Ontario, 1974.

4. The American Association of State Highway and Transportation Officials, *Standard Specifications for Highway Bridges*, Twelfth Edition, 1977.

5. CSA CAN3 S16.1-M78, *Steel Structures for Buildings - Limits States Design*, Canadian Standards Association, Rexdale, Ontario, 1978.

6. Fisher,J.W., Frank,K.H., Hirt,M.A., and MaNamee,B.M., *Effect of Weldments on the Fatigue Strength of Steel Beams*, NCHRP Report 102, Transportation Research Board, Washington, 1970.

7. Fisher,J.W., Albrecht,P.A., Yen,B.T., Klingerman,D.J., and McNamee,B.M., *Fatigue Strength of Steel Beams with Welded Stiffeners and Attachments*, NCHRP Report 147, Transportation Research Board, Washington, 1974.

8. Marshall,P.W., *Basic Considerations for Tubular Joint Design in Offshore Construction*, Bulletin 193, Welding

Research Council, New York, N.Y., 1974.

9. De Koning,C.H.M., and Wardenier,J., *The Fatigue Behavior of Welded N-type Joints Made of Square Hollow Sections*, CECA - con. nr. 6210.KD-1-103, TNO - I.B.B.C report nr. BI-77-107/05.3.31310, Dec. 1977.
10. Davie and Giddings, *Research into the Strength of Welded Lattice Girder Joints in Structural Hollow Sections*, University of Sheffield, Sheffield England, CIDECT Programme 5EC, CIDECT Issue 71/7/E, 1971.
11. Blockely,D.I., Eastwood,W., Osgerby,C., and Wood,A.,A., *An Experimental Investigation into the Behavior of Joints Between Structural Hollow Sections*, University of Sheffield, Sheffield England, Feb. 1970.
12. Bijlaard,P.P., *Stresses From Local Loadings in Cylindrical Pressure Vessels*, Transactions, American Society of Mechanical Engineers, Vol. 77, No. 6, pp. 805-814, Aug. 1955.
13. Dundrova ,V., *Stresses at the Intersection of Tubes: Cross and T - Joints* , University of Texas, SFRL Tech Report P550-3 1966.
14. Scordelis,A.C., and Bouwkamp,J.G., *Analytical Study of Tubular Tee - Joints*, Journal of the Structural Division, ASCE, Vol. 96, No. ST1, Proc. Paper 7016, Jan. 1970, pp. 65-87.
15. Greste,O., *A Computer Program for the Analysis of Tubular K-Joints*, University of California Structural Engineering Lab. Report No. 69-19, 1969.

16. Kwan,C., and Graff,W.J., *Analysis of Tubular T - Connections by the Finite Element Method, Comparison with Experiments*, Paper No. OTC 1669, Fourth Annual Offshore Technology Conference, Houston, Texas, May 1-3, 1972.

17. Greimann,L.F., DeHart,R.C., Blackstone,W.R., Stewart,B., and Scales,R.E., *Finite Element Analysis for Complex Joints*, Paper No. OTC 1823, Fifth Annual Offshore Technology Conference, Houston, Texas, April 30 - May 2, 1973.

18. Reber,B.J., *Ultimate Strength of Tubular Joints*, Journal of the Structural Division, ASCE, Vol. 99, No. ST6, Proc. Paper 9793, June 1973, pp. 1223-1240

19. Clough,R.W., and Felippa,C., *A Refined Quadrilateral Element for Analysis of Plate Bending* , Proceedings 2nd Conf. on Matrix Methods in Structural Mechanics AD 703-685 Air Force Institute of Technology, Wright Patterson Air Force Base, Ohio, TR 68-150, pp. 399-440, Dec. 1969.

20. Liaw,C.Y., Litton,R.W., and Reimer,R.B., *Improved Finite Elements for Analysis of Welded Tubular Joints* , Paper No. OTC 2642, Eighth Annual Offshore Technology Conference, Houston, Texas, May 3-6, 1976.

21. Potvin,A.B., Kuang,J.G., Leick,R.D., and Kahlich,J.L., *Stress Concentrations in Tubular Joints* , Society of Petroleum Engineers Journal, Vol. 17, No. 4, pp. 287-299, Aug. 1977.

22. Visser,W., *On the Structural Design of Tubular Joints* , Journal of Engineering for Industry, Transactions of the ASME, Vol. 97, Series B, pp. 391-399, May 1975.

23. Dijkstra,O.D., Hartog,J., and Wardenier,J., *Study of Literature Regarding the Fatigue Behavior of Unstiffened Tubular Joints: Stress Concentrations Factors in Tubular Joints*, TNO-IBBC Report Nr.BI 77-58/05.3.31315, May 1977.

24. Eastwood,W., Wardle,S., Osgerby,C., Wood,A.A, and Shinouda,V., *Analysis of Tubular Joints Consisting of Two Web Members and a Boom Member in a Plane Framework*, The University of Sheffield, Sheffield England, Feb. 1968.

25. Eastwood,W., Osgerby,C., Wood,A.A., and Blockely,D.I., *A Theoretical Investigation into the Elastic Behavior of Joints Between Structural Hollow Sections*, University of Sheffield, Sheffield England, Nov. 1967.

26. Mang,F., and Dutta,D., *Fatigue Strength of Welded Joints of Hollow Sections*, Symposium on Tubular Structures, Delft, Netherlands, Oct. 1977.

27. Bouwkamp,J.G., *Behavior of Tubular Truss Joints Under Static Loads*, Structures and Materials Research, Report No. SESM 65-4, University of California, Berkeley, July 1965.

28. Beale,L.A., and Toprac,A.A., *Analysis of Inplane T, Y, and K, Welded Tubular Connections*, Bulletin No. 125, Welding Research Council, New York, N.Y., Oct. 1967.

29. Graff,W.J., *Design Correlation of Elastic Behavior and Static Strength of Zero Eccentricity T, Y, and K Tubular Joints* , Paper No. OTC 1310, Second Annual Offshore Technology Conference, Houston, Texas, April 22-24, 1970.

30. Toprac,A.A., and Louis, B.G., *Research on the Fatigue Behavior of Tubular Connections* , Structures Fatigue Research Laboratory Dept. of Civil Eng., The University of Texas, Austin Texas, May 1970.

31. Bouwkamp,J.G., and Stephen,R.M., *Tubular Joints Under Alternating Loads (Phase 2, Part 1)* , University of California Structural Engineering Laboratory, University of Calfornia, Berkeley, Nov. 1967.

32. Maeda,T., Uchino,K., and Sakurai,H., *Experimental Study on the Fatigue Strength of Welded Tubular T and X Joints* , IIW Document No. XV 270-69, July 1969.

33. Kurobane,Y., Makino,Y., and Sagawa,M., *Low-cycle Fatigue Research on Tubular K-Joints* , Progress Report Dept. of Architecture, Kumanuto University, Kumanuto 860, Japan, Feb. 1970.

34. Eastwood,W., and Wood,A.A., *Welded Joints in Tubular Structures Involving Rectangular Sections - Conference on Joints in Structures* ,University of Sheffield, Sheffield England, July 1970.

35. Wardenier,J., *Testing and Analysis of Truss Joints in HSS (Predominantly Statically Loaded)* , Paper presented to the International Symposium on HSS, Toronto, Canada,

May 25, 1977.

36. Mouty J.A., *Theoretical Prediction of Welded Joint Strength* , Paper presented to the International Symposium on HSS, Toronto, Canada, May 25, 1977.
37. Packer,J.A., *A Computer Program for the Structural Analysis of Welded Tubular Joints with RHS Chords* , Advances in Engineering Software, Vol.1, No.4, 1979.
38. Uchino,K., Sakurai,H., and Sugujama,S., *Experimental Study on the Fatigue Strength of Welded Tubular K-Joints* , IIW Doc. No. XV 344-73, Sep. 1973.
39. Kurobane,Y., Makino,Y., and Sagawa,M., *Low Cycle Fatigue Research on Tubular K-Joints*, Welding Research Abroad, Vol. X1X, No. 1, Jan. 1973.
40. Kurobane,Y., and Konomi,M., *Fatigue Strength of Tubular K-Joints, S-N Relationships Proposed as Tentative Design Criteria* , IIW Doc. XV 340-73, 1973.
41. Babiker,D.B., *The Fatigue Behavior of Welded Joints Between Structural Hollow Sections*, Ph.D thesis at the University of Sheffield, Sheffield England. CIDECT Program 5C, Issue 811, Dec. 1967.
42. Eastwood,W., Osgerby,C., Wood,A.A., and Babiker,D.B., *The Fatigue Behavior of Welded Joints Between Structural Hollow Sections* , The University of Sheffield, Sheffield England, Feb. 1970.
43. BS 153, British Standard 153, *Specifications for Steel Girder Bridges*, British Standards Institution, 1972.
44. Marshall,P.W., and Toprac,A.A., *Basis for Tubular Joint*

Design, Welding Research Supplement 201-S, May 1974.

45. Rolfe,S.T., and Barsom,J.M., *Fracture and Fatigue Control in Structures, Applications of Fracture Mechanics*, Prentice Hall, N.J., 1977.
46. Pan,R.B., and Plummer,F.B., *A Fracture Mechanics Approach to Non-Overlapping Tubular K-Joint Fatigue-life Prediction*, Paper No. OTC 2645, Eighth Annual Offshore Technology Conference, Houston, Texas, May 3-6, 1976.
47. Bouwkamp,J.W., *Fatigue Behavior of Tubular Joints in Offshore Structures* , Paper No. OTC 2207, Sixth Annual Offshore Technology Conference, Houston, Texas, May 6-8, 1974.
48. Fisher,J.W., and Hirt,M.A., *Fatigue Crack Growth in Welded Beams* , Engineering Fracture Mechanics, Vol. 5, 1973.
49. Maddox,N., and Wildenstein,A., *Spectral Analysis for Offshore Structures*, Paper No. OTC 2261, Seventh Annual Offshore Technology Conference, Houston, Texas, May 5-8, 1975.
50. Gurney,T.R., *Fatigue of Welded Structures* , British Welding Research Association, London, 1968.
51. Munse,W.H., and Grover,L., *Fatigue of Welded Steel Structures* , Welding Research Council, New York, N.Y., 1964.
52. Blockely,D.I., *Joints Between Structural Hollow Sections*, Civil Engineering and Public Works Review, Vol. 67, No. 796, pp. 1148-1153, Nov. 1972.

53. Dasgupta,A., *The Behavior of Joints in Tubular Trusses* , Ph.D thesis at the University of Nottingham, England, Nov. 1972.

54. Tajima,J., Okukawa,A., Sugizaki,M., and Takenouchi,H., *Fatigue Tests of Panel Point Structures of Trusses made of 80 Kg/sq.mm High Tensile Strength Steel* , IIW Doc. X111-831-77, July 1977.

55. Sharpe,M.L., and Nordmark,G.E., *Fatigue Strength of Welded Tubular Aluminum Trusses* , Journal of the Structural Division, ASCE, Vol. 103, No. ST8, Proc. Paper 13140, pp. 1619-1629, Aug. 1977.

56. Cran,J.A., Gibson,E.B., and Stadnyckyj,S., *Hollow Structural Sections: Design Manual for Connections* , First Edition, The Steel Company of Canada Ltd., Hamilton, Canada, 1971.

57. American Welding Society, AWS D1.1-79, *Structural Welding Code - Steel 1979*, American Welding Society Inc., Washington, D.C., 1979.

58. Comeau,M., and Kulak,G.L., *Fatigue Strength of Welded Steel Elements* , Structural Report No. 79, Department of Civil Engineering, The University of Alberta, Edmonton, Alberta, Oct. 1979.

59. Bathe,K.J., Wilson,E.L., and Peterson,F.E., *SAP1V, A Structural Analysis Program for Static and Dynamic Response of Linear Systems* , College of Engineering, University of California, Berkeley, California, Nov. 1972.

60. Rodabaugh,E.C., *Review of Data Relevant to the Design of Tubular Joints for Use in Fixed Offshore Platforms*, WRC Bulletin 256, ISSN 0043-2326, Jan. 1980.

61. Mang,F., and Striebel,A., *Fatigue Strength Results*, (in German) Internal Doc., University of Karlsruhe, W. Germany.

62. Paris,P.C., *Fatigue - An Interdisciplinary Approach*, Proceedings, 10th Sugamore Conference, Syracuse University, Syracuse N.Y., p.104, 1964.

63. Albrecht,P., and Yamada,K., *Rapid Calculation of Stress Intensity Factors*, Journal of the Structural Division, ASCE, Vol. 103, No. ST2, Proc. Paper 12742, pp. 377-389, Feb. 1977.

64. Dover,W.D., Holdbrook,M.S.J., Hibberal,R.D., and Charlesworth,F.D.W., *Fatigue Crack Growth in T-Joints; Out-of-Plane Bending* , Paper No. OTC 3252, Tenth Annual Offshore Technology Conference, Houston, Texas, May 8-10, 1978.

65. Hibberal,R.D., and Dover,W.D., *Random Load Fatigue Crack Growth in T-Joints* , Paper No. OTC 2853, Ninth Annual Offshore Technology Conference, Houston, Texas, May 2-5, 1977.

66. Maddox,S.J., *An Analysis of Fatigue Cracks in Fillet Welded Joints*, International Journal of Fracture, Vol. 11, April 1975.

Appendix A - Fracture Mechanics Approach to HSS Joint Design

Many welded steel details have simple geometries and are attached to structural members in regions where nominal stresses are easily computed and severe changes in stresses do not occur. Examples of such details are the various beam details examined by Fisher et al. (6,7). In order to determine fatigue strength for attachments such as these, experimenters have usually adopted the following procedure.

A constant amplitude sinusoidally varying load is applied to the specimen, resulting in a nominal stress range in the detail under investigation. Cycling is continued until failure occurs. This is repeated for several identical specimens at several stress ranges. A linear regression analysis of the stress range versus cycle life data generally yields a straight line of the form:

$$\text{Log}\,Sr = A + B\,\text{Log}\,N \qquad (A.1)$$

where:

Sr = stress range

N = number of cycles

A,B = constants

It is convenient to show these results on a plot of Log Sr versus Log N. The procedure is repeated for other types of

details and a series of regression lines are built up on the Log Sr versus Log N graph. The categories found in CSA S16.1 - M78, for example, have been generated in this manner.

Typically, after the experimental development of a stress range versus cycle life curve, investigators attempt a theoretical check using fracture mechanics. The check most often involves the integration of the semi-empirical crack growth rate law proposed by Paris (62):

$$\frac{da}{dN} = C_1 (\Delta K)^{C_2} \qquad (A.2)$$

where:

a = crack length

N = load cycles

C_1, C_2 = material constants

ΔK = change in stress intensity factor

ΔK may be expressed as:

$$\Delta K = Y \Delta \sigma \sqrt{\pi a} \qquad (A.3)$$

where:

Y = compliance factor

$\Delta\sigma$ = applied stress range

For simple geometries, Y can be determined theoretically and

solutions for several cases are available in the literature (45). C_1 and C_2 are usually obtained from crack growth records of simple plate specimens recorded in the form Log da/dN versus Log N . Substitution of Eq. A.3 into Eq. A.2 and integration, assuming Y constant, leads to the expression:

$$N = \frac{1}{C_1 Y^{C_2} \alpha S_r^{C_2}} (a_i^{-\alpha} - a_f^{-\alpha}) \qquad (A.4)$$

where:

a_i = initial crack (flaw) size

a_f = final crack size

$$\alpha = \frac{C_2}{2} - 1$$

Since a_f is usually much greater than a_i , Eq. A.4 can be simplified:

$$N = M S_r^{-C_2} \qquad (A.5)$$

where:

$$M = \frac{1}{C_1 Y^{C_2} \alpha a_i^{\alpha}} \qquad (A.6)$$

In logarithmic form, Eq. A.5 appears as:

$$\text{Log } N = P - C_2 \text{ Log } Sr \qquad (A.7)$$

where:

$$P = \text{Log } M$$

It can be seen that Eq. A.7 is of the same form as Eq. A.1 and the theoretical check mentioned earlier usually involves the comparison of these equations. Most investigators (6,7) have been able to show reasonable agreement, although the fracture mechanics approach is sensitive to initial flaw size and the selection of material constants. With regard to initial flaw size, experimental evidence shows that cracks usually initiate from flaws, porosities, or slag inclusions associated with weldments. Investigators have been able to produce satisfactory values for a_i based on visual observation of these flaws. The values are averages and usually involve a calibration to account for initial flaw shape (48).

The complexity of HSS joints and the number of parameters (β,γ,τ,etc.) involved means that it is not practical to consider testing as the principal means of establishing specification limitations for these elements. Rather, a slightly more analytical approach must be used. For example, "hot spot" stresses obtained through an elastic analysis of the joint can be used in conjunction with Log Sr versus Log N curves developed for simple welded plate specimens. This practice has been used for the design of offshore structures and involves the use of stress range versus life cycle curves such as AWS D1.1 - 79 curve 'X' which is based on tests of simple butt welded plates (8).

In such an analysis it is assumed that stress distribution, stress gradients and the change in load transfer with crack length, will be similar for both simple specimens and HSS joints. Because the AWS curve 'X' is based on groove welds, Marshall (8) has proposed calibration factors to account for more severe weld profiles (Fig. 4.15). The procedure followed has been described in Chapters 2 and 4 and involves the use of stress concentration factors from an elastic analysis and also the use of a cumulative damage law such as Miner's Rule. Rodabaugh (60) has compared fatigue life estimates based on the method just described with experimental data for C-C gap K-type joints published by several investigators. For medium and long fatigue lives (N>1000), the approach appears to be conservative.

The complexity of HSS joints also makes fatigue life predictions based on fracture mechanics very difficult. Most of this difficulty is associated with the calculation of the compliance fator, Y, in Eq. A.3. Albrecht and Yamada (64) have expressed Y as:

$$Y = F_E F_S F_W F_G \qquad (A.8)$$

where:

F_E = elliptical integral, associated with crack aspect ratio

F_S = surface effect, also dependent on crack aspect ratio

F_W = finite width adjustment, dependent on crack depth to

wall thickness ratio

F_E = effect of stress gradient due to local geometry, also dependent on crack depth to wall thickness ratio.

The factors above have been determined analytically for simple crack shapes and plate geometries (45). However, establishing these factors for more complex configurations requires sophisticated analysis techniques, usually involving the finite element method. Although a solution for a non-load-carrying fillet weld has been obtained (66), there is no indication that such an analysis has been attempted for more complicated geometries such as tubular joints.

Several investigators have attempted to determine the compliance factor, Y, using experimental crack growth records. Pan and Plummer (46) have used this approach drawing on data published by Kurobane et al. (33) for non-overlapping C-C K-type joints. Substitution of Eq. A.3 into Eq. A.2 gives:

$$\frac{da}{dN} = C_1 (Y \Delta\sigma \sqrt{\pi a})^{C_2} \qquad (A.9)$$

In this formula, $\Delta\sigma$ is the hot spot stress range as determined by an elastic analysis. Pan and Plummer used the stress concentration factors derived by Potvin et al. (21). The constant C_2 is taken as the slope of the Log Sr versus

Log N plot for K-type joints. A corresponding value of C_1, is selected from the literature. Both these constants are average values in that they are derived from a variety of steel grades and weld materials. Eq. A.9 is non-dimensionalized using the chord wall thickness and web-chord intersection length and then is solved for Y. Y can then be determined as a function of the non-dimensional crack length since da/dN and a are available from crack growth records and $\Delta\sigma$ is also known. Once a solution for Y is obtained, then Eq. A.9 can be integrated for any C-C gap K-type joint, providing that values for C_1 and C_2 are available. Pan and Plummer found good agreement between predicted fatigue life and actual test records using this method.

Dover, et al. (64) and Hibberal and Dover (65) have also attempted to determine the compliance factor, Y, using experimental crack growth records. In this case, the joints studies were C-C T-type joints tested for both in-plane and out-of-plane bending. The constants C_1 and C_2 were determined from crack growth measurements on simple plate specimens made from the same material as the full size joints. For the in-plane bending tests an attempt was made to separate the compliance factor into two effects:

$$Y = Y_s Y_\sigma \qquad (A.10)$$

where:

Y_S = surface or crack shape effect

Y_σ = stress effect

Comparing Eq. A.8 to Eq. A.10, it can be seen that $Y_\sigma = F_W F_G$ and $Y_S = F_E F_S$. A solution for Y_σ, which will change as the crack grows, can be obtained only if Y_S is known. On the basis of previous high load tests, Dover felt that crack growth took the form of an edge crack, in which case Y_S = 1.12. Using this assumption and an approach similar to Pan and Plummer (46), Y_σ was found to be a steadily decreasing function of crack depth which eventually reached a constant value. Later examination of the crack growth record, however, showed that cracks did not grow strictly as simple edge cracks. In the early stages of life the cracks grew as independent surface cracks followed by a transition period where the cracks began to coalesce. Only in the later stages of growth was cracking the result of a single edge crack. Since no simple solution for Y_S could be assumed it was felt that it would be possible to determine only the product $Y_\sigma Y_S$. For similar reasons it was only possible to compute the product $Y_\sigma Y_S$ for out-of-plane bending. In both these cases and for Pan and Plummer's work, Y was found to be a steadily decreasing function which eventually reached a constant value. The significance of this decline in Y with increasing crack length is that later stages of crack growth become more important. The crack

rate does not increase as rapidly with crack length as might be expected for, say, a simple plate specimen, thus tending to increase fatigue life. For the same reason, fatigue life is less sensitive to a_i, the initial crack size, a commonly stated objection to the fracture mechanics approach.

Dover, et al. (64) and Hibberal and Dover (65) found that for both in-plane and out-of-plane bending, fracture mechanics gave a better fatigue life estimate than the conventional stress range versus cycle life approach using AWS curve 'X'. In both cases, the estimates were conservative.

A fracture mechanics approach to the fatigue strength of HSS joints requires more information than a stress range versus cycle life approach. This includes the material constants, C_1 and C_2, the initial crack size, a_i, and general expressions for, Y, the compliance factor. If this information can be determined, then a more accurate life prediction than that of a stress versus life approach would be expected since a stress versus life analysis does not include such factors as change in load transfer due to crack growth or initial flaw size. The lack of such information is reflected in the scatter found in stress versus life data. At the present time much more work is required before geometries as complex as HSS joints can be designed on a fracture mechanics basis. The stress versus life method using curves such as AWS 'X' and stress concentration factors such as those presented by Potvin et al. (21) remains the only practical design guide.

RECENT STRUCTURAL ENGINEERING REPORTS

Department of Civil Engineering

University of Alberta

73. *Double Angle Beam-Column Connections* by R.M. Lasby and R. Bjorhovde, April 1979.

74. *An Effective Uniaxial Tensile Stress-Strain Relationship for Prestressed Concrete* by L. Chitnuyanondh, S. Rizkalla, D.W. Murray and J.G. MacGregor, February 1979.

75. *Interaction Diagrams for Reinforced Masonry* by C. Feeg and J. Warwaruk, April 1979.

76. *Effects of Reinforcement Detailing for Concrete Masonry Columns* by C. Feeg, J. Longworth and J. Warwaruk, May 1979.

77. *Interaction of Concrete Masonry Bearing Walls and Concrete Floor Slabs* by N. Ferguson, J. Wongworth and J. Warwaruk, May 1979.

78. *Analysis of Prestressed Concrete Wall Segments* by B.D.P. Koziak and D.W. Murray, June 1979.

79. *Fatigue Strength of Welded Steel Elements* by M.P. Comeau and G.L. Kulak, October 1979.

80. *Leakage Tests of Wall Segments of Reactor Containments* by S.K. Rizkalla, S.H. Simmonds and J.G. MacGregor, October 1979.

81. *Tests of Wall Segments from Reactor Containments* by S.H. Simmonds, S.K. Rizkalla and J.G. MacGregor, October 1979.

82. *Cracking of Reinforced and Prestressed Concrete Wall Segments* by J.G. MacGregor, S.K. Rizkalla and S.H. Simmonds, October 1979.

83. *Inelastic Behavior of Multistory Steel Frames* by M. El Zanaty, D.W. Murray and R. Bjorhovde, April 1980.

84. *Finite Element Programs for Frame Analysis* by M. El Zanaty and D.W. Murray, April 1980.

85. *Test of a Prestressed Concrete Secondary Containment Structure* by J.G. MacGregor, S.H. Simmonds and S.H. Rizkalla, April 1980.

86. *An Inelastic analysis of the Gentilly-2 Secondary Containment Structure* by D.W. Murray, C. Wong, S.H. Simmonds and J.G. MacGregor, April 1980.

87. *Nonlinear Analysis of Axisymmetric Reinforced Concrete Structures* by A.A. Elwi and D.W. Murray, May 1980.

88. *Behavior of Prestressed Concrete Containment Structures - A Summary of Findings* by J.G. MacGregor, D.W. Murray, S.H. Simmonds, April 1980.

89. *Deflection of Composite Beams at Service Load* by L. Samantaraya and J. Longworth, June 1980.

90. *Analysis and Design of Stub-Girders* by T.J.E. Zimmerman and R. Bjorhovde, August 1980.

91. *An Investigation of Reinforced Concrete Block Masonry Columns* by G.R. Sturgeon, J. Longworth and J. Warwaruk, September 1980.

92. *An Investigation of Concrete Masonry Wall and Concrete Slab Interaction* by R.M. Pacholok, J. Warwaruk and J. Longworth, October 1980.

93. *FEPARCS5 - A Finite Element Program for the Analysis of Axisymmetric Reinforced Concrete Structures - Users Manual* by A. Elwi and D.W. Murray, November 1980.

94. *Plastic Design of Reinforced Concrete Slabs* by D.M. Rogowsky and S.H. Simmonds, November 1980.

95. *Local Buckling of W Shapes Used as Columns, Beams, and Beam-Columns* by J.L. Dawe and G.L. Kulak, March 1981.

96. *Dynamic Response of Bridge Piers to Ice Forces* by E.W. Gordon and C.J. Montgomery, May 1981.

97. *Full-Scale Test of a Composite Truss* by R. Bjorhovde, June 1981.

98. *Design Methods for Steel Box-Girder Support Diaphragms* by R.J. Ramsay and R. Bjorhovde, July 1981.

99. *Behavior of Restrained Masonry Beams* by R. Lee, J. Longworth and J. Warwaruk, October 1981.

100. *Stiffened Plate Analysis by the Hybrid Stress Finite Element Method* by M.M. Hrabok and T.M. Hrudey, October 1981.

101. *Hybslab - A Finite Element Program for Stiffened Plate Analysis* by M.M. Hrabok and T.M. Hrudey, November 1981.

102. *Fatigue Strength of Trusses Made From Rectangular Hollow Sections* by R.B. Ogle and G.L. Kulak, November 1981.